

# **Influence of mandrel's surface on the properties of joints produced by magnetic pulse welding**

Alexandra Martins Ramalho

***Master Thesis / Dissertação do MIEM***

Orientadora na FEUP: Professora Doutora Ana Reis

Orientadora no INEGI: Doutora Inês Oliveira

Mestrado Integrado em Engenharia Mecânica



## **FEUP**

Faculdade de Engenharia da Universidade do Porto

Departamento de Engenharia Mecânica

Janeiro de 2017



# ABSTRACT

---

Nowadays, an increasing number of structural applications require high performance materials with a high strength-weight ratio, high electrical and thermic conductivity and an improvement on the corrosion resistance. This is only possible to obtain when combining different materials, benefiting from the combination of both mechanical and physical properties. However, joining two workpieces is not always easy, especially when these are dissimilar materials. Due to the difference in melting temperature and thermal properties, it is in most cases impossible to use fusion welding techniques to weld dissimilar materials such as aluminum-copper, unless they exhibit comparable characteristics.

Electromagnetic pulse technology (EMPT) provides non-contact process for joining, welding, forming and cutting metals with great potential to join similar and dissimilar materials besides the conventional welding techniques often used in the industry. Magnetic pulse welding (MPW) is a cold solid-state welding process, it consists in an impact welding process when at least one of the joining parts is electromagnetically accelerated against the other with a certain velocity, under a certain impact angle which results in a high impact pressure. The physical effects described by Maxwell state that a temporarily varying magnetic field induces electrical currents in nearby conductors and additionally exerts forces, so called Lorentz forces. These Lorentz forces act like forming forces causing the dynamic deformation of the workpiece if the magnetic pressure is higher than the yield strength of the workpiece. The present dissertation intends to provide a contribution for understanding how the state of the surface influences the joining between copper and aluminum using magnetic pulse welding technology. Different surface conditions were tested: machined, blasted, polished, chemically etched, greasy surface and threaded. Through the results obtained is possible to notice that the surface topology may have an influence on the welding quality. MPW is often considered as a solid-state welding process; However, through the results of this study, the occurrence of melting was verified.

---

---

## RESUMO

---

Atualmente, inúmeras aplicações estruturais exigem materiais de alto desempenho permitindo beneficiar de uma boa relação resistência mecânica/peso, alta condutibilidade térmica e elétrica e, por exemplo, uma melhoria na resistência à corrosão. Estas características são possíveis de obter quando se combinam materiais diferentes, permitindo beneficiar das propriedades mecânicas e físicas de ambos, simultaneamente. No entanto, unir duas peças nem sempre é um processo fácil, especialmente quando se tratam de materiais diferentes. Devido à diferença entre pontos de fusão, entre outras propriedades térmicas, torna-se difícil o recurso às técnicas de soldaduras por fusão para soldar materiais diferentes, tal como no caso do alumínio e cobre, a não ser que ambos exibam propriedades semelhantes.

A tecnologia de pulso eletromagnético (EMPT) permite a união, soldadura, conformação e corte de metais, exibindo um grande potencial para unir materiais com diferentes propriedades térmicas. Esta tecnologia consiste numa alternativa aos processos de soldadura convencionais. A soldadura por impulso magnético (MPW) é um processo de soldadura a frio em fase sólida. Consiste numa soldadura por impacto em que, pelo menos, uma das peças a unir é magneticamente acelerada contra o alvo. A peça é acelerada a uma determinada velocidade, com um determinado ângulo, originando uma pressão de impacto. O fenómeno físico descrito por Maxwell defende que um campo magnético variável induz correntes elétricas nos condutores próximos que por sua vez exercem forças – conhecidas como forças de Lorentz. Estas atuam como forças de conformação, deformando dinamicamente os materiais envolvidos, caso a pressão exercida pelo campo magnético seja superior ao limite de elasticidade dos mesmos. Esta dissertação pretende estudar a influência da preparação das superfícies na qualidade de soldadura, utilizando MPW, entre cobre e alumínio. Diferentes superfícies foram testadas: maquinado, granalhado, polido, atacado quimicamente, contaminado com óleo e roscado. Analisando as interfaces de soldadura obtidas é possível verificar que a topologia de superfície poderá ter influência na qualidade da junta obtida. MPW é, frequentemente, considerado um processo de soldadura na fase sólida, no entanto, a ocorrência de fusão foi detetada.

---

# AGRADECIMENTOS

---

Endereçar os maiores agradecimentos à Professora Doutora Ana Reis, orientadora deste trabalho, pela oportunidade de desenvolver uma tese nesta área científica e por todo o apoio e incentivo.

À Doutora Inês Oliveira, orientadora deste trabalho, pela partilha do seu conhecimento científico que foi essencial para a realização desta dissertação. Estou muito grata pela constante orientação e pelo incedível apoio, tanto a nível técnico como pessoal.

Ao INEGI, Instituto de Engenharia Mecânica e Gestão Industrial, endereço os meus agradecimentos por todos os meios disponibilizados durante a realização deste projeto.

Aos meus professores, com quem tive o privilégio de aprender para além de engenharia. Pela constante partilha de conhecimentos, essencial para o meu desenvolvimento profissional e pessoal.

À Bárbara Libório, por ser uma constante fonte de inspiração e motivação e por se ter tornado, desde a minha entrada na FEUP, uma grande referência para mim.

Ao Bruno Azevedo, por todo o apoio e amizade que se excedem à minha passagem pela FEUP.

À Leonor Babo, por todos os momentos de amizade, compreensão e partilha que transformaram todas as dificuldades em momentos que não esquecerei.

A todos os meus amigos de curso, cujo apoio me permitiu conciliar o curso com outras atividades extra-curriculares. Por todas as horas de estudo e partilha e, acima de tudo, por todos os momentos que tornaram esta minha passagem pela FEUP verdadeiramente inesquecível.

Aos meus pais que foram um apoio essencial ao longo de todo este percurso. Tudo o que sou e serei, devo-o a vocês.





# CONTENTS

---

<b>Abstract</b> .....	<b>iii</b>
<b>Resumo</b> .....	<b>v</b>
<b>Agradecimentos</b> .....	<b>vii</b>
<b>Contents</b> .....	<b>ix</b>
<b>List of Figures</b> .....	<b>xi</b>
<b>List of Tables</b> .....	<b>xv</b>
<b>List of Symbols</b> .....	<b>xvii</b>
<b>1 Introduction</b> .....	<b>1</b>
1.1 Motivation .....	1
1.1.1 Explosive Impact Welding (EXW) .....	3
1.1.2 Vaporizing foil actuator welding (VFAW) .....	7
1.1.3 Magnetic Pulse Welding (MPW) .....	9
1.2 Scope and layout of the thesis .....	11
<b>2 Literature Review</b> .....	<b>13</b>
2.1 Magnetic Pulse Welding .....	13
2.2 Theoretical background .....	15
2.3 Advantages and disadvantages of EMPT .....	19
2.4 Magnetic Pulse Welding Equipment .....	21
2.4.1 Capacitor Bank .....	21
2.4.2 Coil .....	22
2.5 Process Parameters .....	24
2.6 Effect of the energy on the weld strength and width .....	28

---

2.7	Effect of standoff distance on the weld strength and width .....	29
2.8	Jetting for bonding mechanism.....	31
2.9	Summary .....	33
<b>3</b>	<b>High velocity impact welding .....</b>	<b>35</b>
3.1	Theoretical background .....	35
3.2	Intermetallic phase formation .....	36
3.3	Effect of initial surface conditions on the weld joint .....	40
3.4	Local Melting and its influence on metallographic .....	43
3.5	Interface wave propagation in MPW .....	45
3.6	Summary .....	49
<b>4</b>	<b>Experimental work .....</b>	<b>51</b>
4.1	Material Characteristics .....	52
4.2	Experimental methodology.....	53
4.3	Analysis of the welding quality.....	59
4.4	Summary and Layout.....	65
<b>5</b>	<b>Analysis of the results.....</b>	<b>67</b>
5.1	Mechanical characterization of the joint .....	67
5.2	Intermetallic phase formation .....	69
5.3	Jetting formation.....	71
5.4	Occurrence of melting.....	72
5.5	Summary .....	73
<b>6</b>	<b>Conclusions .....</b>	<b>75</b>
6.1	Conclusions .....	75
6.2	Future work.....	77
<b>7</b>	<b>References .....</b>	<b>79</b>

# LIST OF FIGURES

---

Figure 1: Principle of collision welding [33].	1
Figure 2: The explosive welding arrangement [3].	3
Figure 3: Formed jet on explosive welding process [63].	4
Figure 4(a) Wave formation for impact of titanium flyer plate (3mm) on titanium base plate (30mm) with an impact velocity of 486m/s (b) Formation of vortices for impact of titanium flyer plate (3mm) on titanium base plate (30mm) with an impact velocity of 606m/s [63].	5
Figure 5: The interface view of bonded samples, increasing the explosive ratio [63].	6
Figure 6: Comparison of flyer velocities in VFAW and MPW at certain distances and energy levels [33].	8
Figure 7: Illustration of MPW Process [44].	10
Figure 8: Interaction between physical phenomena in magnetic pulse welding [79].	10
Figure 9: The magnetic pulse process [61].	13
Figure 10: The Spicer® Bi-Metallic Stub-Shaft was produced using magnetic pulse welding technology. With this technology, aluminum was joined to steel to make the driveshaft [45].	14
Figure 11: Electromagnetic phenomena representation [19].	15
Figure 12: Equivalent circuit diagrams (adapted from [73]).	16
Figure 13: Directions of the current, the magnetic field lines and the pressure during a) electromagnetic compression b) electromagnetic expansion c) electromagnetic sheet metal forming [73].	17
Figure 14: Sketch of the magnetic field distribution for a fieldshaper (adapted from [73]).	18
Figure 15: Examples of MPW applications a) Audi space frame structure; b) Structure of BMW-C1E [61].	20
Figure 16: Schematic view of electromagnetic sheet metal forming process and his components [7].	21
Figure 17: Oscillation of a typical discharging current [81].	22
Figure 18: Cylindrical coil types: a) the bobbin; b) the helix; c) the spiral; d) the single-turn coil [73].	23
Figure 19: Example of pancake coil [69] and a real flat spiral coil [70].	23
Figure 20: Principle of electromagnetic tube compression with an outer coil (left), and tube expansion with an inner coil (right) [69].	23

---

Figure 21: Process parameters on MPW [68].	24
Figure 22: The weldability window [64, 100].	24
Figure 23: Specimen for uni-axial tensile test showing break in the parent metal [43].	25
Figure 24: Al to Al electromagnetically welded sample showing weld and no-weld zones [46].	26
Figure 25: Magnified view of the weld zone indicated in the Fig.24 [46].	26
Figure 26: Lorentz forces acting on the sheets at the time of collision. Force in the center is normal to the sheet while it has a shear component elsewhere [46].	27
Figure 27: Cross sections of the coils [46].	28
Figure 28: (a) Rectangular coil: effect of energy on the shear strength of the weld, with standoff distance = 2.5 mm, (b) tapered coil: effect of energy on the shear strength of the weld with standoff distance $\frac{1}{4}$ 2.5 mm [46].	29
Figure 29: Schematic of MPW welding process of two tubes before and after welding [61].	30
Figure 30: Scheme of impurity removal, Jetting [61].	31
Figure 31: Aluminum (flyer metal) velocity just before collision [61].	32
Figure 32: Experimental setup of MPW process [84].	33
Figure 33: Main effects plot for burst pressure [84].	34
Figure 34: Comparison between Al/Cu weld (a) and Al/Al weld (b) for an interface shape from straight to wavy – Al–Cu intermetallic occurrence independently of the interface shape [77].	37
Figure 35: Typical porous structured intermetallic, and cracking driven by pores interactions [77].	37
Figure 36: Typical fracture surface of the intermetallic observed at the pores scale [77].	38
Figure 37: Influence of the intermetallic on the mechanical behavior of the weld [77].	38
Figure 38: Macroscopic observation of the fracture surface given by the torsion shearing test: (a) Al/Al interface and (b) Al/Cu interface [77].	39
Figure 39: As-machined Al and Cu tube samples before welding (a) and the produced surface scratches on the Cu tubes in hoop direction (b). The further sanded surface is shown in (c) [102].	40
Figure 40: SEM micrographs of two interface regions and their local enlargements. The rough Cu surface was from chemical etching [102].	42
Figure 41: The Al–Cu binary phase diagram, computed with commercial software and with available thermodynamics database [102].	43
Figure 42: The optical micrograph of a sample welded at 6.0 kV, and a round pore with a smooth surface was observed (a). By refocusing at the pore bottom (b) some surface cracks were revealed [102].	44
Figure 43: Kelvin–Helmholtz instability creation (from left to right $u_1 > u_2$ ) [10].	46
Figure 44: The periodic wave formation [61].	46
Figure 45: Typical wavy interface showing the intermetallic phase located in a “melted pocket.” Cracks and pores are also characteristic to the wavy location of the intermetallic layer [90].	47
Figure 46: Setup used for the welding process.	55
Figure 47: Welding window illustration [67].	55
Figure 48: Setup used for the tensile tests.	56
Figure 49: Workpiece during the tensile test.	57
Figure 50: Projected grip (using SOLIDWorks®).	57
Figure 51: Metal Plugs for Testing Tubular Specimens, Proper Location of Plugs in Specimen and of Specimen in Heads of Testing Machine - ASTM A370.	58

---

Figure 52: Force-displacement curves obtained experimentally for different specimens. ....	59
Figure 53: Machine surface: a) weld interface SEM analysis for M1 (magn. 500x); b) Force-displacement curve for M2 and M3 machined specimens. ....	60
Figure 54: Blasted surface: a) weld interface SEM analysis for G1 (magn. 250x); b) Force-displacement curve for G2 and G3 blasted specimens. ....	60
Figure 55: Polished surface: a) weld interface SEM analysis for P1 (magn. 500x); b) Force-displacement curve for P2 and P3 polished specimens. ....	61
Figure 56: Chemically-attacked surface: a) weld interface SEM analysis for Q1 (magn. 500x); b) Force-displacement curve for Q2 and Q3 chemically-attacked specimens. ....	61
Figure 57: Greasy surface: a) weld interface SEM analysis for O1 (magn. 250x); b) Force-displacement curve for O2 and O3 oil-contaminated specimens. ....	62
Figure 58: Threaded surface: a) weld interface SEM analysis for R1 (magn. 250x); b) Force-displacement curve for R2 and R3 threaded specimens. ....	63
Figure 59: Weld interface for the R2 screwed specimen with almost non-intermetallic phase (magn. 100x). ....	63
Figure 60: Failure occurred in the aluminum part at 19,70 kN load. ....	64
Figure 61: Cracking observation for machined sample (M). ....	68
Figure 62: Weld interface (magnification 500x): a) Machined specimen (M1); b) Shot-blasted specimen (G1). ....	68
Figure 63: EDS study on MPW welded Al-Cu interface zones for different surface preparations: a) machined; b) blasted; c) polished; d) chemical etching; e) greasy; f) threaded. ....	69
Figure 64: Analysis of the content for the different surface conditions. ....	70
Figure 65: Flat interface observed a) Greasy surface b) Threaded surface. ....	71
Figure 66: SEM observation for G1 workpiece. ....	72

---

# LIST OF TABLES

---

Table 1: Thermal properties of materials [54].	2
Table 2: Explosive ratio, explosive quantity and impact speed of upper plate [32].:	5
Table 3:Electrical resistivity and conductivity at 20 °C	17
Table 4: Standard chemical composition of the Al6060T6 and Cu specimen [77]	36
Table 5: Some physical properties of Al6060T6 and Cu (adapted from [77])	36
Table 6: Peeling test results and bonded percentage lengths for different welding conditions. The percentage is the bonded length over the total interface length estimated from micrographs of sectioned surfaces [102].	41
Table 7: Chemical composition of the copper.	52
Table 8: Mechanical properties of the copper R300.	52
Table 9: Mechanical properties of the Aluminum AA 6063-T5.	52
Table 10: Different surface preparation for copper specimens.	53
Table 11: Roughness measurements of the copper R300.	54
Table 12: Welding parameters.	55
Table 13: Tensile tests parameters according to ASTM A 370.	57
Table 14: Surface roughness and average maximum bond strengths for different surface conditions.	64
Table 15: EDS study on MPW welded Al-Cu interface-zones for different surface conditions.	70

---



## LIST OF SYMBOLS

Symbol	Unit	Description
$V_p$	m/s	Impact velocity
$V_w$	m/s	Collision point velocity
$\beta$	°	Collision angle
$T_b$	s	Burst time
$V_0$	V	Charging voltage
$I$	A	Current
$E$	J	Energy
$F$	N	Force
$C$	$\mu\text{F}$	Bank capacitance
$U_{\text{set}}$	kV	Set voltage level
$P_1$	$\text{N}/\text{m}^2$	Pressure
$\alpha$		Factor for effects that limits deformation
$\sigma_y$	$\text{N}/\text{m}^2$	Yield strength
$R$	m	Radius
$\delta$	m	Skin depth
$L$	H	Inductance
$R$	$\Omega$	Resistance
LWZ	mm	Overlap distance
$m$	kg	Mass
$A_0$	$\text{M}^2$	Cross sectioned area
$R_a$	nm	Mean roughness
$R_q$	nm	Mean square roughness
EMPT		Electromagnetic pulse technology
MPW		Magnetic pulse welding
EXW		Explosive impact welding
VFAW		Vaporizing foil actuator welding
RLC		Resistance-inductance-capacitance
EDS		Energy Dispersive Spectroscopy
SEM		Scanning Electron Microscope

---

TCC

Thermal contraction coefficient

# 1 INTRODUCTION

---

## 1.1 Motivation

Design of multi-material structures for complex lightweight applications becomes more and more important nowadays. The joining of different materials started at prehistoric times when simple techniques of forging welding were applied. Perfectly, the nature would supply the materials as demanded to fulfill human's needs. However, sometimes tough and lasting constructions are required and should be developed using human techniques. That's the main reason why welding process is increasingly indispensable: to create bonds between different materials which together will make the perfect couple to answer to our overwhelming needs. Solid-State impact welding processes are those in which different materials are joined below their melting point. The main difference between solid-state welding and conventional welding processes is that the heat conventionally used to join the materials is partly replaced by applying pressure on the materials wanted to be joined, this pressure to join the workpieces is created through impact. These processes do not require the addition of brazing filler metal. When a piece of metal collides with another at an appropriate speed and angle, a weld may be created. There are some processes related to solid-state welding: Explosive impact welding (EXW), magnetic pulse welding (MPW) and vaporizing foil actuator welding (VFAW). In all these processes time, temperature and pressure individually or in combination produce coalescence of the base metal without reaching their melting point [54]. All mentioned joining technologies are based in the same physical mechanisms, which are represented in Fig.1.

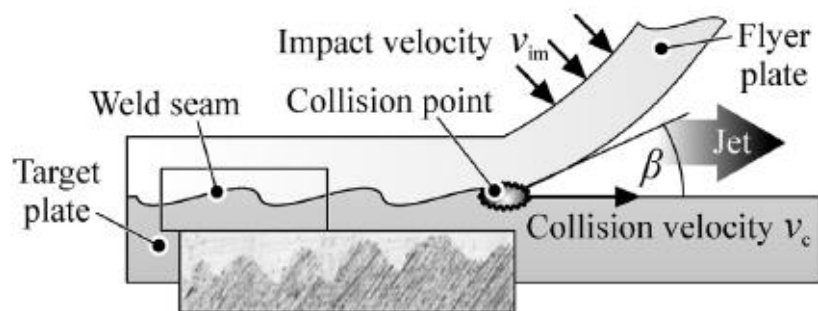


Figure 1: Principle of collision welding [33].

When welding two materials by using the conventional processes it is crucial to assure that they have similar characteristics. Due to the difference in melting points, thermal conductivity, volumetric specific heat and in thermal expansion coefficient, the solid state welding consists in a more interesting technology when compared to the conventional one. In the first one the difference between properties does not mean a restriction for its use. Fusion welding techniques for example laser spot welding and brazing have been used for creating joints between Al/Cu joints without suitable results, due to the formation of brittle phases in the weld [51]. It is known that at temperatures higher than 120° C the interaction between Al and Cu will result in brittle, low strength and high electrically resistant intermetallic compounds [51]. For that reason, it is desirable to develop new technologies to find new solutions for joining dissimilar materials. Solid state bonding processes have been experiencing in industrial environments for the production of Al/Cu joints. In Tab.1 is possible to compare the thermal properties of different materials and analyze the difference between the melting point of Aluminum and Copper (nearly 424° C) which is a constraint to bond this both metals through conventional welding techniques.

<b>Material</b>	<b>Melting Temp. (°C)</b>	<b>Thermal Conduct. (W /m.K)</b>	<b>Expansion Coeff. (10<sup>-6</sup>/K)</b>	<b>Specific Heat (kJ/kg.K)</b>
<b>Aluminium</b>	660	237	23.0	0.91
<b>Copper</b>	1084	353 - 386	17.0	0.39
<b>Titanium</b>	1670	16 - 22	11.0	0.54
<b>Carbon Steel</b>	1425 - 1540	36 - 54	10.8	0.49
<b>Stainless steel</b>	1510	16.3	17.3	0.50

*Table 1: Thermal properties of materials [54].*

Solid state impact welding gives the opportunity of joining dissimilar materials as the melting point is not a constraint in this process, this could be very interesting for different industries, as automotive and heat-transfer systems. A good understanding of the welding bonding mechanism for dissimilar materials is required in order to take the most possible advantages from the process.

Solid-state welding offer certain advantages when compared to the conventional welding processes since the base metal does not melt and form a nugget, the metals retain their original properties without heat-affected zone problems involved. When dissimilar metals are being joined their thermal expansion and conductivity is less important with solid state welding than in the conventional welding processes [54, 37]. Depending on the type of solid welding processes it could involve one of the following phenomenon or more than one at the same time [41]:

1. Diffusion, what means the transfer of the atoms across an interface and/or;
2. Pressure, where higher the pressure the stronger will be the interface and/or;
3. Relative interfacial movements which creates clean surfaces;

There are some other processes related to solid-state impact welding with some similarities with magnetic pulse welding: vaporizing foils and explosive welding. In the following, a general overview about the different processes and a deeper approach related to MPW is given.

The main aim of this thesis is to study the influence of the surface when welding two dissimilar materials. Different surface preparations were studied: machined, blasted, polished, chemically

etched, greasy and threaded. Studying different surface preparations enables to state different conclusions and analyze different behaviors of the welds. According to some authors, there is no need of cleaning the workpiece surface in order to achieve a good quality of welding. Joining two materials through magnetic pulse welding creates a jet. This jet formed consists in a quick burst that acts as a clean agent of the surface. However, testing a greasy surface would provide a better understanding and would be helpful to state how relevant is to clean the surface before welding.

### 1.1.1 Explosive Impact Welding (EXW)

Explosive welding process has been applied since several years ago and is the most used solid-state impact welding technique [32]. Although it is considered as a solid-state welding process, according to some authors, it is also considered as a fusion welding process. Mousavi and Al-Hassani, in [63], mention that high temperature in the collision point may lead to a phase change. The fusion welding theory consists on the dissipation of the kinetic energy at the interface while the pressure theory is based on the assumption that large plastic deformations lead to clean surfaces which are allowed to be formed and a solid diffusion process take place [20]. Explosive welding is generally used to bond two dissimilar metal plates and is most often used when the combination of metals makes conventional welding impractical. In this process, a wavy interface is usually generated between two flat and smooth plates. The still solid material acts like a fluid under the intense pressure at the welding front in order to form a wavy interface (Fig.4). In EXW, two plates (flyer and base) one placed above the other, and separated by a defined distance, as shown in the Fig.2. In this process, an explosive is responsible to give a certain amount of energy through its detonation. Usually the explosive is a powder and its detonation accelerates the flyer plate across the standoff gap, forcing it to collide at high velocity against the target plate. These high-velocity impact forces the two surfaces to become plastic at the collision zone, creating a jet. The jet consists of a left-over combination of both metals which is ejected from their middle. It is responsible for clean the surface of the plate leaving the metal prepared for bonding [3].

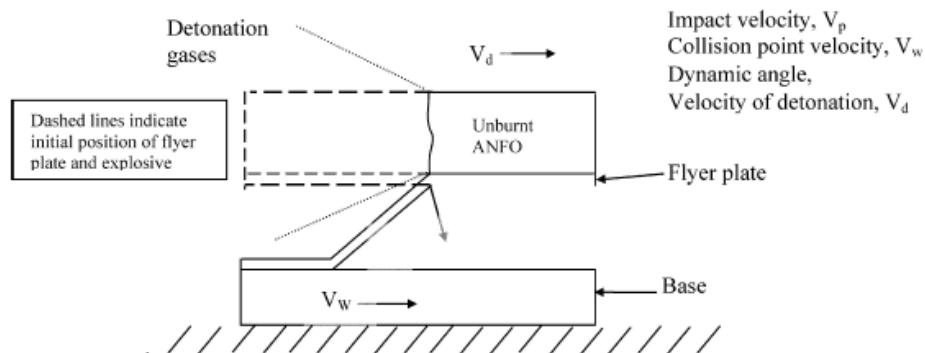


Figure 2: The explosive welding arrangement [3].

The velocity detonation of the explosives plays a very important role for the success of the process. In some applications, the velocity of the commercial explosives is generally too fast. Thus, sometimes a “slower” powder mix of ammonium nitrate and diesel fuel oil and an inert material such as perlite or sand is used [3]. The collision angle between the flyer plate, velocity

of detonation, collision point velocity  $V_w$  and plate impact velocity  $V_p$  is given through the Eq.(1).

$$V_p = 2V_w \sin\left(\frac{\beta}{2}\right) \quad (1)$$

Literature mentions that successful welds generally occur at angles between  $5^\circ$  and  $20^\circ$  and for impact velocities ranging from 150 m/s to 1500 m/s [33]. Due to the high velocity collision of metal plates, a high velocity forward jet is formed between the metal plates as shown in the Fig.3. The surface layers on the metals, containing non-metallic films such as oxide films that are detrimental to the establishment of a metallurgical bond, are swept away in the jet. The pressure has to be sufficiently high and for a sufficient length of time to achieve inter-atomic bonds. The successful solid diffusion could be compromised due to the few microseconds during when the pressure is maintained as this time could be not enough to guarantee the success of the technique [63].

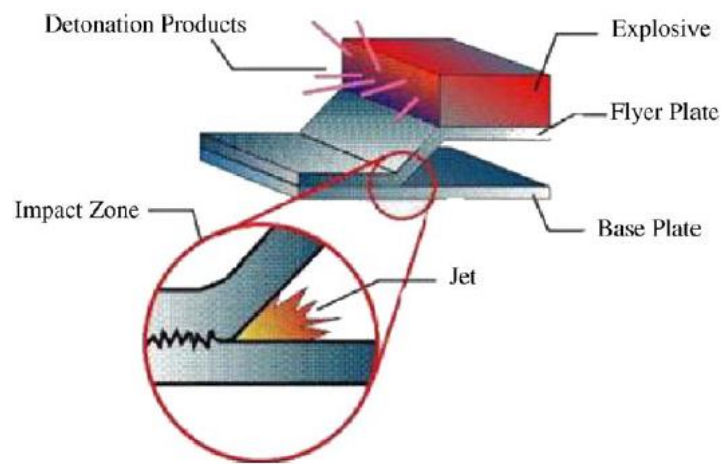


*Figure 3: Formed jet on explosive welding process [63]*

The interface of explosive welded metals can vary widely depending on the velocity and the angle, as described above. Thus, there are several possible types of interfaces ranging from straight smooth waves, small waves, large waves, waves with vortices (as shown in Fig.4), waves with solidified melt pockets, and continuous fused molten layers. According to [38] the waves are created behind the collision zone as a result of a velocity discontinuity across the interface which involves a salient jet. However, several studies and different theories have been carried out to better understand the wave formation during the collision and the conclusions are widely different from each other. The authors conclude that the waves were observed on surface of metals which had been subjected to oblique collision, where neither welding nor jetting has occurred [27, 3, 54]. The fact that the interface is wavy increases the contact surface between the materials, higher mobility of atoms and effective removal of contamination. The wavy bond without an apparent intermediate layer is preferred, as this layer, generally, yields the most desirable properties [63].

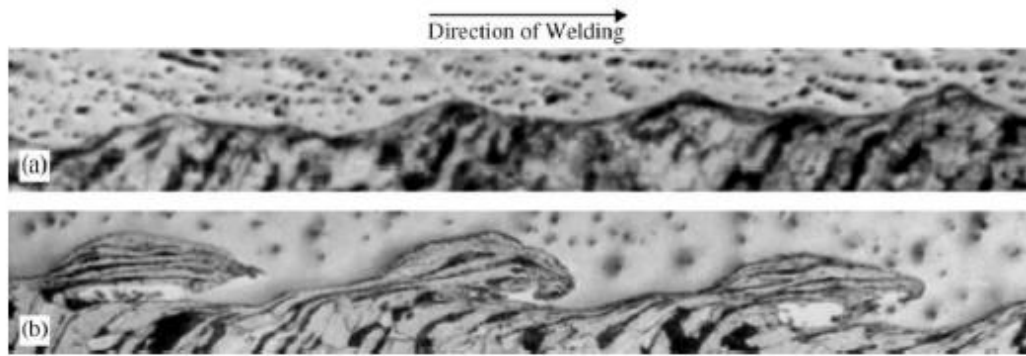


Figure 4(a) Wave formation for impact of titanium flyer plate (3mm) on titanium base plate (30mm) with an impact velocity of 486m/s (b) Formation of vortices for impact of titanium yer plate (3mm) on titanium base plate (30mm) with an impact velocity of 606m/s [63].

In the work presented in [32], the weldability of aluminum (Al) sheet and copper (Cu) sheet by explosive welding and the effect of explosive ratio on the joint interface were studied. Al and Cu are two materials which can not be joined though conventional welding process due to the difference between their melting points, as mentioned above (see Fig.1). However, it is possible to join them using the explosion welding process [32]. In the work presented in [32] the joint interface was changed from linear to wavy by increasing the explosive ratio, which is one of the major parameters on interface quality. Explosive ratio is the proportion between the explosive and flyer mass. The higher this ratio, the more explosives used and thus the more powerful the explosion will be.

In the Tab. 2 is clear that the explosive ratio is increasing from one specimen to another and the effect of this increasing on the microstructure consists in an increased wavy interface, as showed in Fig.5. Analyzing the Fig.5 it is clear that the bonding interface of the welding couples tend to become wavy with increasing explosive ratio, due to the crash angle. As described through the Eq.1, the impact velocity depends on the collision angle and on the collision point velocity. For each configuration there is an optimal angle which increases the value of the impact velocity. Some previous research proves that the higher the explosive ratio is, the bigger the waviness bonding will be [32, 22].

Sample	Weight of upper plate (g)	Explosive ratio (R)	Amount of explosive (g)	Speed of upper plate $V_p$ (m/s)
1	216	1.2	260	985
2	216	1.5	324	1124
3	216	2	432	1305
4	216	2.5	540	1452
5	216	3	648	1570

Table 2: Explosive ratio, explosive quantity and impact speed of upper plate [32].:

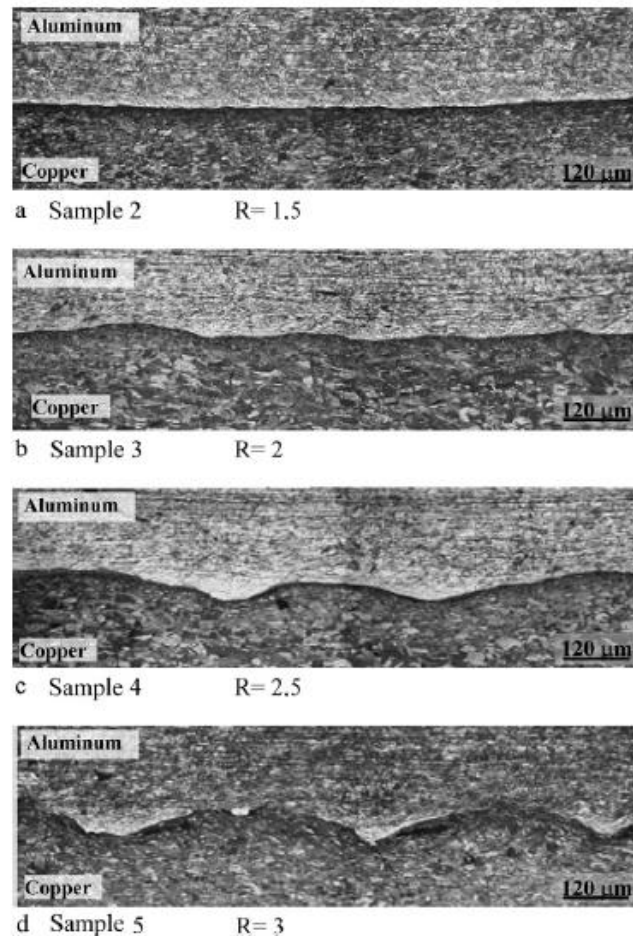


*Figure 5: The interface view of bonded samples, increasing the explosive ratio [63].*

The study referred above ([32]) concludes that after analyzing the interface from the microstructural images (see Fig.5) a mechanical bonding starts because of waviness interface with increasing explosive ratio and the mechanical properties were improved as well. Also, the sample which does not show a wavy interface was not bonded. This fact proves the importance of the waves to have a successful joint. The hardness tests showed that the hardness of the sample increased in the inner and outer sides with increasing explosive ratio because of the bigger deformation values [32]. The jet formation is a very important issue which should be well understood and improved in order to achieve the desired results. Due to its high velocity, the jet acts as a cleaning agent to both surfaces, removing the detrimental substances as all oxides and surface contaminants in the weld area. Thus, a metallurgical bond can be established what means an atomic bonding can be achieved between the two mating metal surfaces [63]. In most situations the explosive welding is a successful technique. This technique shows a bunch of advantages, being the most important the quality of the joint which is generally good with high mechanical strength. As it is a designed “cold method” the bonded metals retain their pre-bond properties. However, great failures sometimes occur and the cause(s) are, most of the time, unknown. Thus, it is important to notice the main disadvantages of EXW and it is possible to refer the danger associated due to the explosion needed [4]. EXW is applied for large scale operations, with weld lengths in the scale of meters. Large and isolated spaces are required to implement this explosive technique which represents an increasing on the overall costs [9].



---

Using the explosive welding has the following disadvantages: irregularity of detonation waves along the edge of the cladding metal sheet, undesirable effects of unstable detonation in the proximity of the detonator, cracking and distortion of the cladding metal sheet along the edges thereof, intrusion of gaseous detonation products into the gap between the cladding metal sheet and the base metal sheet, and ineffective bond and cracks of the clad metal caused by the foregoing difficulties [12, 6]. EXW and MPW are the most common techniques; however a novel method for welding driven by rapid metal vaporization has been studied [73].

### 1.1.2 Vaporizing foil actuator welding (VFAW)

Comparing with EXW, above described, MPW is more suitable for smaller scale operations, on the order of millimeter. Vaporizing foil actuator welding (VFAW) consists in a new and alternative method to explosive welding (driven by chemical explosives) and to magnetic pulse welding (driven by magnetic forces). In VFAW thin foil and/or wires are vaporized by the passage of a high current driven by a capacitor bank. This phenomenon can create a region of high pressure and consists basically in an electrical explosion of conductors. During the violent vapor expansion, a discharge current of the capacitor rapidly vaporizes a thin foil in order to accelerate the metal flyer plate and deform it plastically. The energy deposited in the conductors increases with increasing input energy from the capacitor bank; however this increase is not linearly proportional. While faster energy deposition improves the energy density in the foil at vaporization, there is a limit to how much energy can be deposited in a foil of a given mass. Foils of greater mass display the potential for greater energy deposition, as may be expected [18]. VFAW was found to be a robust collision welding technique, able to successfully weld various dissimilar metal pairs as it is possible to prove through the study presented in [93] where very different couples of materials were tested and different successful bonds were created: copper–titanium, copper–steel, aluminum–copper, aluminum–magnesium and titanium–steel. In the research done in [93] the main goal was to use vaporizing conductor technique as an alternative to EXW, creating similar bonds at much smaller length scales. In the work presented in [33], vaporizing foil actuator welding is described as a competitor technology to magnetic pulse welding. Actually, the high issue about MPW is the concern about the longevity of the actuator while in VFAW there is no issue about the longevity of the coil and even low conductivity materials can be launched without the use of a driver sheet [93, 33]. The current cause some physical changes to occur in the thin metallic conductor and basically it is possible to brief them in five steps [33]:

1. the heating stage;
2. the melting stage;
3. the heating stage of liquid metal;
4. the vaporizing stage;
5. the plasma forming stage;

The beginning of the violent expansion or burst time  $-t_b-$  is indicated by the peak in voltage and by the destruction of the dynamic equilibrium between the expansive vapor pressure and the counteracting Lorentz force around the conductor [94]. From the  $t_b$  on, the intense pressure of the expanding vapor or plasma acts as forming pressure for the plate. The velocity of the flyer plate or consequently the pressure achieved is directly related with the amount of the electrical

energy  $E_D$  deposited into a metal wire until it bursts [80]. Increasing the current rate from 20 to 150 A/ns allowed the deposition of almost three times more energy [33]. The fact of the amount of energy stored is increasing with the current rate conflicts with some literature where the storable energy per unit mass is a constant for a given metal [83]. This amount of energy can be estimated through the following Eq.(2):

$$E_D = \int_0^{tb} UI dt \quad (2)$$

Where,  $U$  represents the voltage drop across the length and  $I$  the current through the foil [92].

VFAW seems to be a promising alternative to MPW because higher flyer velocities can be reached, there are no tool longevity problems since foils are disposable low-cost actuators and workpieces do not need to be good electrical conductors [33].

Although in case of magnetic pulse welding the peak currents are higher than in VFAW, the most notable fact is that vaporizing foils provide flyer velocities up to three times higher than MPW, nearby 930m/s versus 300m/s at the maximum [33]. As shown in Fig.6 for an identical experimental configuration the VFAW velocities exhibit deviations of up to 25% with regard to the average value and the values are clearly bigger comparing to MPW velocities. Flyer impact velocities up to 900m/s were recorded for VFAW experiments which is a good advantage compared to MPW as it is directly related with the energy stored in the wire, as described before [95, 93].

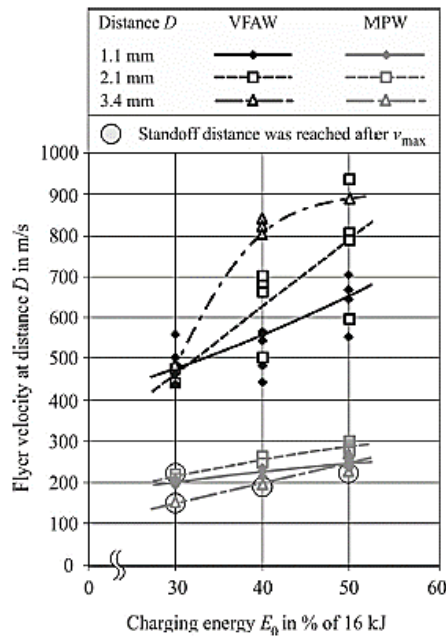


Figure 6: Comparison of flyer velocities in VFAW and MPW at certain distances and energy levels [33].

However vaporizing wires have also found limited use in industry with hydroelectric forming, their use has proven difficult to commercialize [34, 18].

---

### 1.1.3 Magnetic Pulse Welding (MPW)

The magnetic pulse welding (MPW) is a combination of electromagnetic, mechanic and heat transfer phenomenon, as described in the Fig.7. MPW consists in a cold welding process which uses high velocity impact to join parts [36]. It could be compared to the EXW but using magnetic pressure to accelerate the object instead of chemical explosives. The magnetic pressure required in this process is associated with a magnetic field. Thus, MPW makes use of the electromagnetic forming technology (EMF) to create a joint between the flyer and the target plate.

In this process the forming force is generated by Lorentz Forces (see Eq.3) whose are created by the two opposite currents (primary in the coil and the secondary current in the workpiece), both of these currents repeal each other creating the required force to deform the plate.

$$\vec{F} = \vec{j} \times \vec{B} \quad (3)$$

where,  $\vec{F}$  is the force acting on the workpiece,  $\vec{j}$  is the current density,  $\vec{B}$  is the magnetic field [73].

The required voltage of the capacitor bank is one parameter to be set before starting the process. This voltage determines the energy that is stored in the capacitors and could be described as follows by the Eq.4:

$$E = \frac{CU_{set}^2}{2} \quad (4)$$

Where, E corresponds to the stored energy [J], C to the bank capacitance [ $\mu$ F] and  $U_{set}$  to the set voltage level [kV] [54].

The magnetic pressure has to be enough to deform the part of the workpiece in the working zone and provide it with enough kinetic energy so that the impact with the inner workpiece makes a good bond. The required value of pressure is possible to estimate through the Eq.5, in this equation the  $P_1$  corresponds to the pressure required for deformation [ $N/m^2$ ],  $\alpha$  is the factor for effects that limit deformation,  $\sigma_y$  is the yield strength of the material [ $N/m^2$ ], t corresponds to the thickness of the workpiece [m] and R is the radius of the workpiece [m].

$$P_1 = \alpha \times \frac{2\sigma_y t}{R} \quad (5)$$

The strength of collision welds can reach or even exceed the one of the weakest parent material [33]. In Fig.7, MPW process is represented and, as can be seen, consists in a short-duration high-magnitude current which is discharged through a coil, creating an eddy current in the outer surface of the outer tube and an intensive magnetic field between the coil and the outer tube. The reaction between the eddy current and the magnetic field generates Lorentz force which expels and accelerates the outer tube towards the inner tube [44].

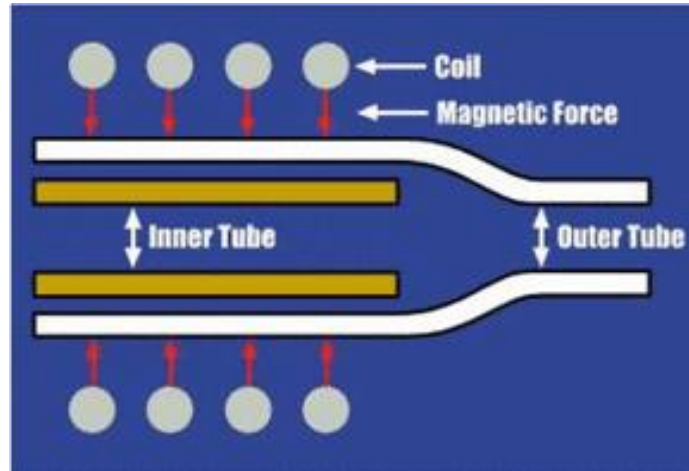


Figure 7: Illustration of MPW Process [44].

As described for EXW and VFAW, the impact velocity and the impact angle are the two important parameters in the forming of weld. In case of magnetic pulse welding the charging voltage level required can be predefined for the capacitors when the geometry is chosen [54]. The peak current generated by a capacitor bank discharge,  $I_{max}$ , can be estimated by the Eq.6:

$$U_{set} = \frac{I}{\sqrt{\frac{C_{\Sigma}}{L_{\Sigma}} \times \delta}} \quad (6)$$

Where [54]:

$I$  is the current peak in the coil [A];

$C_{\Sigma}$  is the total capacitance of the system [F]

$L_{\Sigma}$  is the total inductance of the system [H]

$\delta$  is the system attenuation coefficient [-]

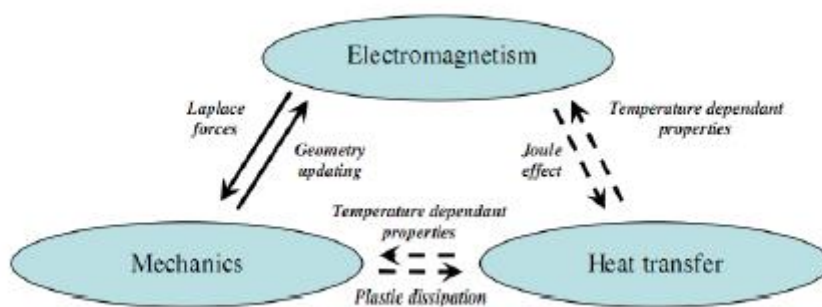


Figure 8: Interaction between physical phenomena in magnetic pulse welding [79].

According to [29] even with lower collision velocities, as compared to those during explosive impact welding method, a metastable wave initiation mechanism take effect during MPW what makes the weld possible to occur. However, one of the well-known issues about MPW is the relatively short lifetime of a coil because the Lorentz forces take effect on both the workpiece and the coil which becomes a concern at high driving pressures [93, 73, 33].

---

The MPW is the principal method explored in this paper concerning it to be an advanced joining technique as it enables the possibility of joining dissimilar materials; contrarily to the conventional welding methods no melting is involved thus avoiding or at least minimizing the heat-affected zone (HAZ) such as the formation of brittle intermetallic phases or cracking in fusion welding. Thus, no major changes in materials properties are expected to take place in this process [13]. MPW process is completed within several microseconds, being so a fast method of joining. Literature says that the parts to weld do not have to be cleaned or degreased and no finishing of the parts is required [29]. Despite of many advantages showed, only electrically conducting materials can be used as flyer material and the parts must overlap to generate the joint.

As referred for EXW process, the velocity and absolute energies are typically much higher than in MPW. Thus, the MPW process seems to be more prone to problems related to removing surface contamination. For this reason, the surface preparation and removal of contamination may influence the joining efficiency. Very different opinions can be related in the literature about considering MPW as a solid-state welding process due to some melting occurrence and the formation of an intermetallic phase in the joint when the temperature increased for values above the melting point. These different topics consist in the main motivation for developing this present work in order to find a reasoned approach about the influence of the surface on the quality of welding.

## 1.2 Scope and layout of the thesis

Taken into consideration the main objectives, this dissertation was divided in 7 chapters. In this present chapter an overview of the work's motivation and an introduction to the main concepts are presented. The **Chapter 2** is related to the literature review and presents the theoretical background of MPW. This literature review includes the description of EMPT phenomenon, a description of advantages and disadvantages of Magnetic Pulse Welding are given in order to compare this process with others. The different components of the equipment used in the process and the process parameters are also described. The jetting formed for bonding mechanism is also approached in this chapter.

**Chapter 3** is dedicated to understand the high velocity impact welding process. The chapter starts with a theoretical background where an amount of different examples is given in order to better understand the bonding between aluminum and copper with different approaches. Other important topics are described related to the interface created. As the intermetallic phase formation, the effect of the initial surface conditions, the local melting sometimes verified and the wavy interface often registered in MPW processes.

**Chapter 4** deals with the experimental work. In this chapter the aluminum and copper used are characterized in terms of mechanical and thermal properties. The different surface preparations tested, the methodology and equipment used for welding are described. Tensile tests at 2 mm/min and microstructure examination were performed to evaluate the welding quality. The data collected from these tests is used to compare with the theoretical background.

**Chapter 5** is about the analysis of the results. Different aspects of the welds are analyzed. The aspect of the interface is analyzed and the effect of the roughness on the mechanical strength of the joint. For each sample tested, the intermetallic phase formation and wavy interface is analyzed.

Finally, in the **chapter 6** the work main conclusions and suggestions for future work are presented.

## 2 LITERATURE REVIEW

---

### 2.1 Magnetic Pulse Welding

Welding requires two atomically clean surfaces to be pressed together to obtain metallurgical continuity [46]. Magnetic pulse welding consists in an impact welding process meaning that at least one of the joining parts - the flyer - is accelerated against the other with an appropriate velocity ( $v$ ) at which it collides with the target plate under a certain impact angle, ( $\beta$ ), resulting in high impact pressure (on the order of gigapascal) [42, 33]. As widely described in literature the high velocity impact of the two surfaces forces them to become plastic at the collision zone and it all comes along with the formation of a jet that removes all oxides and surface contaminants in the weld area allowing the creation of an atomic bonding between the two metal surfaces [29, 10, 33, 73].

The magnetic pulse welding is similar to the explosive welding principle but the impact energy is induced by electromagnetic force which is generated by interaction among discharge pulse current running through the coil, induced magnetic flux around the coil and eddy current produced at the plate surface, as described in the Fig.9. The welding is normally achieved within 10 microseconds with a negligible temperature increase [96].

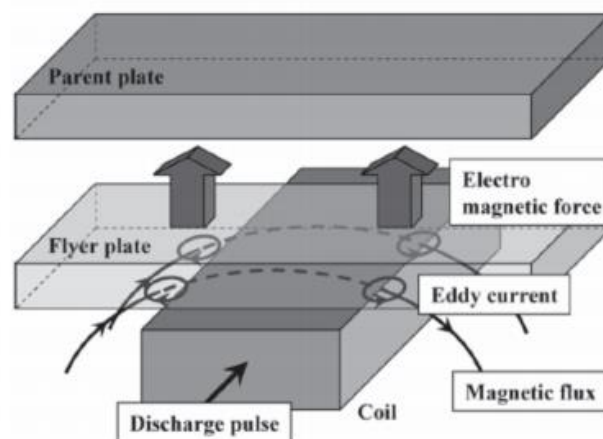
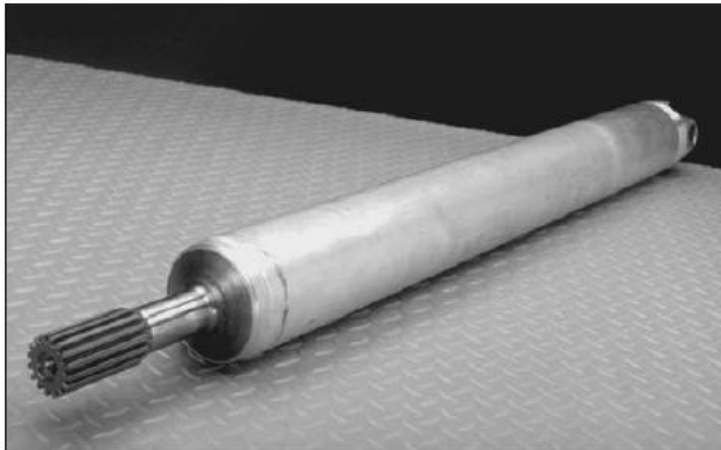


Figure 9: The magnetic pulse process [61].

This welding process can be applied to dissimilar material combinations in physical and mechanical properties such as melting point, heat conductivity, and hardness [96]. It represents an extremely interesting finding for automotive industry (see Fig.10) as the sector is currently highly focused on cutting vehicle emission through weight reduction [45]. On the other hand, besides the emission reduction the idea of joining a strong material to a lightweight one could provide for industry a new tool for obtaining optimum strength at minimum weight, which sounds really attractive for the users [45]. Metallurgical bonding can be obtained in a wide variety of similar and dissimilar metals and alloys without any external application of heat or the use of any intermediate metals [86]. This consists in a very important finding for the development of new material combination with improved mechanical and physical properties.



*Figure 10: The Spicer® Bi-Metallic Stub-Shaft was produced using magnetic pulse welding technology. With this technology, aluminum was joined to steel to make the driveshaft [45].*

New developments in magnetic pulse welding are opening up new applications for the technology. Actually, magnetic pulse welding has been available for more than 60 years, but its use has been very limited up until now [45]. Whereas previously, the process could only weld small diameter (less than 25mm) parts made of soft alloy materials, it is now capable of joining large parts made from hard materials, which have been pre-heat treated before. Although one of the greatest advantages of magnetic pulse welding as referred before is that it is suitable for joining dissimilar metals it has the limitation that one of the two parts (the one which moves) should be a good conductor of electricity [33]. Thus, it is mandatory to choose a good enough conductor as aluminum, magnesium, titanium or copper by contrast of steel, for instance [96, 52].

The development and improvements on electromagnetic pulse technology are playing a very important role especially in the automotive industry due to the possibility of implementing lightweight construction concepts. In electromagnetic forming processes the ductility of the workpiece increase significantly when compared to conventional forming processes, though the reason behind this increase in ductility is still being debated [73].



## 2.2 Theoretical background

Electromagnetic pulse technology (EMPT) provides non-contact processes for joining, welding, forming and cutting of metals [81, 88]. This technology uses pulsed magnetic fields to apply forces to the metal workpiece preferably made of a high electrical conductor material [19]. The principles of this technology are explained by physical effects described by Maxwell (1873). Maxwell explained that a temporarily varying magnetic field induces electrical currents in nearby conductors and additionally exerts forces - Lorentz forces [60]. Kapitza (1924) founded the electromagnetic forming process generating enough magnetic field strengths to deform solid conductors [73]. This principle is represented in Fig.11 and described in the following.

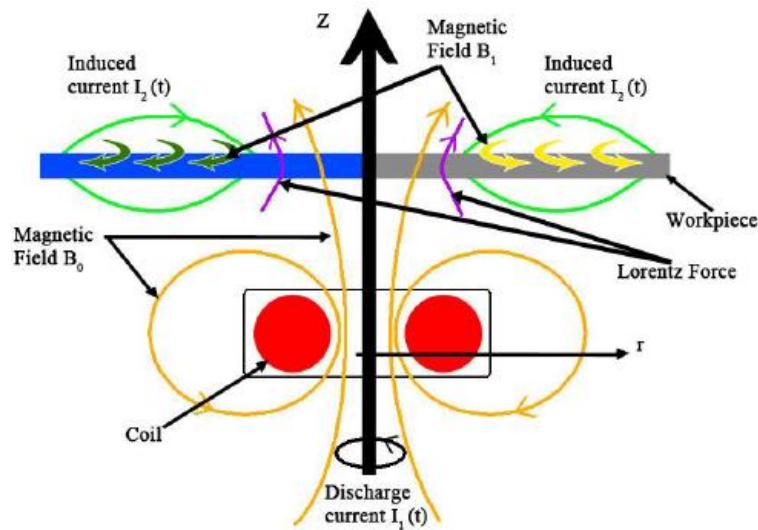


Figure 11: Electromagnetic phenomena representation [19].

The required energy for the process is stored in the capacitor bank (with the total capacitance  $C$ ), charged at an initial voltage  $V_0$ . This stored energy is instantaneously discharged -  $I_1(t)$  - and flows through a coil (which could have different geometries depending on the required shape). As a result of the discharged current, a transient magnetic field  $B_0$  is produced in the coil that penetrates the workpiece which is placed as close as possible to the coil. This transient magnetic field  $B_0$  induces Eddy currents in the workpiece responsible for limiting the penetration of the magnetic field  $B_0$  into the workpiece and for creating its own magnetic field in an opposite direction -  $B_1$  - which interacts with  $B_0$  producing body forces on the workpiece - the so called Lorentz forces. Then, this body force - Lorentz force- acts like a forming force causing the dynamic deformation of the workpiece if the magnetic pressure is higher than the yield strength of the workpiece [19, 26, 73].

As mentioned above, the MPW process makes use of the electromagnetic pulsed technology in order to join the flyer and the target plate. The welding tool consists of an electrically insulated coil which is connected to a capacitor bank pulse power supply, known as EMPT machine. The capacitor discharge accelerates the flyer electromagnetically within few microseconds. At the same time, this welding tool - coil - is placed close to the workpiece or flyer [33]. Within this high velocity forming process, pulsed magnetic fields are used to form metals with an high electrical conductivity [73]. The entire system may be approximated by a simple series RLC (resistance-

inductance-capacitance). Thus, the forming machine is represented by a serial circuit consisting of a capacitor  $C$ , an inductance  $L_i$  as well as a resistor  $R_i$ . The tool coil can be represented by its resistance  $R_{coil}$  and its inductance  $L_{coil}$ , both connected in series to the pulse power generator, as represented by the Fig.12 [33].

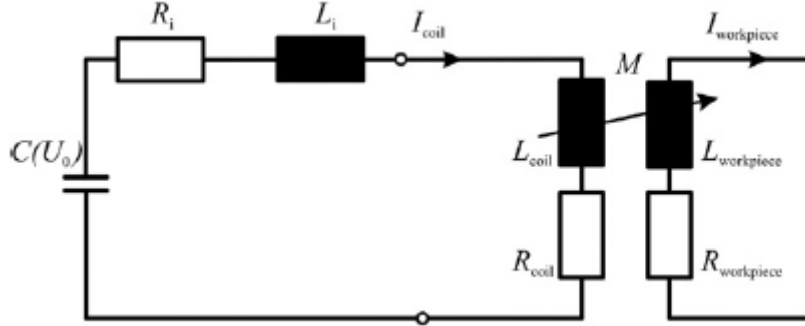


Figure 12: Equivalent circuit diagrams (adapted from [73]).

The intensity of the current can be determined through Eq.7:

$$I = I_0 e^{-\frac{t}{\tau}} \quad (7)$$

Where,  $I_0$  is the maximum current intensity, the current frequency and the damping factor, which characterizes the exponential decay of the discharge current, which are computed by:

$$I_0 = v_0 \sqrt{\frac{C}{L_t}} \quad (8)$$

$$\tau = \frac{2L_t}{R_t} \quad (9)$$

$$\omega_0 = \frac{1}{\sqrt{L_t C}} \quad (10)$$

Where,  $V_0$  is the voltage applied to the circuit,  $C$  and  $L_t$  are the capacitance of the capacitor bank and the total inductance of the circuit, respectively, while  $R_t$  is the total resistance of the circuit. As mentioned above, the magnetic field will penetrate the workpiece and this penetration should be limited. Otherwise, the magnetic field would penetrate so depth and would not repel the opposite magnetic field. Thus, the skin-depth (Eq.11), which represents the penetration of current in the workpiece, is an important parameter to consider and can be calculated by the relation:

$$\delta = \sqrt{\frac{2\rho}{\mu_0 \omega}} \quad (11)$$

$$\rho = \frac{1}{\sigma} \quad (12)$$

Where,  $\rho$  is the resistivity of the workpiece [88, 73, 19]. The resistivity of the material can be calculated through the Eq.12, it is inversely proportional to the conductivity of the material. Due to the skin-depth dependence of the resistivity, the metal of this component should be wisely chosen; it should have enough resistivity to assure that the magnetic field will repel the opposite one. In the Tab.3 it is possible to compare values of conductivity and resistivity for different

materials. Through this table and analyzing the Eq.11 it is explainable why EMPT is suitable for good electrical conductors as aluminum and copper and not for steel, because of the high skin depth penetration that steel will allow to the magnetic field.

Material	Resistivity [ohm . m]	Conductivity [S/m]
Copper	$1.68 \times 10^{-8}$	$59,6 \times 10^7$
Aluminium	$2,82 \times 10^{-8}$	$3,5 \times 10^7$
Steel		$7 \times 10^7$

Table 3:Electrical resistivity and conductivity at 20 °C

As already explained, two opposite direction of flowing current create a large magnitude magnetic repulsion force between the coil and the metal object (workpiece) and if the force of this repulsion is sufficient to stress the workpiece of metal beyond its yield strength a permanent deformation occurs [26]. Then, hollow profiles can be compressed or expanded as well as 2D or 3D sheet metal can be shaped, joined or cut. Different setups and geometries of coils are required for electromagnetic compression, expansion of tubes and for the setup of electromagnetic sheet metal forming, as represented in the Fig.13. In tube compression processes the setup is frequently complemented by a fieldshaper, which is positioned between the tool coil and workpiece [73]. The fieldshaper (see Fig.14) is a component made of an electrically high conductive material [26].

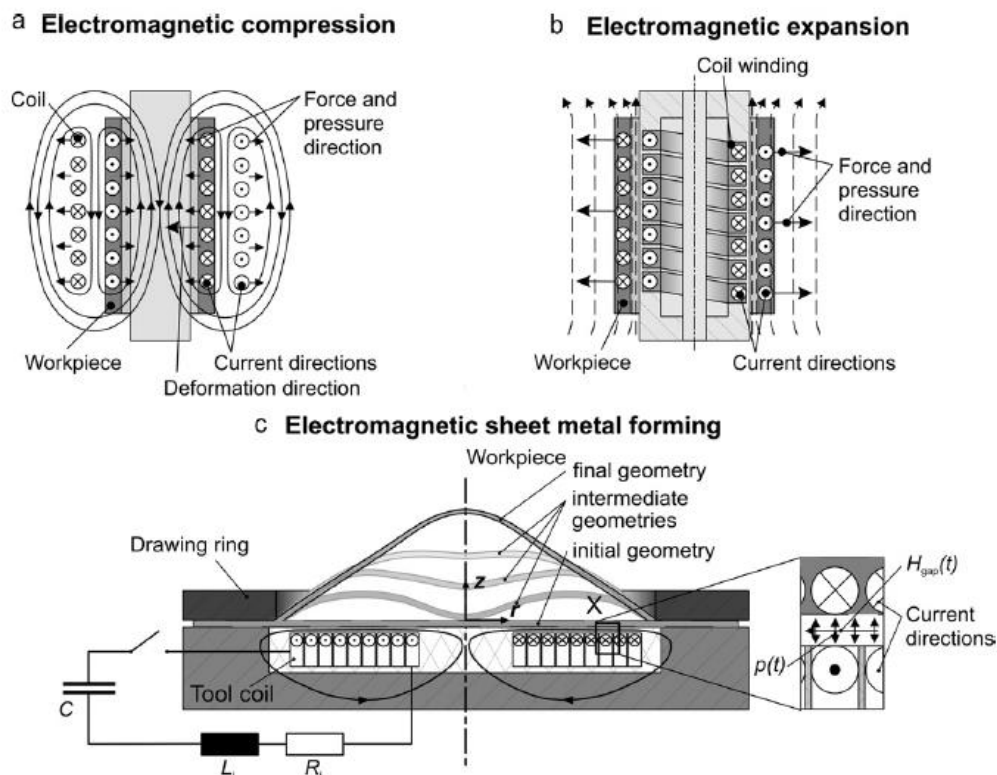


Figure 13: Directions of the current, the magnetic field lines and the pressure during a) electromagnetic compression b) electromagnetic expansion c) electromagnetic sheet metal forming [73].

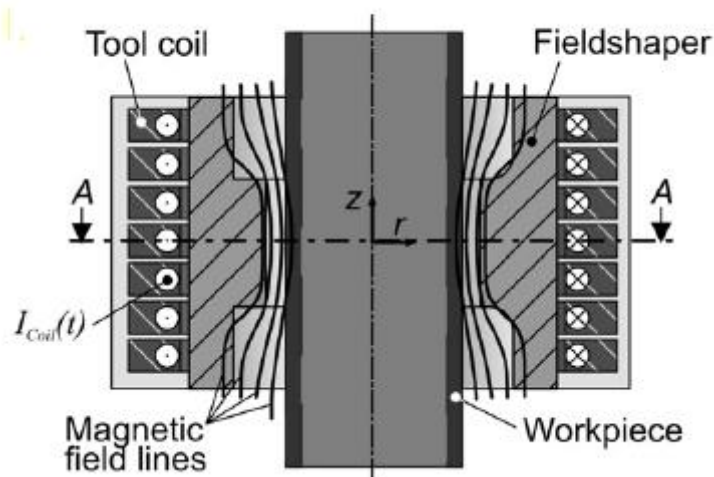


Figure 14: Sketch of the magnetic field distribution for a fieldshaper (adapted from [73]).

In EMPT the workpiece is deformed at high strain rate in comparison to conventional processes [26]. As mentioned above, due to these three different processes variants, different types of coils can be used (see Fig.13). The coil is responsible to convert the electrical current discharge into electromagnetic forming pressure. The coil itself shall be made of a highly conductive material, usually its made by copper or aluminum alloy and can be a single-turn or multi-turn coil. During the process of tube expansion the coil is placed inside the workpiece (tube) and the final shape of the tube is defined by the die surrounding the tube. Related to the compression process the coil surrounds the tubular workpiece which generates compressive loads on the tube walls. For the sheet metal forming the die shape determines the final shape of the metal sheet [26, 73]. It is important that the electromagnetic pressure distribution from the discharge coils is appropriate for the part desired to form. A very common problem usually found during the designing of an efficient coil is the non-uniform distribution of pressure, specially a significant drop in pressure in the area close to the centre of the coil for flat pancake coils. Uniform pressures is developed if the current in the coil and sheet are both uniform and the gap between them is constant [88]. In case of forming, the energy required is the amount enough for accelerate the metal against the die. However, in case of welding, instead of a pattern the flyer plate will reach the target plate and should reach it with the enough velocity and angle to create a jet which will clean both of the surfaces and create an atomic bond. Thus, the pressure used is what differentiate welding from forming noting that a less amount of energy is required in case of forming [26].

This process is not limited to electrically conductive material. A comparison between electromagnetic forming through an elastic medium and direct electromagnetic forming is possible to find in Livshitz et. al. (2004).

The acting loads responsible for deforming the metal through an electrical discharge, depend on many different parameters which can be classified as machine parameters: as the capacity, the inner inductance, inner resistance, the ringing frequency and the charging energy; the tool parameters as the geometry, the inductance, the material of the coil, the fieldshaper properties

---

and the die/mandrel and workpiece parameters: as the geometry, the material, the electrical conductivity and the mechanical properties [73].

### 2.3 Advantages and disadvantages of EMPT

The electromagnetic pulse technology has several advantages when compared to conventional, quasistatic processes. It is possible to summarize them as follows [73, 26, 33]:

1. The risk of impureness or imprint occurrence is reduced due to the contact-free force application between the tool coil and the workpiece.
2. Because no lubricants are used in this process it is considered as an environmental friendly [73];
3. The jet formation explained above works as a clean agent of the surface. Thus, according to some authors, there is no need of cleaning the workpiece surface what consists in a simplified workpiece processing; However, this is will be studied during this thesis.
4. Once the charging energy and the voltage is adjusted once a high repeatability could be achieved. Forming energy can be dosed precisely up to 1% what means a very accurate estimation could be done [71].
5. The possibility of joining very dissimilar materials is a very important finding for several industries as the automotive industry. Combinations of metal and glass, polymers, composites and different metals are possible due to this technology and very interesting combination of high mechanical properties with lightweight could be achieved.
6. The economic cost of the process is relatively low when compared to conventional processes because EMPT only uses one form defining tool, what makes this process very attractive [72].
7. Springback effect is reduced in comparison to conventional quasistatic forming operations, what simplifies the die design significantly.
8. High production rates could be achieved, especially if the process is automatized and mechanized could reach an output of 3600 operations per hour or even more.
9. Due to the fact that magnetic forces penetrate low conductive materials like glass, ceramics and polymers, applications within a vacuum, an inert gas atmosphere or under clean room conditions are possible. [72]
10. The workpiece exhibits a high velocity (about 150 m/s) and high strain rates in the range of  $10^4 \text{ s}^{-1}$ , thus the mechanical properties of the workpiece material can be improved compared to quasistatic ones. As proved in several research studies, the forming behavior of some materials can significantly differ from the quasistatic forming behavior if high forming velocities are applied as the ductility of specimens loaded in dynamic tensile tests is higher than in the case of quasistatic experiments [73].
11. The same coil may be used to form workpieces of different configurations which offers a high technological flexibility of the process.

Nevertheless, there are as well some disadvantages which are important to refer in order to better understand and reduce the side effects as much as possible:

1. The main limitation for the process is the mechanical and the thermal loading of the tool coil. Up to now efforts have been made to build coils which can withstand this load long-term. A promising concept of a durable flat coil is presented in [30];
2. The process is most suitable for materials with a high electrical conductivity and low flow stress. Authors specified that the maximum specific resistance should not be lower than 15

$\mu\Omega\text{cm}$ , which corresponds to a specific electrical conductivity of about 6.7 MS/m [73]. However, much recent studies say that lower conductive materials can be formed successfully if the electromagnetic pulse machine has a high discharge frequency (60-100 Hz) or a so-called driver foil is used. This foil could be done by aluminum or copper because of the high conductivity of both of these materials [73];

3. The efficiency of the technology is relatively low because only a small part of the charging energy is used for the plastic deformation, the ratio of deformation energy and capacitor charging energy is not higher than 20% [73];
4. Significant requirements regarding safety aspects are necessary, because high currents and high voltages resulting in strong magnetic fields can occur [72];
5. Is difficult to realize a deep drawing state by electromagnetic forming. In order to reach this strain state it is necessary to form the workpiece by various coils which must fit to the shape of the workpiece [73];

Some companies use MPW to produce space frame structures made of aluminum or steel contributing for the lightweight of final assembly, maintaining the strength of the steel at the joints (see Fig.15). Some examples of applications are in the Aerospace industry, as for components of fuel pumps, tubular space frames. For the automotive industry is possible to use this technology to produce space frames drive shafts, fuel filters and for tubular seat components [45].

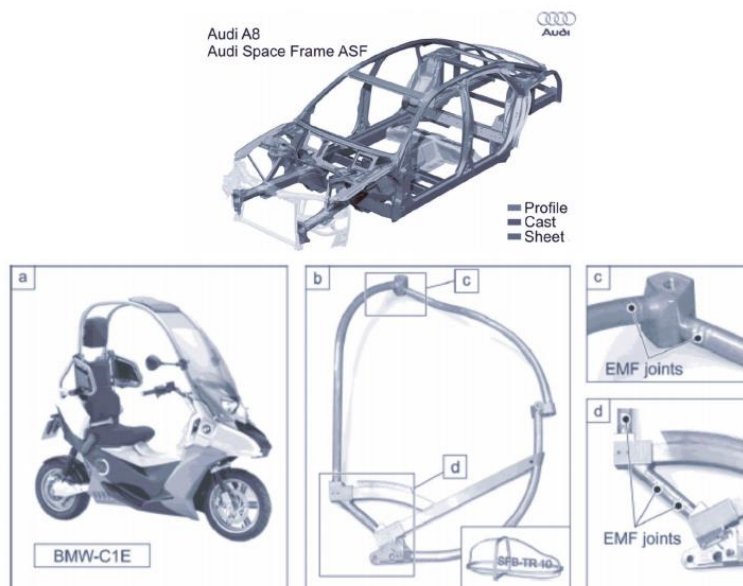


Figure 15: Examples of MPW applications a) Audi space frame structure; b) Structure of BMW-C1E [61].

## 2.4 Magnetic Pulse Welding Equipment

The equipment applied in the electromagnetic pulse technology strongly influences the process and the achievable results, as it is for the conventional welding processes as well [73]. For this technology there are some essential components as the welding machine which is the pulsed power generator - capacitor bank - and the tool coil (including a fieldshaper if the process is about a compression). However, despite of the importance of the geometry and mechanical properties of the components in case of electromagnetic welding also the electrical parameters play a very important role and need to be adapted and planned for the forming task. The Fig.16 illustrates the schematic view of the circuit for electromagnetic pulse technology, as it is possible to describe, the systems is equipped with a pulsed power generator (capacitor bank), a conductive coil and the workpiece to be deformed.

### 2.4.1 Capacitor Bank

High electrical energies are required in a very short time. Thus, is necessary to store enough energy to induce the required strong magnetic field. Several theories and solutions were thought and the most economic and effective solution achieved was the capacitor storage. Therefore, a capacitor bank is used in modern pulse power generators and should exhibit a low self-inductance and should stand a high number of pulse discharges. Furthermore, it should be minimum weight and dimensions as possible for economic and ergonomic reasons.

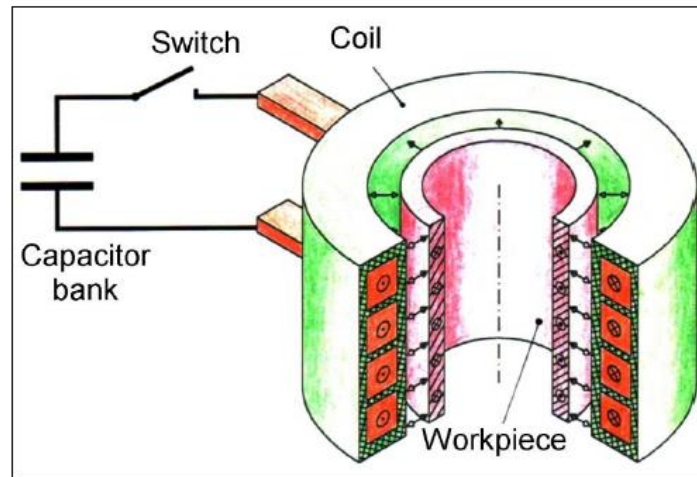


Figure 16: Schematic view of electromagnetic sheet metal forming process and his components [7]

The two characteristics parameters of the capacitor are its capacitance  $C$  and the maximum allowable charging voltage,  $U_{max}$ , which together determine the maximum allowable capacitor charging energy  $E_c max$ . The stored charging energy of a capacitor bank could be calculated according to the Eq.13:

$$E_c(t) = \frac{1}{2}CU(t)^2 \quad (13)$$

Where  $C$  is the capacity and  $U(t)$  is the charging voltage. This energy is suddenly discharged as an electrical current  $I(t)$  [73, 26].

The discharged current  $I(t)$  is a highly damped sinusoidal oscillation (see Fig.17) and depends on the electrical properties of the circuit and is related to the corresponding magnetic field, which is concentrated between the workpiece and the tool coil [57, 19].

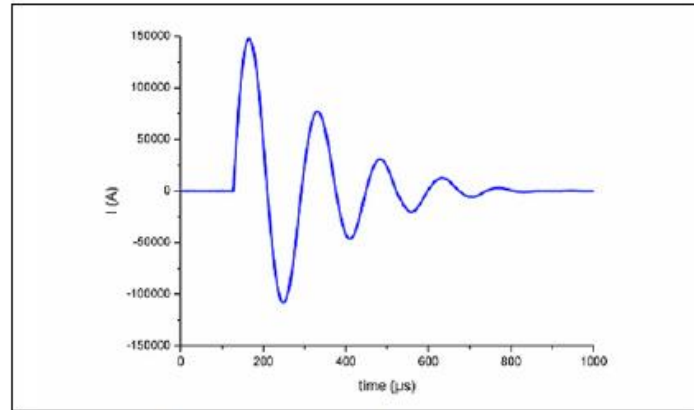


Figure 17: Oscillation of a typical discharging current [81].

#### 2.4.2 Coil

The coil is the actual tool of the EMPT and analogous to conventional forming processes it needs to be adapted to each specific welding task. The major task of the tool coil is conducting the current and consequently establishing a suitable temporary course and local distribution of the magnetic field and pressure [73]. Considering the strength and – related to this – the durability of a tool coil it needs to be considered that according to the third Newton axiom “action = reaction”, the forces required in order to achieve the desired deformation of the workpiece act also as so-called reaction forces on the tool coil in the opposite direction.

Therefore, the coil has to exhibit some characteristics as [53, 26, 73]:

- High conversion coefficient of the capacitor bank energy to the work of the workpiece deformation;
- High mechanical resistance in order to resist to high pressures and high number of charges cycles;
- Guarantee a reliable connection to the machine;
- Have a simple design performance;
- Has to absorb the reaction forces as well as forces between the separate turns of the winding without any deformation;
- Conduct extreme currents at high voltages;
- Should resist to heating since the thermal loading occurs at high cycle times and at high discharge currents, the temperature increases and can cause thermal fracture on components of the coil such as winding, connectors, etc.

The design of the geometry of the coil is as important as its mechanical properties, specially the strength to avoid undesired burst during the work cycle. In case of tube expansion or



compression the cylindrical coils are typically used. As illustrated in the Fig.18, there are four different types of cylindrical coils.

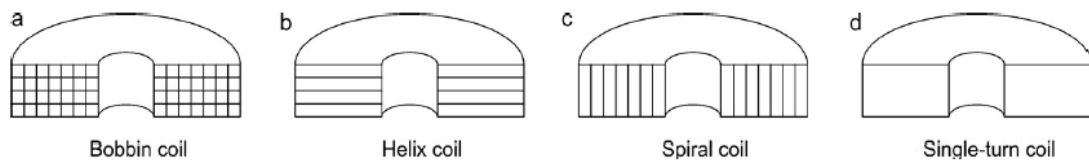


Figure 18: Cylindrical coil types: a) the bobbin; b) the helix; c) the spiral; d) the single-turn coil [73].

The helix coil complemented with the fieldshaper is usually used for tube compression and the single-turn coil is the cylindrical coil used in this work. While for sheet lap joints the most common coils are the spiral coil type, which is often known as pancake-coil (see Fig.19), is typically applied for forming rotationally symmetric sheet metal components [72, 26, 73]. In the specific case of this work, the coil which will be used during the experimental part is the single-turn coil, represented in the Fig.18. Although the scope of geometries for tool coils used in EMPT is much wider (trident coil geometry, ellipsoidal, super-ellipsoidal, so on) it is not worthy to describe all of them due to the specific frame of this work, however it is possible to find detailed information about very different coils geometries in [73].

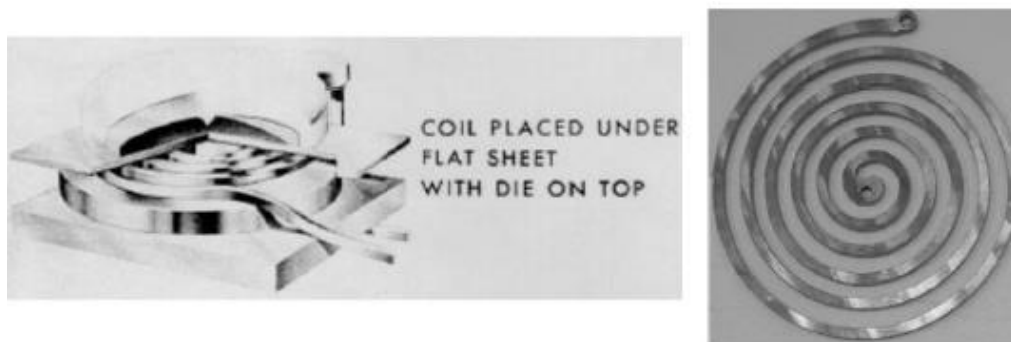


Figure 19: Example of pancake coil [69] and a real flat spiral coil [70].

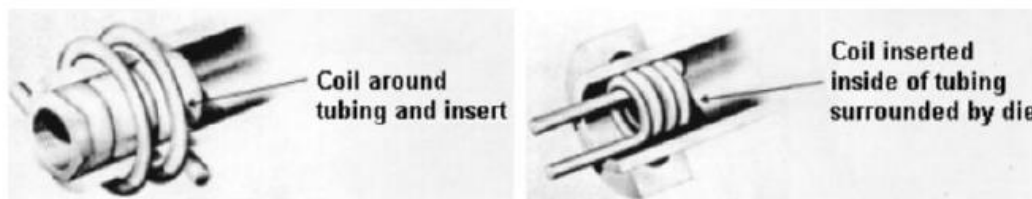


Figure 20: Principle of electromagnetic tube compression with an outer coil (left), and tube expansion with an inner coil (right) [69].

## 2.5 Process Parameters

The quality of the joints obtained by MPW are dependent on the impact velocity and the impact angle ( $\alpha$ ) which are dependent on energy, standoff energy ( $S$ ) and LWZ. In Fig.21, LWZ represents the length of the tube inside the coil and  $S$  the distance between the two plates being welded.

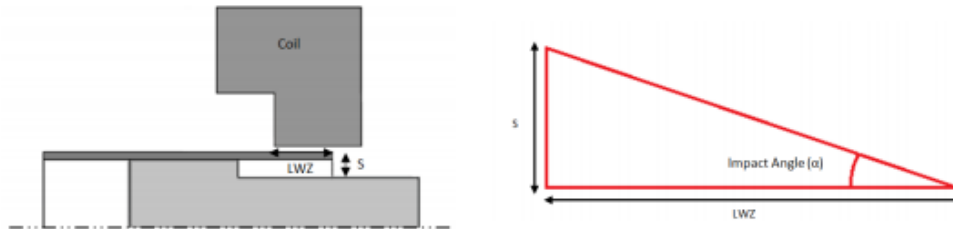


Figure 21: Process parameters on MPW [68].

The process parameters referred above have a strong effect on the weld strength. One very useful tool to analyze the process parameters and its influence in the quality of the weld is the welding window (see Fig.22). Through the Fig.22 is given the explanation of the directly dependence between the collision angle and the speed of impact [68]. The impact velocity is related to pressure and kinetic energy (EEEE) and depends on the material's characteristics and as well on the set up. The velocity should be enough to accelerate the flyer against the target plate and ensure the bonding between the two parts.

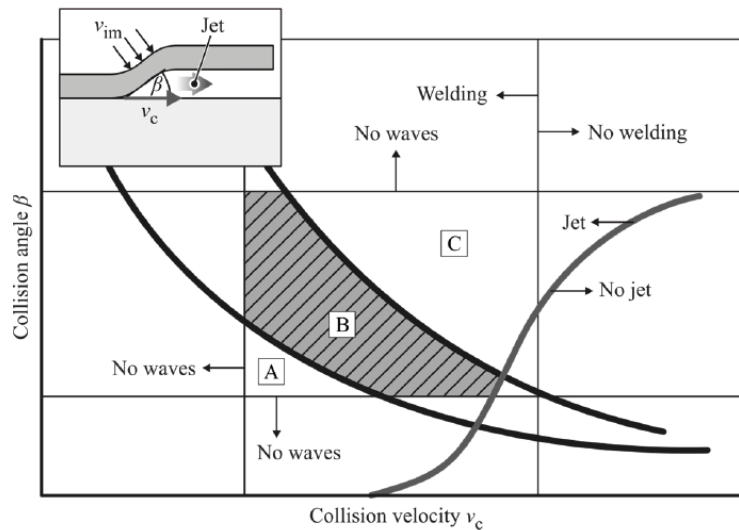


Figure 22: The weldability window [64, 100].

In the Fig.21 it is represented the impact angle, LWZ and  $S$ . The impact angle depends strongly on the geometry of the workpieces. The impact velocity depends on the gap, LWZ, energy and other material characteristics while the impact angle depends on the gap and LWZ. The Fig.22 was adapted from a work related to explosive welding ([54, 55]), however it could be useful to explain the concept of a welding window. Broadly, if the collision angle and the impact velocity are in the range of the weldability zone a jet will be created when the collision between the two surfaces occurs creating thus the bond. The values for each parameter are strongly dependent

on the material's properties, thus it is barely possible to adapt optimum values from one experiment to another. The optimum impact angle is hard to calculate as it varies for each experiment. However, the literature based in several previous experiments says that depending on the application the value of the initial angle should be in the range of 6° to 18° [26]. The shearing stress present in the weld affects its behavior under working conditions. Some studies were carried out in [46] and this value of shearing strength of the lap weld obtained by EM welding could be determined by uni-axial tensile test and calculated using the Eq.14:

$$\sigma_y = \frac{F}{A_l} \quad (14)$$

Where,  $\sigma_y$  is the stress in uniaxial tension; F represents the axial load on tensile test at failure and  $A_l$  is the area of the lap welded joint. The Eq.14 could be defined as Eq.15 as well.

$$\tau = \frac{UTS \times A_0}{A_l} \quad (15)$$

Where,

$$k = \frac{\sigma_y}{\sqrt{3}} \quad (16)$$

Where  $\tau$  is the shear stress,  $A_0$  is the area of the cross-section of the  $A_l$  sheet,  $\sigma_y$  is the stress in uniaxial tension and k is the yield strength under shear:

If  $\tau/k \geq 1$  then sample failed in the weld;

If  $\tau/k \leq 1$  then sample failed in the parent metal;

When the yield strength under shear (k) is greater than the shear stress ( $\tau$ ) the sample fails in the parent metal creating a weld stronger than the parent metal.

In the studied carried out at [46] some of the samples tested for uni-axial tensile test satisfy the condition  $\tau/k \leq 1$  and failed in the parent metal as shown in the Fig.23. This indicates that welds obtained are stronger than the parent metal, which is a desirable result.

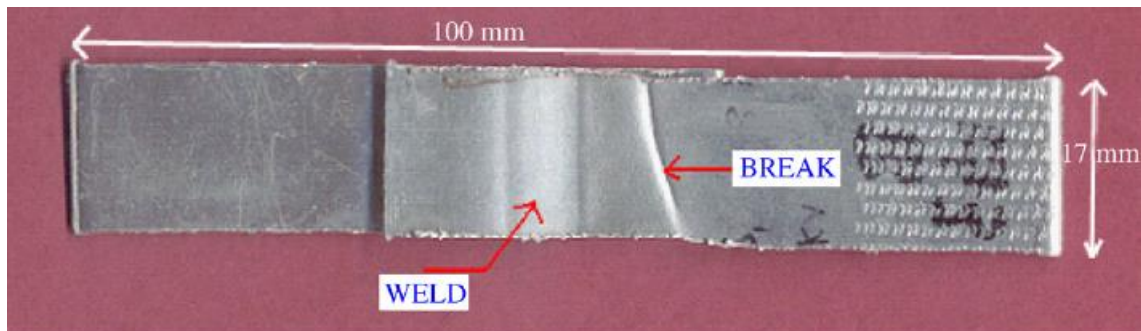


*Figure 23: Specimen for uni-axial tensile test showing break in the parent metal [43].*

The metallographic study of the Al–Al welded samples shows the weld and no-weld zones and it's represented in the Fig.24. Two welded zones and one non-welded zone at the center are clearly seen.

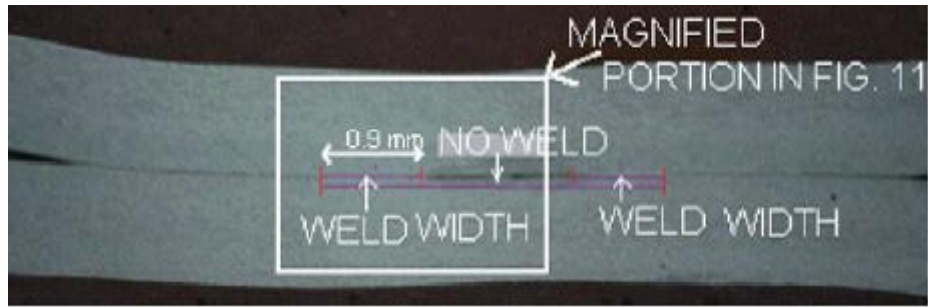


Figure 24: Al to Al electromagnetically welded sample showing weld and no-weld zones [46].

In the Fig. 25 it is possible to see the magnification of the welded zone. The welded zone shows the total metallurgical continuity of the metals. The transition zone between welded and non-welded zone has wavy interface as the physical boundaries of the two sheets are retained.

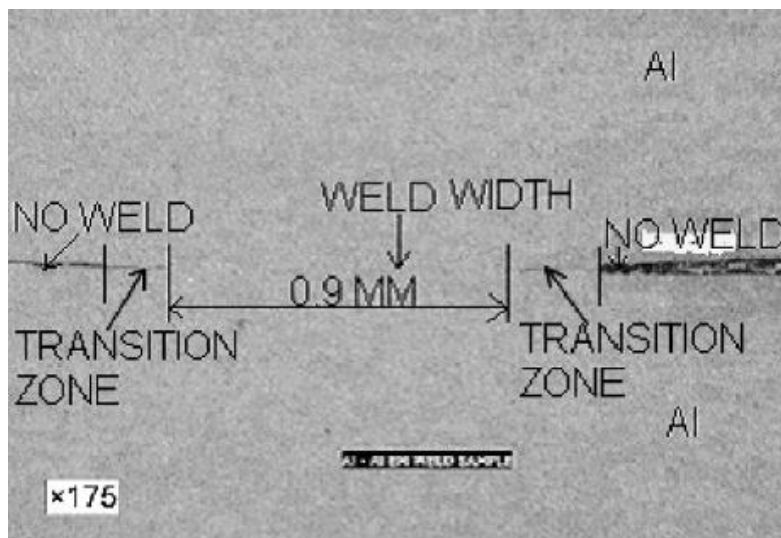
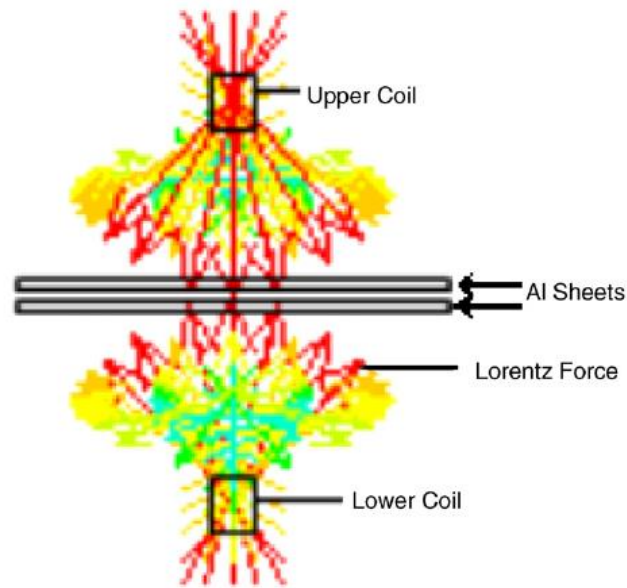


Figure 25: Magnified view of the weld zone indicated in the Fig.24 [46].

Possible reasons for the non-welded zone at the center are:

1. At the time of collision the Lorentz forces acting on the Al sheets are normal to the sheet at the center and it has shear component elsewhere as shown in Fig.26. Al sheets collide with each other at the center and this gives rebound effect leading to non-welded zone at the center. As there is no rebound effect away from the center, the colliding sheets remain in contact with each other leading to welded zones.
2. Entrapment of oxide on the colliding surfaces of the Al sheets at the center because the two sheets are placed parallel to each other, unlike the case where an angular placement of the sheets enables expulsion of the oxides effectively.
3. The other possible reason that may be contributing is complex deformation state at the interface. This need to be further investigated.



*Figure 26: Lorentz forces acting on the sheets at the time of collision. Force in the center is normal to the sheet while it has a shear component elsewhere [46].*

Is possible to determine the weld width by using the Eq.17:

$$\%Weld_{width} = \frac{Width_{total}}{Width_{section}} \times 100 \quad (17)$$

Where,  $Width_{total}$  is the total width of the weld and  $Width_{section}$  is the width of the web cross section of the coil. Increase in discharge energy for welding increases the magnetic field generated, and thus increases the shearing strength and the width of the weld for a given standoff distance [46, 48].

The coil geometry also plays a very important rule as in the study [46] two coils were applied, on rectangular and one tapered. The conclusion says that the reduction in the cross-section area of the coil (e.g. tapered coil) increases the current density leading to an increase in the shearing strength of the weld.

## 2.6 Effect of the energy on the weld strength and width

As described before, MPW is closely analogous to explosive welding. However, rather than explosives, it uses electromagnetic force to accelerate the flyer plate. Therefore, MPW can be safely reproduced to use in production environments controlled by an electric power supply and the fine adjustment to parameters [107]. The energy level of an experiment is set through the charging voltage level of the capacitor bank [54]. Stored energy in the capacitor bank is discharged into the coil and this energy is responsible for the movement of the flyer metal. Thus, it is essential to ensure that the voltage imposed to the capacitor bank is enough to perform the weld. Discharge energy takes place in a very short time in the range of a few microseconds in order to accelerate the flyer metal against the other part at high velocity [61, 43]. As mentioned above, this energy depends mainly on the material properties and dimensions of the flyer. In order to avoid efficiency losses as much as possible, it is important to guarantee low penetration of the magnetic field into workpiece. This magnetic field penetration is measured through the skin-depth, mentioned above.

In [46] the shearing strength and the width of the weld were found to increase with an increase in discharge energy. In [46] two different coils were studied in order to establish a reasonable relation between the influence of the coil on the discharge energy, thus two coils were used, flat rectangular coil and tapered coil, respectively (Fig.27). Fig.28 shows the dependency of the shearing strength on the energy for flat rectangular coil. Increase in energy enhanced the shearing strength of the welds for both coils.

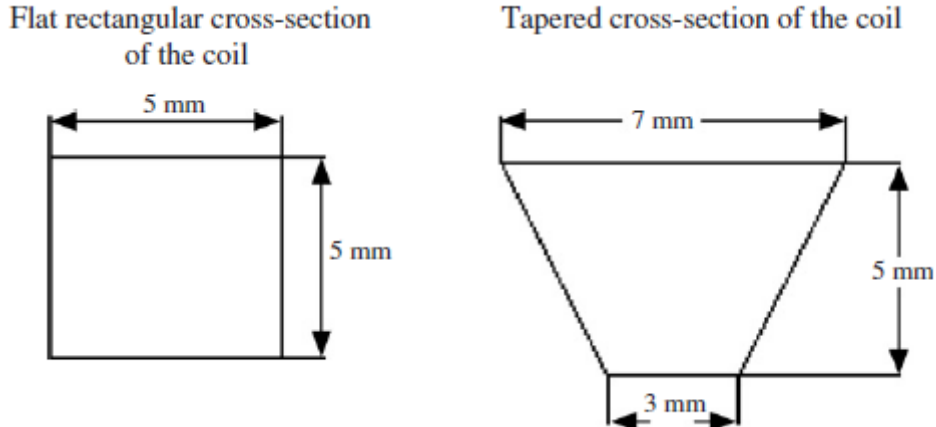


Figure 27: Cross sections of the coils [46].

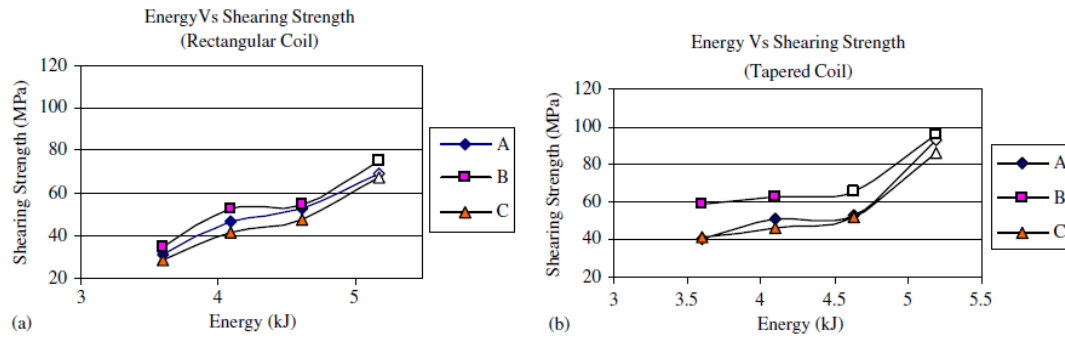


Figure 28: (a) Rectangular coil: effect of energy on the shear strength of the weld, with standoff distance = 2.5 mm, (b) tapered coil: effect of energy on the shear strength of the weld with standoff distance  $\frac{1}{4}$  2.5 mm [46].

The increase in energy for the welding has enhanced the shearing strength of the welds in both cases, enhancing the quality of welding.

When the two sheets collide with each other the kinetic energy gets transformed into impact energy and due to jetting and the expulsion of oxides the weld takes place.

The increase in energy also increases the width weld. For the same joining materials, a continuous weld is possible to find for higher levels of energy while the discontinuous weld appear for lower discharge energy values. This occurs because at the lower values of energy the velocity of impact is not enough to create a continuous weld and the discontinuous weld is characterized by a discontinuous wavy interface [46, 104]. A relation between sheet's thickness and discharge energy is possible to establish, meaning that less thickness sheets need less discharge energy to weld [87, 66, 103].

## 2.7 Effect of standoff distance on the weld strength and width

The standoff distance is basically the distance between parts prior to the discharge and the main aim of having this gap (Fig.29) in every welding processes is to accelerate the plate to the impact velocity [46, 84]. During this gap, the metal flyer gains velocity – impact velocity - and acquire kinetic energy which is going to be transformed into impact energy [61]. Thus, the standoff distance, or gap, should be high enough so that the outer workpiece will have the time to accelerate due to the electromagnetic impulse up to the desired velocity [54]. This value of standoff distance has an optimum value which varies according to the welding materials. Aluminum sheets kept at some standoff distance get accelerated due to the electromagnetic impulse. At some optimum value of standoff distance the sheets achieve a maximum velocity and acquire the corresponding high kinetic energy [46]. This optimum value strongly depends on the set-up and as well on the material properties. For the lower values of standoff distance, collision takes place before sheets attain the maximum velocity, whereas, for higher values the velocity attained drops to a lower value at the time of collision. Meaning that when the gap is too small, it is necessary to increase the pressure on the flyer, and some cracks may appear in the material [75]. On the other hand, if the standoff distance becomes too high, the velocity might start decreasing again [54]. Therefore, maximum strength of the weld is achieved only at the optimum value of the standoff distance for a given set of other process parameters. The effect of standoff distance on the strength and width of the weld was investigated at constant discharge energy of 5 kJ [46]. In terms of discharge energy, the higher the gap, the higher should

be the discharge energy in order to obtain a good quality weld [61]. Therefore, it is possible to conclude that for a given set of process parameters the standoff distance has one optimum value that gives the maximum shearing strength and width of the weld.

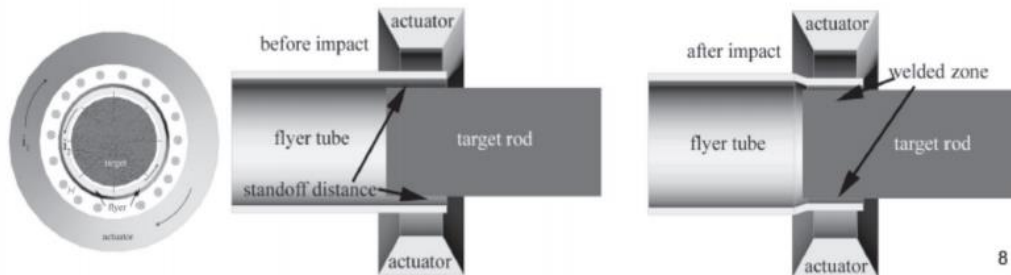


*Figure 29: Schematic of MPW welding process of two tubes before and after welding [61].*

In [54] several experiments were done in order to better understand the influence of the different parameters. The standoff distance is one of the parameters that was varied the most in the experiments. It was found in this experiments that this value have a strong influence in the weld length in the aluminum-aluminum experiments. In this case, welds were successfully achieved for standoff distances of 2.0 mm, 2.5 mm, 3.0 mm and 3.5 mm and the optimal standoff distance for aluminum workpieces with a thickness of the outer tube of 1.5 mm and a voltage level of 15 kV is then in the range 2.5mm-3.0mm . It was found that for higher standoff distance the welding lengths were shorter and for standoff values lower than 2.5 mm the results found were unable to be welded.

In [1] different welding interfaces as straight, wavy and continuous solidified-melted were used with changing explosive welding parameters as standoff distance and explosive loading in order to study the influence of the parameters on the welding quality. Joined metals were investigated under heat-treated and untreated conditions and the bending strength of heat-treated samples was generally higher than for untreated samples. When the explosive loading and standoff distance were increased the bonding interface changed from straight to wavy structure. Whereas for wavy interfaces, when the explosive loading was increased the wavy length and amplitude increased.



## 2.8 Jetting for bonding mechanism

Welding requires two atomically clean surfaces to be pressed together to obtain metallurgical continuity. This continuity in Al-based alloys is interrupted by  $\text{Al}_2\text{O}_3$ , adsorbed gases and surface contamination [61]. However, these are removed during the well-known process of jetting (see Fig.30). The jet formation consists in a thin layer of metal which at high-velocity impact (in the range of the sound velocity) is disintegrated and ejected as a result of the high pressure impact. Thus, the surfaces of two impacting sheets become atomically clean at the time of collision. As the two sheets come together leading to atomically clean surfaces coming together the requirement of weld formation is satisfied and a weld is formed at the interface establishing the metallurgical continuity [46, 68]. On the basis of experimental evidence it is generally accepted that the phenomenon of jet formation at the collision point is an essential condition for welding. The jet chemically cleans the mating surfaces by removing films and other contaminants, thereby making it possible for the atoms of the two materials to approach to within inter-atomic distances when subjected to the explosively produced pressure waves. The collision pressure associated with the dissipation of kinetic energy must reach a sufficient level and be maintained for a sufficient length of time at this level to achieve the stable inter-atomic bonds. In this case, the impact velocity determines the pressure, whereas the velocity at the collision point governs the time available for bonding [63].

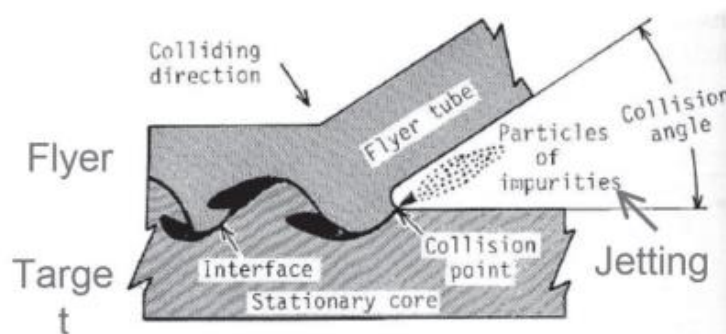


Figure 30: Scheme of impurity removal, Jetting [61].

The impact velocity is influenced by the energy and the standoff distance. The impact velocity usually is about 1500-3000 m/s and the collision of the metals creates the jet consisting of a mixture of metal, air and oxides, ejected from the surfaces of both metals [10]. From the Fig.31 it is possible to conclude that velocity and discharged energy vary accordingly [61]. At the impact point, the shock waves travel in both metals with a radial front, and an angle depicted in Fig.30.

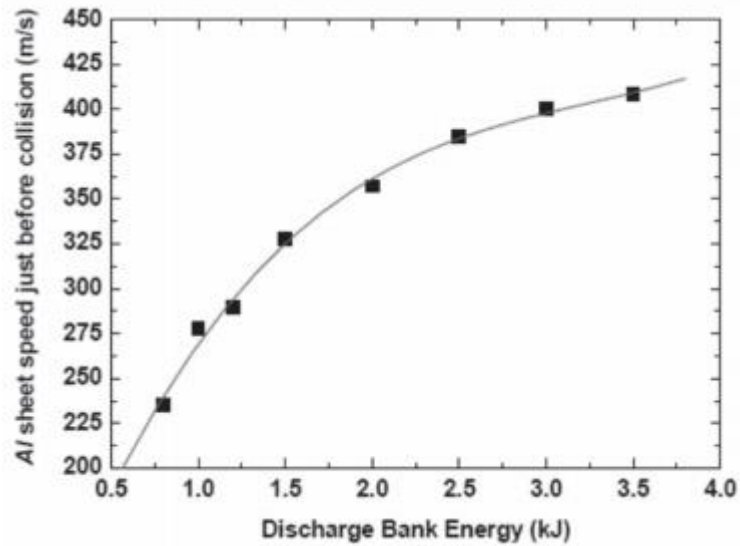


Figure 31: Aluminum (flyer metal) velocity just before collision [61].

It has been noted that most of the jetting material, as known as back flow material, comes from the flyer part. The thickness of this removed layer is generally less than 0.05 mm. Due to its thickness which is greater than the height of microroughness on the base material, the way of jet can severely deform the microroughness and damage the inert surface layer removing undesired material [54]. Due to the high speed verified, nearby 50% of the kinetic energy of the flyer plate can be concentrated in this jet flow, which reaches values of speed 30-50% bigger than the impact velocity. The strength of the material is also lowered by the jet due to the increased of the temperature induced [54].

## 2.9 Summary

MPW is one of the most useful welding processes of the dissimilar metal joining which uses cylindrical materials such as pipe or a tube. The quality of joint is decided by several process parameters in magnetic pulse welding, so it is really difficult to control quality of the products. In [84] a mathematical model was developed in order to investigate the effect of process parameters for the setup represented in Fig.32.

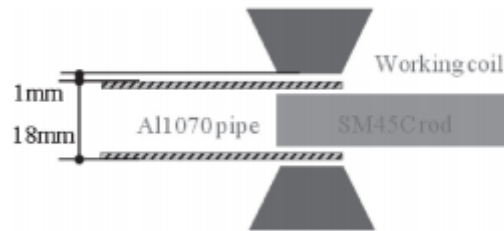


Figure 32: Experimental setup of MPW process [84].

It was found that the process parameters could be approached as a quadratic polynomial model including three squared terms, three interaction terms, three linear terms and one intercept term as shown in Eq.18. MPW uses electromagnetic collision energy from high current discharged through working coil which develops collision energy in outer pipe to be welded. Simultaneously, the gap between inner rod and outer pipe and the thickness of outer pipe take the role of accelerating the speed of collision. Therefore the factors in this experiment were the charged voltage ( $X_1$ ), the gap between inner rod and outer pipe ( $X_2$ ) and thickness of outer pipe ( $X_3$ ) [84].

$$Y = b_0 + b_1X_1 + b_2X_2 + b_3X_3 + b_{11}X_1^2 + b_{22}X_2^2 + b_{33}X_3^2 + b_{12}X_1X_2 + b_{13}X_1X_3 + b_{23}X_2X_3 \quad (18)$$

Where, Y is the response burst pressure,  $b_0$  is the average of the results of the replicated center point,  $b_1$ ,  $b_2$  and  $b_3$  are the main half-effects of the coded variables  $X_1$ ,  $X_2$  and  $X_3$  respectively.  $b_{12}$ ,  $b_{13}$  and  $b_{23}$  are two factor interaction half-effects. After developing the mathematical model the plot of main effect was checked and plotted in Fig.33 where V, G, T refer to the charged voltage, the gap between outer and inner pipe and the thickness of outer pipe, respectively.

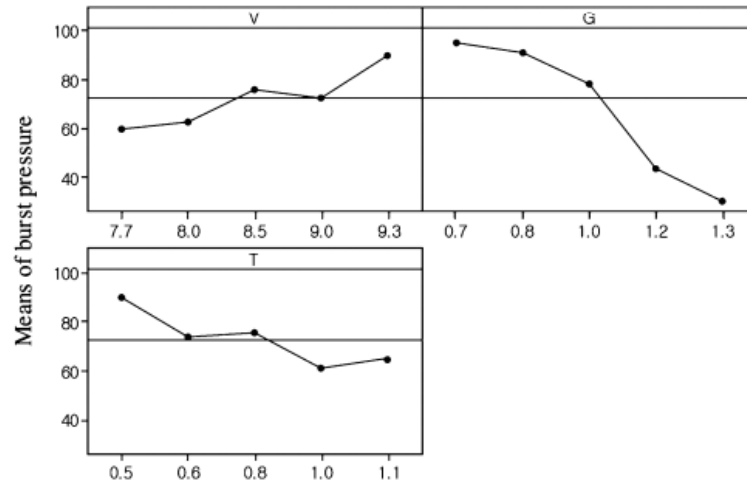


Figure 33: Main effects plot for burst pressure [84].

After developing the mathematical model in order to investigate the effect of process parameters, the plot of main effect was checked and plotted and the following conclusions can be withdrawn:

- As the level of gap between inner and outer pipe has been increased, burst pressure has been decreased sharply;
- While the charge voltage and thickness have been increased the burst pressure has been varied slightly;
- As a result it is found that the gap between inner and outer pipe is the most effective factor on the quality of joint.

# 3 HIGH VELOCITY IMPACT WELDING

---

## 3.1 Theoretical background

New cold welding methods like impact welding provide crucial alternatives for welding highly dissimilar metal combinations as Aluminum with Copper. The use of pulsed magnetic fields to generate the impact by Lorentz forces action makes the MWP a fast, clean, reliable and cost-efficient process [77]. Several studies agree that a wavy interface indicates a good bonding. In [76] multi scale characterizations of an Al/Al joint have shown a strengthening of the weld with an increased wave. However, for dissimilar pairs there are some doubts that a wavy interface guarantees a good bonding [77, 78]. In [39], it was shown that both, straight or wavy shaped Cu/Ti joint, have a quite similar mechanical bonding resistance. In MPW process, influence of the dissimilar metal combination on the weld formation should be widely analyzed since the joint features strongly depend on it. In [74] welding of Al/Cu instead of Al/Al shown that introducing copper instead of aluminum strongly decreased the welding range due to appearance of an intermetallic phase which damage the surface at high impact energies. This is because when welding dissimilar materials an intermetallic phase with defects such as voids and cracks could occur [28, 77].

In [77], aluminum Al6060 T6 is used for the Al/Al joint and as flyer for the Al/Cu pair with a pure copper inner part. Properties of both materials are presented in Tab.4 and Tab.5. Aluminum is a lightweight material and has a wide of applications in automobile and aerospace industries although formability and weldability still remain major issues for aluminum [8]. Special surface preparation is not necessary for carrying out the electromagnetic impact welding of Al sheets, since the surface oxides are removed during the phase of jet formation that precedes the phase of bond formation [46]. Both of these materials have comparable mechanical properties but very different thermo-physical properties [77]. This joint allows combining high thermal conductivity with highly dissimilar mechanical properties.

	Mg	Si	Fe	Mn	Cr	Zn	Ti	Cu	Al
Al6060T6	0.8-1.2	0.4-0.8	0.7	0.15	0.04-0.35	0.25	0.15	0.15-0.4	Balance
Cu	-	-	-	-	-	-	-	99.9	-

Table 4: Standard chemical composition of the Al6060T6 and Cu specimen [77]

	Tf (°C)	$\lambda$ (W/mK)	$\rho$ (kg/m <sup>3</sup> )	E (GPa)	G (GPa)	Ar (%)	Hv
Al6060T6	650	209	$2.7 \times 10^3$	70	26	10	80
Cu	1065	401	$8.9 \times 10^3$	124	46	14	80

Table 5: Some physical properties of Al6060T6 and Cu (adapted from [77])

### 3.2 Intermetallic phase formation

Intermetallic compounds are found in the dissimilar materials MPW joints [11]. The MPW joint mechanical properties are largely dependent on the microstructure evolution, the welding defects, base metal composition, and metallurgical states [10]. The metallographic observations reveal the occurrence of an intermetallic layer at the interface of the Al/Cu weld (see Fig.34). This intermetallic phase is non-uniform along the weld due to the heterogeneity of the collision at the interface [77]. The intermetallic phase is a compound of aluminum and copper mainly ( $Al_xCu_y$ ) and the thickening of the intermetallic leads to a randomness geometry including discontinuity amorphous phase which could be nanograins, randomly unstructured crystals or both [77]. The occurrence of melting at the interface Al/Cu magnetic pulse joints, welded with different energies were evidenced in [7] because as proven in [23], the impact temperature far exceeds the melting temperature of aluminum and copper, thus the impact heating enables to melt the Al/Cu interface. In this interface of an intermetallic component, cracks may occur and grow in multiple directions inside the thick layers. These defects result from a solidification cracking due to both strong thermal gradient and solidification shrinkage at the interface. Tensile stresses are then developed during the solidification and may exceed the strength of the solidified phase depending on the severity of the thermal gradient and the shrinkage, leading thereby to the appearance fractures. It is difficult to identify the preferred direction propagation due to the non-uniformity of the interface behavior during the collision which leads to a random crack propagation [77]. The porosity (see Fig.36) within the intermetallic zone is another defect responsible for the direction of crack propagation (see Fig.35). The most plausible source of pores formation is the phenomenon of cavitation. At the beginning of the solidification a drop of the temperature occur and there are germination of bubbles and then a coalescence with the increase of tension surface on the inner wall until the mechanical equilibrium is reached. Basically, the cavitation is about a “hole” formation when a liquid phase is subjected to rupture tensions [77, 99, 97].

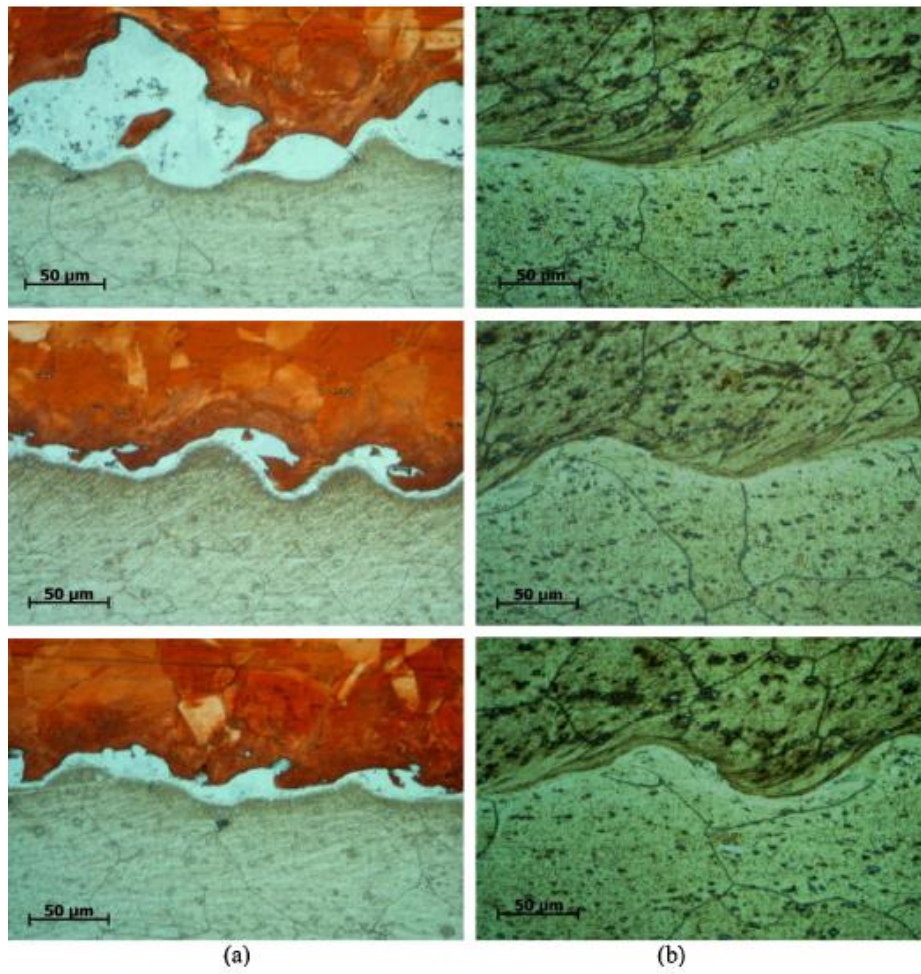


Figure 34: Comparison between Al/Cu weld (a) and Al/Al weld (b) for an interface shape from straight to wavy – Al–Cu intermetallic occurrence independently of the interface shape [77].

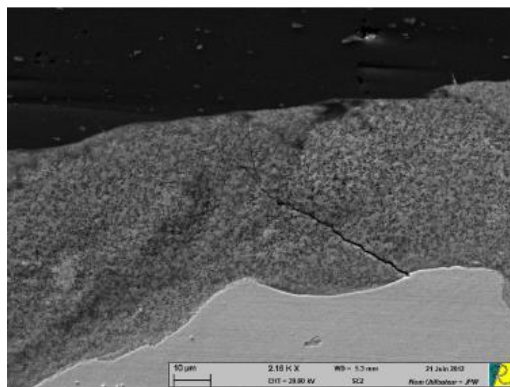
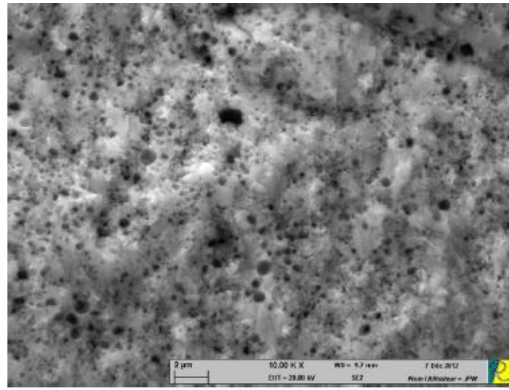
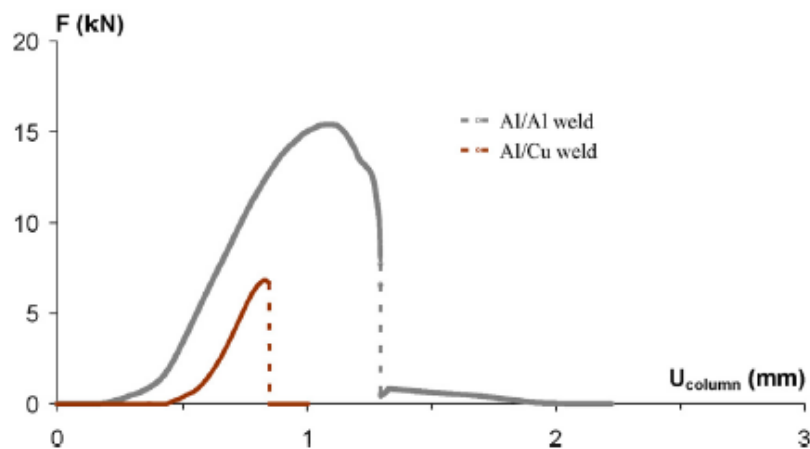


Figure 35: Typical porous structured intermetallic, and cracking driven by pores interactions [77].



*Figure 36: Typical fracture surface of the intermetallic observed at the pores scale [77].*

The occurrence of intermetallic phase, cracks and pores could influence the weld performance and the mechanical properties of the intermetallic generated will determine the behavior of the joint. In [77], the intermetallic is classified as a bulk metallic glass known to be a brittle material. In Fig.37 a comparison between the joint mechanical behavior of Al/Al and Al/Cu is represented. Analyzing the fracture surfaces from the torsion-shear tests it is possible to compare both welds. For the joint Al/Al it undergoes plastic deformation and ductile damage before the moment of rupture while the Al/Cu joint breaks immediately soon the yield strength is reached. Also, because of the detrimental defects explained above related to the intermetallic phase and porosity, the force level is very low and enough to drive the dissimilar joint to the rupture [77].



*Figure 37: Influence of the intermetallic on the mechanical behavior of the weld [77].*

The joint Al/Cu does not have the plastic deformation prior to the rupture and this fact is proved when analyzing the fracture surfaces it is found that the Al/Cu interface is debonded without any trace of residue as opposed to the Al/Al weld which shows a residue on the inner part (see Fig.38).



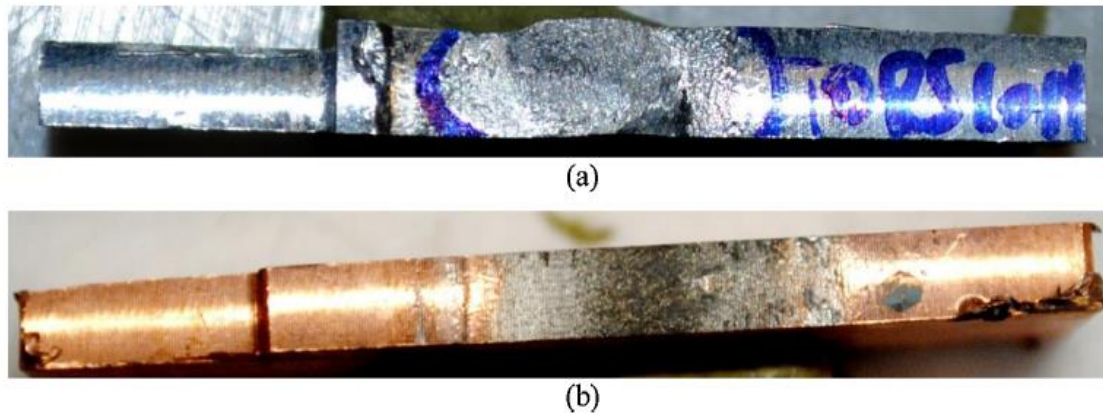


*Figure 38: Macroscopic observation of the fracture surface given by the torsion shearing test: (a) Al/Al interface and (b) Al/Cu interface [77].*

When subjected to collision by magnetic pulse Lorenz force, the interface of dissimilar metal pairs suffers several phenomena that downgrade the joint features. Basically, the comparison of two different joints, one composed of two dissimilar materials and another one with similar materials, Al/Cu and Al/Al, respectively, allows the drawing of some conclusions:

- An intermetallic phase was observed at the interface of the Al/Cu weld whereas the Al/Al joint is bonded with a metal continuity;
- The intermetallic phase is found to be an amorphous phase which results from an hypercooling of a molten Al-Cu compound confined at the interface;
- The intermetallic is characterized by a strong porous media with a highly dispersed pore size and a random allocation of the pores;
- The most plausible source of pores formation is the cavitation phenomenon during the melting at the interface;
- Cracks in multiple directions occur inside thick layers due to both shrinkage solidification and propagation governed by rupture tensions and pores interactions;
- The mechanical characterization of the weld behavior using push-out test shows a brittle behavior with a catastrophic rupture of the Al/Cu weld due to intermetallic layer, and a ductile behavior for the Al/Al joint until the total failure;
- Fracture surface of the interface tested by torque shearing force highlights for the Al/Al weld a plastic deformation by a presence some residues, and for the Al/Cu weld a brittle rupture by fragmentation of the intermetallic layer;

For a given discharge energy the shear strength of the welds reached the maximum value at an optimum coil standoff distance, and the geometry of the coil also has important effect on the product strength [102]. On welding Al to Cu, [59] studied the microstructures and temperatures at the aluminum–copper interface, and the results showed the formation of a hard copper rich intermetallic phase with the same composition as the equilibrium  $\gamma - Cu_2Al$ . Further analytical model analyses proved a strong probability of interface melting during the welding process.

### 3.3 Effect of initial surface conditions on the weld joint

In [102] MPW of Cu/Al tube is further studied with the focus on the effect of initial surface conditions (surface topology and contamination) on the joint establishment. The welded interfaces were characterized, and the new phase formation was identified and analyzed, and more important, some direct evidences on interface melting were obtained. Also the mechanisms of MPW and the means of process improvement were discussed. For these experiments a 5-turn-coil was used with a capacitor bank and a high voltage cabinet for charging the capacitors, capable for generating 30 kJ at a charging voltage of 9 kV. The aluminum alloy (AA6063-O) and pure copper (C110) were machined by lathe turning on both inner and outer surfaces over the joint lengths. In order to investigate the influence of the surface in the welding process, three initial different copper surface conditions were prepared:

1. **Surface condition A:** The as-machined tube surface, produced by lathe turning with the finishing surface containing tangential scratches over its length (see Fig.39);
2. **Surface condition B:** After the lathe turning (condition A) additional manual sanding was performed on the Cu outer surfaces with 200-grit coarse sand papers along the axial direction, which replaced the original tangential lathe scratches (see Fig.39 -b) with a new set of axial scratches on the Cu outer surface (see Fig.39 -c), in order to investigate the surface topology effect;
3. **Surface condition C:** After the lather turning (condition A) a silicon-based high-viscosity lubricant oil was applied over the welding zone surfaces, to produce an artificially contaminated interface (exaggerated) before welding, in order to investigate if the high impact force can break down the contamination layer to establish weld;

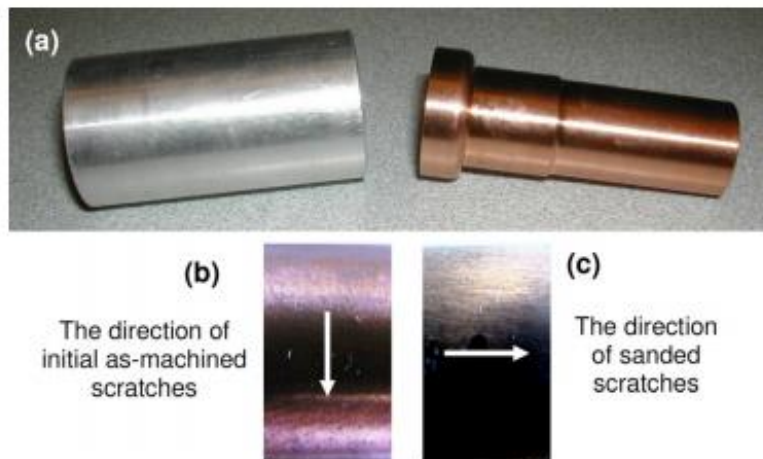


*Figure 39: As-machined Al and Cu tube samples before welding (a) and the produced surface scratches on the Cu tubes in hoop direction (b). The further sanded surface is shown in (c) [102].*

To study the effect of the energy and the power discharged to the coil, three different voltages were applied for charging the battery bank: 4.6 kV, 5.2 kV and 6.0 kV. The quality of welding was evaluated by peeling test and microstructure examination on the sectioned/polished central plane surfaces. The percentage of the welded length over total interface length on the sectioned surface is given in Tab.6.

	<b>Cu surface condition</b>	<b>4.6 kV</b>	<b>5.2 kV</b>	<b>6.0 kV</b>
<b>A</b>	Scratches in hoop direction	welded (55%)	welded (63%)	welded (73%)
<b>B</b>	Scratches in axial direction	N/A	welded (59%)	N/A
<b>C</b>	Oil-contaminated over A	N/A	N/A	welded (10%)

*Table 6: Peeling test results and bonded percentage lengths for different welding conditions. The percentage is the bonded length over the total interface length estimated from micrographs of sectioned surfaces [102].*

As it is possible to conclude with the experimental results presented in Tab.6, Al–Cu tubes have been successfully welded by applying electromagnetic pulse force over Al tube outer surfaces, under different electromagnetic power input levels and surface conditions except for condition C. The comparison of samples with and without oil contamination under the same applied higher voltage (6.0 kV), the contaminated surface did not establish welded interface in the majority contact area, under similar condition or has higher effective strain probably due to the reduced interface friction from oil lubrication allowing the tube to move in axial direction freely. This indicates the oil contaminated surface cannot be easily broken by magnetic pulse pressure, even with significant plastic deformation. This is different from the oxidation layer that can be broken by magnetic pulse force. Therefore, it was found that for a successful welding on magnetic pulse technology a clean surface is required to establish a strong bonding [102]. The microstructure was examined on the polished central plane surfaces in order to evaluate if the Al and Cu are connected without gap or if this gap really exists. It was found that for condition A the percentage welded length increases with voltage, for condition B the welded length is slightly lower than A and even lower for the contaminated surface C.

The processing parameters that affect welding strength include not only the chemical property and compatibility of two joining materials. Besides the power used in the electromagnetic welding, the quality of welding has to do also with the surface topological conditions (the surface roughness, scratch orientations and contamination).

Fig.40 shows SEM micrographs of two welded interface regions, where a transition zone between two base metals can be clearly seen, called intermetallic phase. The results show for the phase a new chemical composition in range of 60-80 % Cu and balanced Al. This mechanical mixing of two metals at the interface which results in an intermetallic phase occurred as the result of severe plastic deformation. Surface topology has important effect on the mechanical mixing and wavy interface formation. The thickness of the intermetallic phase obtained in [102] was in 0-5  $\mu\text{m}$ , depending on the applied energy and the surface conditions. Chemical bonding from intermetallic formation has two opposite effects on bonding strength: it greatly increases the bonding strength but on the other hand it tends to form microcracks under the condition of a high temperature gradient, a high thermal stress, and a large plastic deformation, especially when the intermetallic layer is too thick [102].

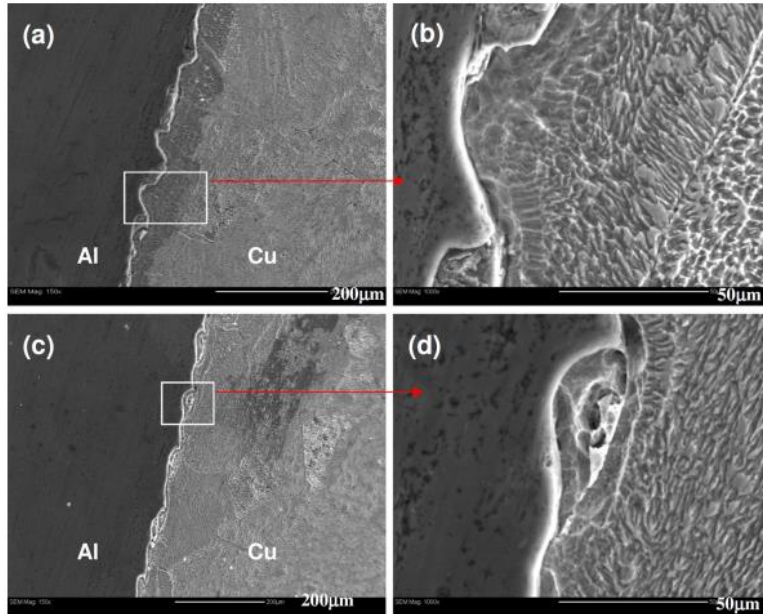


**Figure 40:** SEM micrographs of two interface regions and their local enlargements. The rough Cu surface was from chemical etching [102].

The equilibrium Al–Cu phase diagram (Fig.41) helps to understand that when heated to above 800 K and cooled down to room temperature, intermetallic compounds can grow with various Stoichiometric atomic ratios, including Al/Cu ,  $Al_9Cu_{11}$  , and  $Al_2Cu_3$ , as labeled at the bottom of the phase diagram.

In [50] another lap joining was studied, this time the welding of low carbon steel (SPCC)/A6111 aluminum alloys was carried out through magnetic pulse welding technology. The formation of the intermediate layer of aluminum grains (around 100 nm) and more fined dispersed intermetallic particles at the weld interface were also observed. The matrix of aluminum close to the weld interface exhibited extremely refined grain structure. Because of this two observations, the multi-phase intermediate layer and grain-refined aluminum layer, they are considered to be the origin of high interfacial bonding strength of the lap joint. A strong joining of both materials was successfully achieved without temperature increasing and the wavy morphology was observed together with the intermetallic layer which shows a strong mechanical bonding. The bonding strength of the joint was quite high and it failed at the parent plate when subjected to tensile tests.

In the case of welding Al/Al and Cu/Cu like performed in [98] was verified that although two parallel welded areas were formed along the both side edges of the coil, no welding occurred between them. The gradual change in collision angle between the flyer plate and parent plate caused a wavy morphology at the welding interface. The wavelength and amplitude of the interfacial wave gradually changed with the distance from the vertical central position of the bulged region. Increasing the discharged energy makes the wave length and amplitude of the interfacial wave also increase due to the high velocity of the flyer plate against the target one, resulting in a large collision pressure.

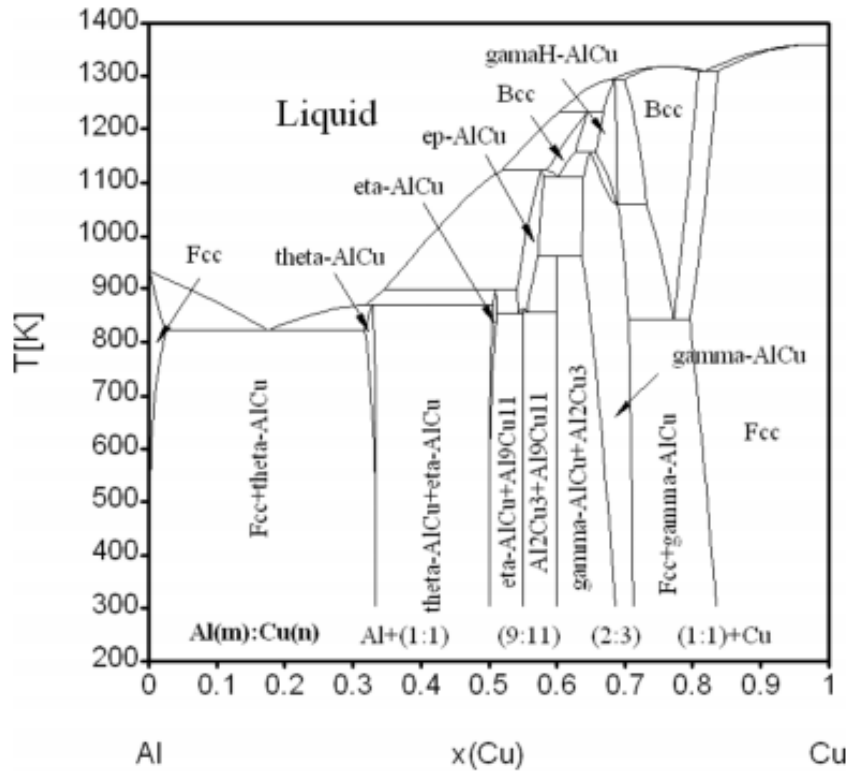


Figure 41: The Al–Cu binary phase diagram, computed with commercial software and with available thermodynamics database [102].

### 3.4 Local Melting and its influence on metallographic

The experimental observations indicate that the formation of intermetallic phase at the interface can occur through two different phenomena [54, 102]:

1. Bonding as a result of solid-state processes based on accelerated mass transfer due to intensive plastic deformation at very high rates;
2. Bonding as a result of solid-liquid interaction: the interface temperature in MPW rises due to the jet and massive deformation of the surfaces, and in some cases, local interface melting and solidification can occur;

The interface melting is not widely observed and is not a necessary condition for intermetallic formation. Thus, the dominating MPW mechanism is still a solid-state process even though the interface temperature increases significantly and depending on the magnitude of applied energy interface, melting may occur. For samples welded at 6.0 kV in [102] there is a direct evidence of interface melting, as shown in Fig.42, where a round pore was found inside the new phase region, and by refocusing to the bottom of the pore it shows the smooth inner surface of the pore with some microcracks within the new phase region. These cracks are stopped at the boundaries of the more ductile base metals and indicate a high thermal stress during rapid solidification [102].

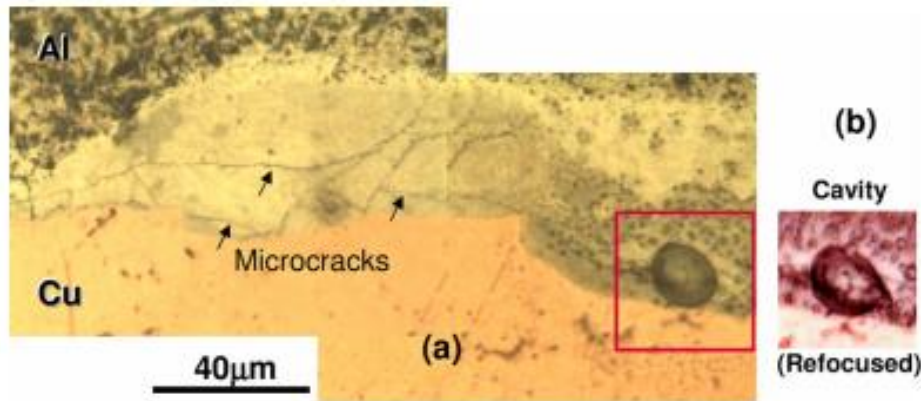


*Figure 42: The optical micrograph of a sample welded at 6.0 kV, and a round pore with a smooth surface was observed (a). By refocusing at the pore bottom (b) some surface cracks were revealed [102].*

The solid-liquid interaction of the intermetallic phase layer shows an increased hardness relative to the base material when welding aluminum with copper. This can be attributed to severe plastic deformation or to a new fine-grained microstructure produced by melting and rapid solidification of the weld interface [54]. This interface achieves a very high temperature, above the melting point, for a few microseconds. This is followed by cooling it at a rate of  $10^5$  K/s and creating thus an ultra-fine grain size [63]. Combining melting with rapid solidification and solid-state deformation /recrystallization can produce a fine-grained microstructure with low dislocation density and with high-angle grain boundaries [102]. As proved in several studies, grains near the interface are generally elongated parallel to the explosion direction what indicates a high degree of plastic deformation [1].

The literature commonly refer to explosion and magnetic pulse welding as a solid state welding process, mainly because metallographic investigation of the bonding area does not show evidence of melting. However, the melting on the interface has been observed on a submicroscopic scale and has been considered as a bonding mechanism. In [49] the bonding of aluminum and copper alloys were studied since a distinct change of the microstructure can be expected if the temperature in the bonding zone exceeds the melting point. Thus, a microstructural analysis of the bonding area by transmission electron microscopy was done in order to clarify if the melting at the interface takes place during the bonding process or not. Since the structure of a material changes considerably when subjected to a temperature above the melting point even for a short time, an analysis of the microstructure showed that it exhibits a large change during welding. It was found that new grains were formed and it could be explained due both recrystallization of heavily deformed material and short time melting. Therefore, the small grains found at the interface of and explosion welds indicate that melting has occurred during the bonding process. All samples prepared from the bonding zone of similar and dissimilar metal welds, with both plane and wavy interfaces, had a 0.5 to 4  $\mu\text{m}$  thick area along the interface with a grain size of 0.1 to 0.3  $\mu\text{m}$ . The existence of these grains refers to a short time melting followed by rapid cooling during the welding process. In [106] the grain boundary crystallographic misorientations of magnetic pulse welded AA6061-T6, in linear and tubular configurations, was studied and the results showed the complex interaction of shock

---

waves with the materials during this impact welding process. However, for the linear weld a refined structure of heavily deformed grains with higher grain boundary angles was observed. In case of tubular weld a significant fragmentation was observed away from the welded region indicating the strain gradient and extensive plastic deformation in this region. This results support the hypothesis of localized deformation in the bulk matrix away from the impacting surface due to the progression of alternating compression and tension deformation waves [106].

### **3.5 Interface wave propagation in MPW**

The bonding interface in impact welding can present three morphologies: wavy, straight and melted layer. For technical purposes, these morphologies depend on the impact velocity and angle [25]. MPW produces either a wavy or waveless morphology at the interface, where the precise shape is determined by the properties of the metals and by the parameters applied [85]. Wavy interface morphology is observed in magnetic pulse welding (MPW) similarly to that of the explosion welding process (EXW) and are formed only at the impact zone and its vicinity, due to induced metal flow in this elevated temperature and high pressure region [10, 2]. Its origin has been analyzed through the welding bond and several mechanisms have been suggested to explain this phenomenon.

In [31] the wave formation is described as a hydrodynamic model, which explains this phenomenon as being analogous to fluid flow behind an obstacle. Thus, the smooth–wavy boundary corresponds to the laminar-turbulent transition. However it has some differences which should be mentioned as in the hydrodynamic model, the waves generated behind an obstacle reach a stable configuration after a certain distance while the waves at the weld interface must be created at the collision point. In [17, 35] was suggested that the source for wave formation is a shear movement of the flyer and base plates creating local vortices in the plastic zone, a stagnation region of the jet acting creates each period vortex as a solid obstacle behind it. However, in [17, 56] it was assumed that indentation of the re-entrant jet into the parent plate surface creates a stagnation point and due to the instability of this region and momentary change in velocity of the metals, the stagnation point “jumps” over the “hump”, and a new “hump” is formed periodically. In [47, 91] another theory is supported based on the Kelvin-Helmholtz instability mechanism [5] in which waves are created as a result of flow velocity discontinuities across the interface (see Fig.43). The main principle of this model is hydrodynamic and says that once two fluids with different velocities interact, instabilities will occur at the interface. These instabilities involve mass flow, usually from the higher density material to the lower one. Whenever instability occurs, it has a direction and a certain velocity (energy) which causes a movement of material from one side of the interface to another creating a wavy interface. The shape and the direction of the wavy interface development are determined by the influence of the mutual velocity of the metals. For this model, the welded metals can be defined as viscous solids [10].

The pressure peak is always at the collision point, because the shock wave travel speed is higher at the start point and decreases with time [61]. The moment of the collision shows a wavy morphology while its amplitude decreases until the end of the weld due to shockwave propagation damping. Fig.44 represents the shockwave propagation, where in Fig.44-b the wave formation is initiated. The instability and new collision points leads to new shock waves. The

pressure peak is always at the collision point, since the speed is higher at that point and decreases retrogressively. Due to decrease of the propagation velocity with the weld progression, the shock wave interference meets the collision point further along and for this reason, the wavelength increases (Fig.44-f). After some point, the velocity of propagation ( $V_c$ ) is so small that the interference are ahead of the collision point and new waves can't be generated [61].

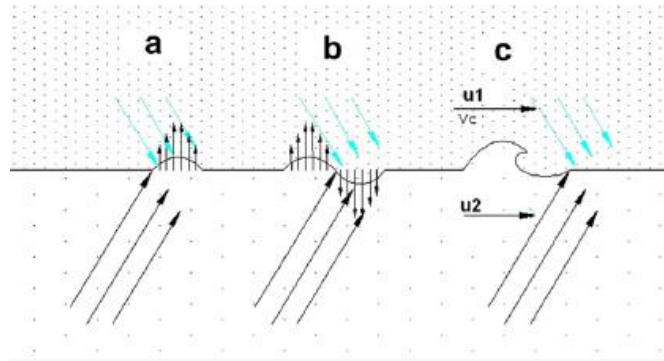


Figure 43: Kelvin-Helmholtz instability creation (from left to right  $u_1 > u_2$ ) [10].

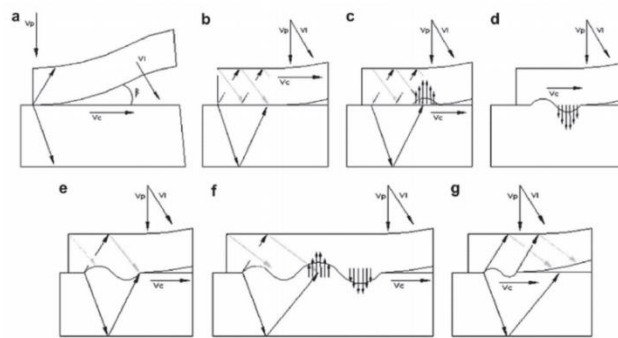
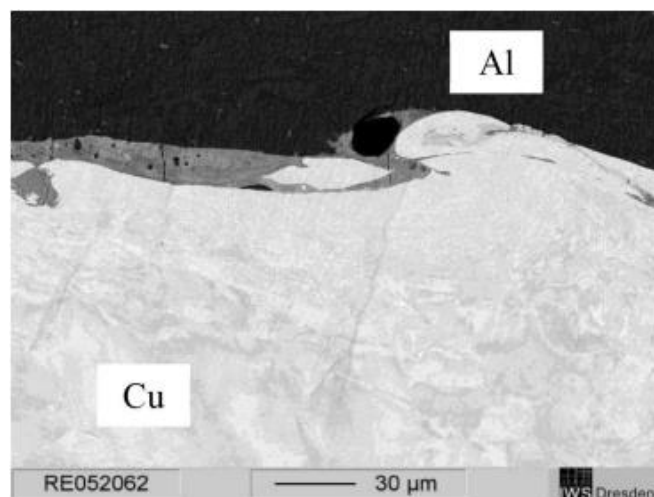


Figure 44: The periodic wave formation [61].

In [10] it was found that interface wave formation in MPW is a consequence of a Kelvin-Helmholtz instability mechanism and the most significant characteristics which influence the wave formation are the collision energy, impact angle and the geometry of the joint. Kelvin-Helmholtz mechanism claims that shock waves that travel through the inner part of the weld are the source for interface interference that initiate wave formation, this shock wave theory claims that shock waves propagate through the metal parts, creating periodic perturbation at the weld interface. It was also proven that wavelength of interface waves are proportional to the free path of shock wave propagation in the inner part of the welded couple. In [10] the free path of shock wave propagation was controlled by drilling a hole in the inner part, thus different path lengths were created (from the surface to the hole) for the incoming shock waves. As represented in the Fig.44 the shock waves, generated at the impact point, travel in both metals with a radial front with an angle proportional to  $\beta$ . The compression waves in the inner part meet their corresponding waves in a rigid collision and are reflected as compression waves towards the interface [10]. Through this theory of Kelvin-Helmholtz for tubular MPW joints, the collision point is under extreme pressure and heat, thus the interaction of the shock waves in combination with mutual movement of the metals, is the source of interface waves. Interface waves are formed only at the impact zone and its vicinity, due to induced metal flow in this



region of high temperature and high pressure. As well the initial gap and the energy of the capacitor influence the impact angle that sets the relationship between the collision point velocity and the weld propagation velocity. Also in [14] it was found that for small collision angles (smaller than  $20^\circ$ ) the jet indentation mechanism occur while for larger values of angles a straight metal interface is obtained. However, for metals with small shear strength values the collision at larger angles than  $30^\circ$  the Kelvin-Helmholtz instability mechanism occur, leading to waves with relatively large length and amplitude. Sometimes what makes the biggest difference between the different studies related to the interface of intermetallic layer is the morphology of the wavy interface. When the interface shows a wavy interface, the intermetallic compounds are typically concentrated in “melted pockets”, typically located at the crests of the interface waves and its thickness increases for high energy rates. The pockets where the melting materials remain are formed by heating, melting, mixing and rapid solidification of wave vortex and show the existence of globular porosity [90]. The high volume of pores registered can be explained due to residual stress during rapid solidification of the molten material and are most probably the initiators of the cracks observed for the higher values of discharge energy as can be analyzed in Fig.45.



*Figure 45: Typical wavy interface showing the intermetallic phase located in a “melted pocket.” Cracks and pores are also characteristic to the wavy location of the intermetallic layer [90].*

Magnetic pulse welding is several times compared to explosive magnetic welding as they both work in similar conditions. The big difference between both of them is the origin of the energy source responsible for initiate the process. In the case of magnetic pulse welding is an electrical source is responsible to accelerate the flyer against the target plate and for the case of explosive magnetic welding the controlled energy of explosives is used to create a metallurgical bond between two similar or dissimilar materials. Thus, and due to the restricted information about the wavy interface in magnetic pulse welding experiments, further one will consider results obtained for explosive pulse welding in order to achieve better conclusions about the waves obtained for MPW experiments. In [40] stainless steel–titanium plates were joined explosively employing oblique geometry route at different explosive ratios. The bonding was analyzed and a transition from smooth bonding interface to a wavy one with increasing explosive ratio was observed. For lower explosion loads the welding interface was flat and after applying higher

explosive loads a wavy interface was clearly seen in the interface. The respective wave length and amplitude of the waves were getting bigger with the increment of explosive loads. Related to the grain size it was also observed that grains near the interface were elongated parallel to the explosion direction due to plastic deformation during the explosion. Hardness was increased with increasing explosive ratio and the highest hardness values were obtained near the bonding interface. Weight increasing due to formation of a stable oxide layer on the welded stainless steel–titanium plates was seen from corrosion tests while weight loss was seen from the other specimens. The weight loss was noticed to increase with increasing explosive ratio. In the tensile-shear test, separation was not occurred in interface and fracture took place within the low strength material. The strength of all welded parts was bigger than the original materials. Although the welding was between two different materials in SEM study, no joining fault was formed in interface, and also no melting voids and intermetallic compounds were observed what confirms that the joining of titanium–stainless steel is successful by means of explosive welding. In [21] bonding ability of copper and steel with explosion welding was investigated, this time using different ratios of explosive and different standoff distance. It was observed that, when explosive ratio was increased smooth bonding interface changed to a wavy bonding interface and the amplitude and wavelength of wave were increased. The use of larger standoff values allowed obtaining wavy interface even for lower explosive ratio however the wavy interface was risen using higher explosive ratio. Thus, the total interface area increased as a result of a bigger wavy interface. When subjected to tensile-shearing tests the wavy interface did not separate proving that the interfaces of the bonded samples were almost perfectly bonded. As for the previous studies analyzed the hardness increased proportionally to explosion rate and standoff distance increment due to the collision of two plates during the explosion welding. Different analysis in this experiment proved that there was no diffusion in the interface zone what means that no melting and intermetallic zone was formed in the interface. Thus, it proved the use steel and copper as a safety couple in explosively welding process [21]. The effects of explosive loading, on the bonding interface of explosive welding, for joining cp-titanium/AISI 304 stainless steel, were carried out in [64]. Due to mechanical and corrosion properties of titanium and stainless steel, they were chosen as overlay plate and base plate, respectively. A low detonation velocity explosive of 2400 m/s and density of 850 kg/m<sup>3</sup> was used and was found that the flat interface is produced and the wavy interface is produced at higher explosive loads. This research study distinguished from the ones mentioned before because the SEM studies show the formation of melted sites in the interface especially at the crest and front slope of waves which grow with explosive load and a number of brittle intermetallic phases such as Fe<sub>2</sub>Ti, Fe<sub>2</sub>Ti<sub>4</sub>O and Cr<sub>2</sub>Ti are identified in the interface at high explosive loads. This melting can be related to adiabatic heating of trapped jet inside vortex at the front slope of waves as a result of density difference or the adiabatic heating of gases compressed between the plates. The molten zone is surrounded by relatively cold metal and subjected to a very high cooling rate. Typical defects in the vortex due to solidification are shrinkage, cracks and gas porosity [64].

As already mentioned, the hardness of the interface layer depends on the properties of the base metals. In case of similar base metal welds the main cause for the hardness increase is the fine grained microstructure formed during the rapid local solidification. For dissimilar base metal welds the increase in hardness is a result of the creation of stable or metastable intermetallic phases and the fine grained microstructure of the interface layer [89].

---

### **3.6 Summary**

Joining dissimilar materials is becoming more important in several industrial applications. However, it is not always easy to join dissimilar materials. Aluminum and copper are two materials with different mechanical and thermal properties which is a constraint for welding them through the conventional welding methods. Magnetic pulse welding technology is a cold welding process under study and could be a solution for welding dissimilar materials as Al/Cu. A good understanding of the welding bonding mechanism for dissimilar materials is required in order to take the most advantages possible from the process. Thus, it is important to analyze how does the surface condition influences the welding quality. Tensile tests and microstructure examination are used to evaluate the welding quality. It is accepted in the literature that impact welding process, as explosive or electromagnetic pulse welding have no restriction on surface cleanliness. Most of the literature supports the theory that the jet action by the strong impact is enough to clean the surfaces. However, the need of pre-cleaning the surface before welding will be investigated in the following of this thesis.



## 4 EXPERIMENTAL WORK

---

In this chapter, the experimental work is presented and explained. The main objective of this thesis is to study the influence of the surface's condition in the welding quality. A total of 18 welds with different surface conditions were performed between samples of copper and aluminum. The experimental results obtained are compared in this section with the theoretical background described before in the literature review of this thesis. In order to develop new knowledge about the process, the following surfaces were tested: machined, shot blasted, polished, chemically attacked, greasy and threaded. The aim of testing different surface conditions is to investigate how the state of the surface influences the welding quality. The welding quality was analyzed through tensile tests and microstructure examination. The importance of pre-cleaning the surface before welding is also another element under analysis in this experimental work and the greasy surface tested would provide a helpful insight on this topic. Some literature review states that the welding would occur either with clean and greasy surfaces. For that reason, greasy surface's specimens were tested and analyzed in order to develop a reasonable approach for this conclusion.

## 4.1 Material Characteristics

In this study of different surfaces, tubes of aluminum were electromagnetically driven against inner cylindrical rods of copper in order to obtain a welded interface. The experiments were performed between copper R300 and aluminum AA 6063-T5. Copper is used as the inner material and the aluminum is the out tube. The Al tube has 1.0 mm wall thickness and an outer diameter of 20 mm. The diameter of the copper rod was defined based on the gap distance that produced the best results in previous work done by the researchers of INEGI [68]. The characteristics of the materials used are important to describe both materials and are described in the following. Copper R300 is a soft copper alloy which is composed for more than 99,9% out of Cu. Its composition is exposed in the Tab.7 and the mechanical properties in the Tab.8. Aluminum alloy 6063-T5 is a commercial alloy and the mechanical properties are presented in the Tab.9.

Component	Composition (At %)
<b>Cu</b>	99,98
<b>Ag</b>	0,0022
<b>O</b>	0,0132
<b>Bi</b>	0,0001
<b>Pb</b>	0,0001

*Table 7: Chemical composition of the copper R300.*

<b>Density</b>	8940-8950	kg/m <sup>3</sup>
<b>Young's modulus</b>	127	GPa
<b>Yield Strength</b>	250	MPa
<b>Shear Modulus</b>	45-50	GPa
<b>Tensile Strength</b>	290-360	MPa
<b>Hardness</b>	90-110	HV
<b>Fracture Toughness</b>	43,2-57,6	MPa m
<b>Melting Point</b>	1083	°C
<b>Electrical Resistivity</b>	1,70-1,74	μΩ cm

*Table 8: Mechanical properties of the copper R300*

<b>Density</b>	2660-2710	kg/m <sup>3</sup>
<b>Young's modulus</b>	67,2-70,7	GPa
<b>Yield Strength</b>	113-125	MPa
<b>Shear Modulus</b>	25,3-26,6	GPa
<b>Tensile Strength</b>	158-175	MPa
<b>Hardness</b>	61,8-68,3	HV
<b>Fracture Toughness</b>	30-36	MPa m
<b>Melting Point</b>	615-655	°C
<b>Electrical Resistivity</b>	3,08-3,21	μΩcm

*Table 9: Mechanical properties of the Aluminum AA 6063-T5*

---

## 4.2 Experimental methodology

In this thesis, a total of 18 copper specimens with six different surface preparations were tested. For each state of the surface a total of three samples were performed. An overview of the different surfaces tested is given in the Tab.10. To study the quality of welding tensile tests and microstructure examination were performed. Two samples of each surface condition were used for the mechanical testing and the spare one for microstructure examination. For this microstructure examination, the samples were cross sectioned and polished through standard metallurgical procedures and then were examined by an optical microscope (OM). The samples were also analyzed through scanning electron microscopy (SEM). The chemical composition distribution across the interfaces was analyzed with an EDS probe, and the obtained chemical compositions were compared with the equilibrium Cu-Al binary phase diagram.

The roughness of the different workpieces was measured using an optical non-contact profiler. For each sample, a total of three measurements were done and the average results are in the Tab.11, where  $R_a$  is the mean roughness and  $R_q$  is the mean square roughness. As it is possible to conclude through the roughness measurements, the highest value of roughness belongs to the shot blasted specimens with an average roughness value nearby 4805 nm and the less rugged specimens are the polished ones, nearby 607 nm. These values are important to analyze how roughness can influence the bond strength.

Run	Surface condition	Specimen identification
1	Machined 1	M1
2	Machined 2	M2
3	Machined 3	M3
4	Shot blasted 1	G1
5	Shot blasted 2	G2
6	Shot blasted 3	G3
7	Polished 1	P1
8	Polished 2	P2
9	Polished 3	P3
10	Chemical attack 1	Q1
11	Chemical attack 2	Q2
12	Chemical attack 3	Q3
13	Greasy 1	O1
14	Greasy 2	O2
15	Greasy 3	O3
16	Threaded 1	R1
17	Threaded 2	R2
18	Threaded 3	R3

*Table 10: Different surface condition for copper specimens.*

As described in Tab.10, six initial copper surface conditions were prepared for analyzing their effects on welding:

- **Machined (M1, M2, M3):** The as-machined surface, produced by lathe and cleaned with acetone;
- **Shot-blasted (G1, G2, G3):** After the lathe turning, the samples were sandblasted. The goal was to replace the machined samples by a new surface topology to study;
- **Polished (P1, P2, P3):** The samples were polished, with 1200-grit sandpaper and the goal was to remove the lathe marks;
- **Chemical attack (Q1, Q2, Q3):** The machined samples were subjected to chemical etching. The specimens were introduced in solution made with 50 mL HNO<sub>3</sub>, 10 mL H<sub>2</sub>N<sub>2</sub> and 50 mL H<sub>2</sub>O, during 90 seconds;
- **Greasy (O1, O2, O3):** After the lathe turning, high-viscosity lubricant oil was applied over the welding zone surfaces. The goal was to study the process when applied to a very contaminated interface aiming to investigate and analyze how relevant it is to clean the surface before welding and if the jet can effectively remove the contamination layer and create a weld.
- **Threaded (R1, R2, R3):** After the lathe turning, a threaded surface with 1 mm pitch was created in order to study a new surface topology.

Copper workpiece	Ra (nm)	Rq (nm)
G1	5244,841	6645,170
G2	4578,090	5834,977
G3	4593,685	5855,302
P1	220,981	311,831
P2	542,146	699,614
P3	1059,465	1221,802
M1	1510,233	1876,141
Q1	1932,056	2363,180
Q3	2176,029	2463,329

*Table 11: Roughness measurements of the copper R300.*

The copper and aluminum parts were subjected to an ultrasonic cleaning device with acetone during five minutes in order to properly clean the surface and assure that there isn't any kind of contaminants which could influence the welding quality. After cleaning both of the parts, the welding procedure was performed. Welding experiments were carried out using a 25/25 magnetic pulse system made by B<sub>max</sub>. It consists in a capacitor bank and a high voltage cabinet for charging the capacitors, capable of generating 25 kJ at a charging voltage of 25 kV. The electromagnetic actuator consists of a single turn coil made of a steel (40CrMnNiMo 7) which is suitable for welding cylindrical parts with an outer diameter of 20 mm. The setup used is shown in the Fig.46.

The geometrical parameters used in the experimental work are represented in the Tab.12. Previous experimental work done by researchers of INEGI for joining aluminum with copper found these parameters acquired to the described work conditions [68]. The same research led to the definition of the welding window for the combination of copper and aluminum (Fig.47). However, it should be clearly noted that the welding window shape always change



through different input parameters, thus each experiment can have its own welding window depending on the values of energy, the LWZ and Gap used.



Figure 46: Setup used for the welding process.

Fixed parameters = C7

Energy [kJ]	Voltage [kV]	LWZ [mm]	Gap [mm]
10,24	16	8	1 ( $\Phi = 16$ mm)

Table 12: Welding parameters.

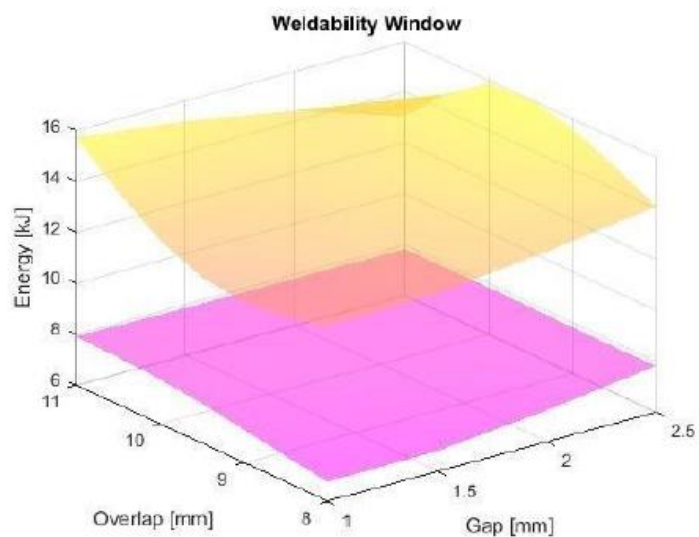


Figure 47: Welding window illustration [67].

One of each different surface preparation was cross-sectioned to observe either the occurrence of joining or not between copper and aluminum. The pictures which are shown in this thesis are the ones that are most representative for the conclusions, but they are only a small part of the total amount pictures that were taken. The welded zone was examined with scanning electron microscopy (SEM) and tensile tests were conducted using the tensile test machine represented in Fig.50. The parameters of the tensile tests according to ASTM A 370 are in the Tab.13. In order to perform the tensile tests, it was necessary to project new grips to proper fix the cylindrical samples during the tests. The projected grips are represented in the Fig.50. To project these new grips was essential to analyze our samples. In this experimental work tension test specimens of full-size tubular sections were used, provided that the testing equipment has sufficient capacity. Snug-fitting metal plugs should be inserted far enough in the end of such tubular specimens to permit the testing machine jaws to grip the specimens properly without crushing. The design used for such plugs in represented in the Fig.51. The plugs shall not extend into that part of the specimen on which the elongation is measured as shown in the Fig.51.

In [68], work performed by researchers of INEGI, the strength of the Al/Cu welds was investigated by compression testing. In the present dissertation the strength will be studied performing tensile tests. A tensile test is a method for determining behavior of materials under axial tensile loading while a compression test is a method for determining the behavior of materials under a compressive load. Tensile tests require a much more complex setup than the compression. During tensile tests, a load is applied in order to elongate the specimen and consequently force them until the maximum force before failure is achieved - tensile strength.



*Figure 48: Setup used for the tensile tests.*

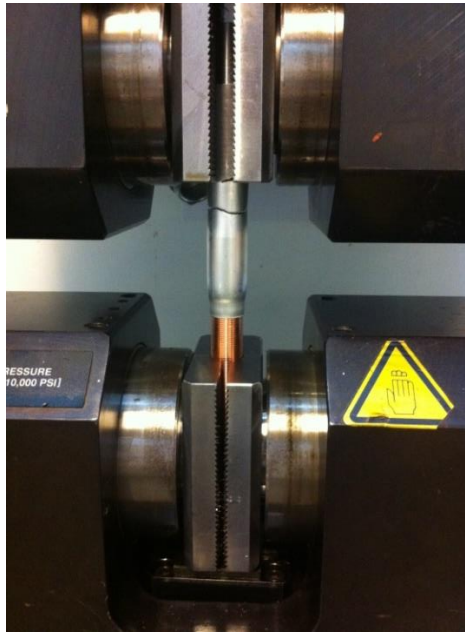


Figure 49: Workpiece during the tensile test.

Cell	200 kN
Type of grip	Hydraulic
Test speed	2 mm/min

Table 13: Tensile tests parameters according to ASTM A 370

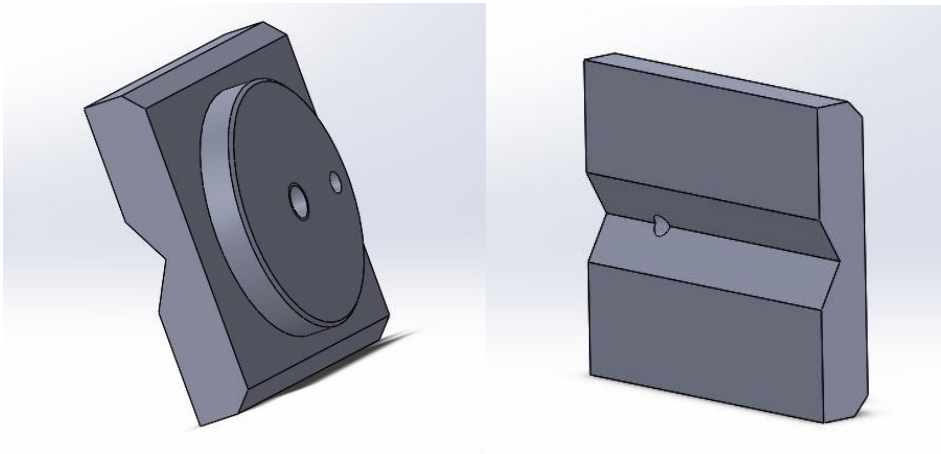
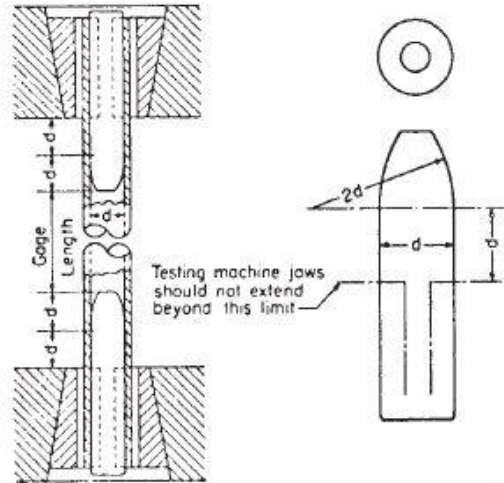


Figure 50: Projected grip (using SOLIDWorks®).



**Figure 51: Metal Plugs for Testing Tubular Specimens, Proper Location of Plugs in Specimen and of Specimen in Heads of Testing Machine - ASTM A370.**

### 4.3 Analysis of the welding quality

After testing, the welding quality was evaluated by tensile tests and microstructure examination. The tensile tests were performed following the standard methods and definitions for cylindrical parts (ASTM A370). The tensile testing machine used was an *Instron model 4507* at a test rate of 2 mm/min. The results obtained are shown in Fig.52. The load-displacement curves for each surface preparation together with the SEM pictures are presented in the following and a general overview for all the workpieces is in the Fig.52. Comparing all the results, the maximum force was obtained for the threaded specimens - R - and it's nearby 19,70 kN. All the joints failed on the welded region except the samples with threaded surface. The tensile experiments were repeated on two samples and the results obtained for both samples of each surface condition are considered consistent. The joint between Cu/Al was, in general, weak as the overall load to pull the jointed parts was only a few kN as described in the Tab.14.

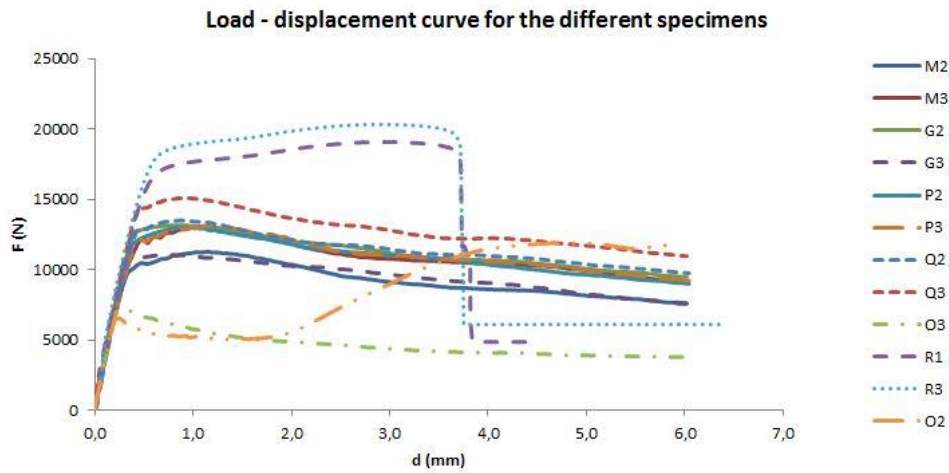


Figure 52: Force-displacement curves obtained experimentally for different specimens.

For the machined specimens (M2 and M3), the tensile tests (Fig.53 b)) showed that the maximum load sustained was nearby 12,14 kN. Analyzing through the SEM images (Fig.53 a)) seems that an intermetallic phase can be observed and a wavy interface is verified. The aspect of the interface and the presence of an intermetallic phase suggest the existence of local melting. Perhaps, the dissipation of the kinetic energy at the interface during the process was a source of heat which could provoke melting across the interface and diffusion within the molten layers.

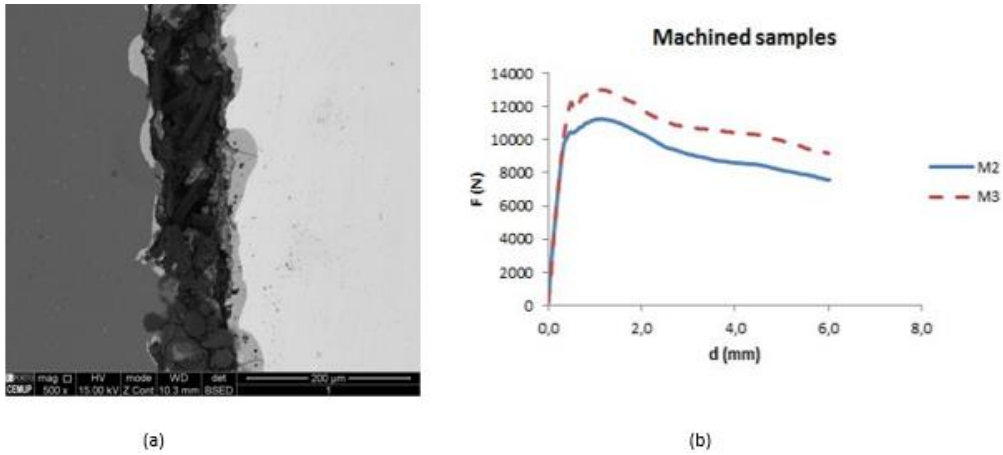


Figure 53: Machine surface: a) weld interface SEM analysis for M1 (magn. 500x); b) Force-displacement curve for M2 and M3 machined specimens.

The tensile tests for blasted specimens (G2 and G3) showed an average maximum load value of 12,11 kN (Fig.54 b)). After analyzing the machined and blasted specimens, is possible to notice that both have very similar maximum load values. The additional sandblasting operation done for G may not represent a significant improvement, regarding the bond strength. The Fig.54 a) corresponds to the SEM analysis for this surface treatment. A wavy interface and an intermetallic phase are also possible to observe. The presence of cracking can also be noticed. The intermetallic zone is full of spherical voids. These voids may result from porosity provoked during the solidification. It probably occurred from the heating above the melting point and thus reaching the fusion zone.

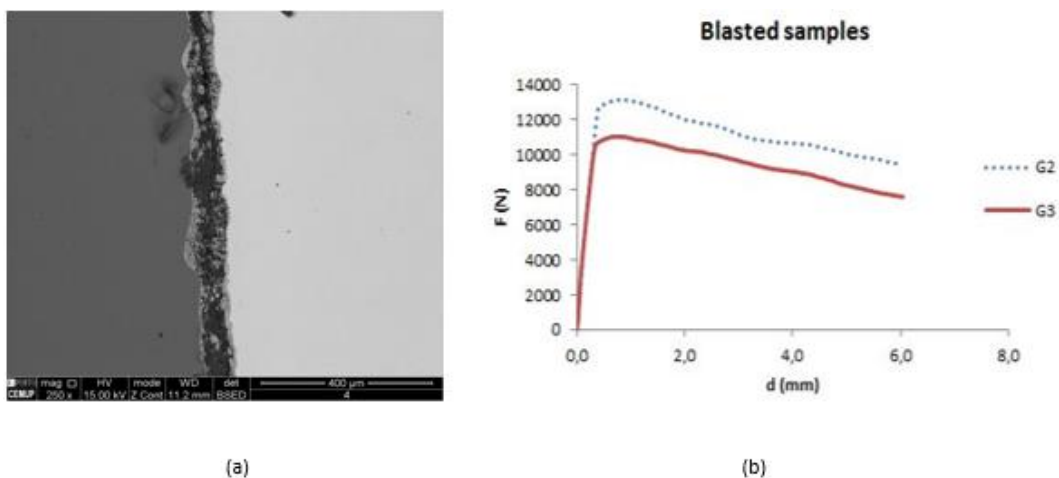


Figure 54: Blasted surface: a) weld interface SEM analysis for G1 (magn. 250x); b) Force-displacement curve for G2 and G3 blasted specimens.

The tensile test's curve for the polished specimens P2 and P3 are in the Fig.55 b) and it was found an average value for the maximum load nearby 13,07 kN, what corresponds to a slightly increasing in maximum force comparing to the M and G samples. The SEM results are in the Fig.55 a). An intermetallic phase is clearly seen although a soft-wavy interface is noticed.

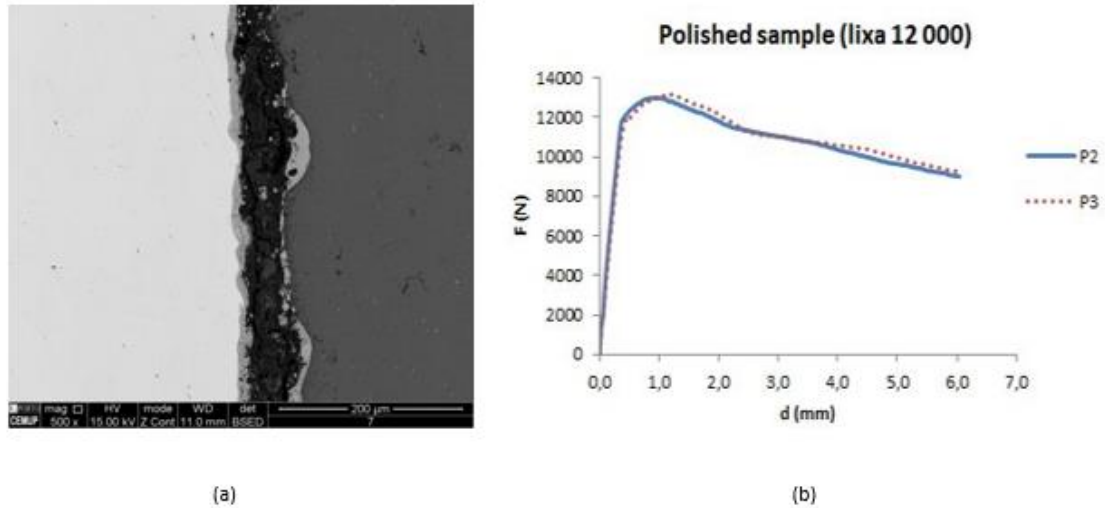


Figure 55: Polished surface: a) weld interface SEM analysis for P1 (magn. 500x); b) Force-displacement curve for P2 and P3 polished specimens.

For the specimens chemically etched the tensile test curve is in the Fig.56 b) and the maximum load suitable exhibits an average value nearby 14,30 kN. Through the SEM analysis (Fig.56 a)) a well expressed wavy interface and cracking are verified.

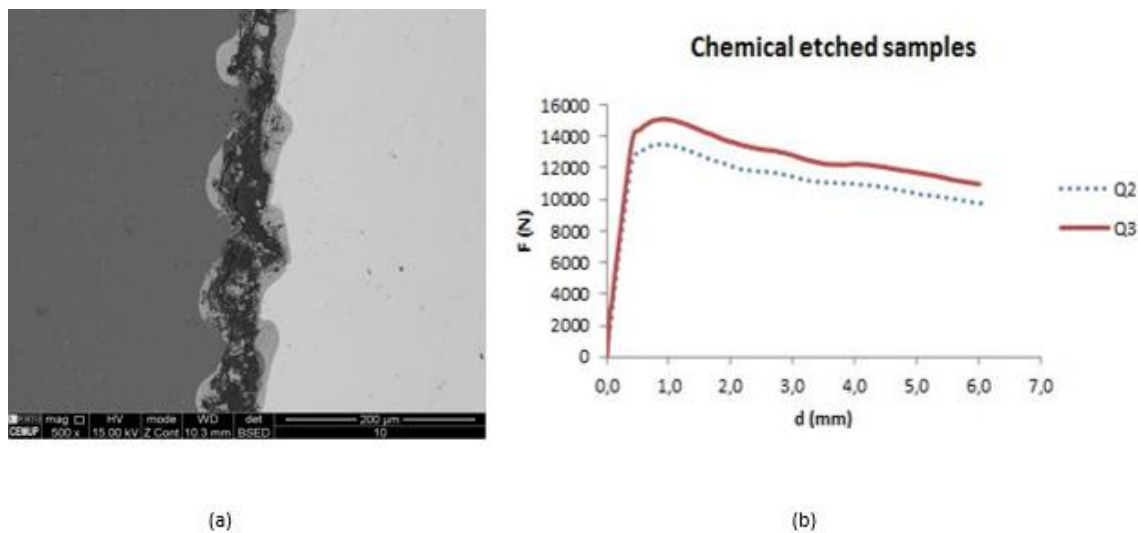


Figure 56: Chemically-attacked surface: a) weld interface SEM analysis for Q1 (magn. 500x); b) Force-displacement curve for Q2 and Q3 chemically-attacked specimens.

For the oil contaminated surface specimens the tensile test's curve is in the Fig.57 b). The average value for the maximum load is 9,57 kN what means that very weak bonding strength was obtained. Interface bonding may not be established due to the excessive contamination. Through the SEM results (Fig.57 a)) is possible to conclude that for these samples the wavy interface was not formed. Having all of this in consideration, the oil in the surface has a detrimental effect on the welding and cleaning the parts before the experiment seems to be necessary.

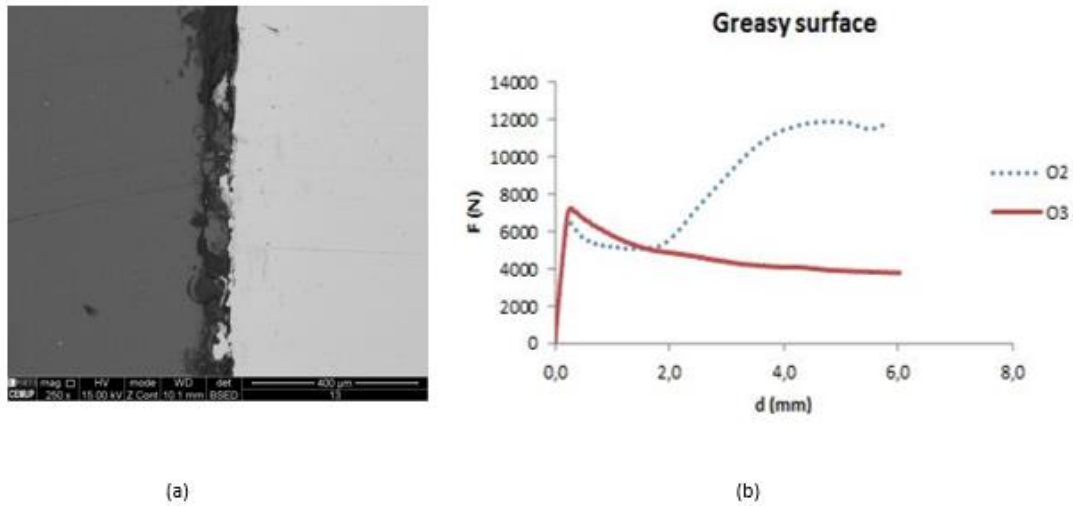


Figure 57: Greasy surface: a) weld interface SEM analysis for O1 (magn. 250x); b) Force-displacement curve for O2 and O3 oil-contaminated specimens.



For the threaded specimens the tensile test curve is in the Fig.58 b). A maximum load showed an average value nearby 19,70 kN which corresponds to the strongest joint achieved. For this experiment the jet and wavy interface was not formed. The Al-Cu joint occurred through a process of crimping instead of welding as expected (Fig.59). For these specimens, failure occurred in the aluminum part at the maximum force (Fig.60). Probably is possible to obtain stronger bonds through the process crimping than welding as the maximum force as higher for this sample. In the Tab.14, the experimental results and observations for all the different surface treatments are registered.

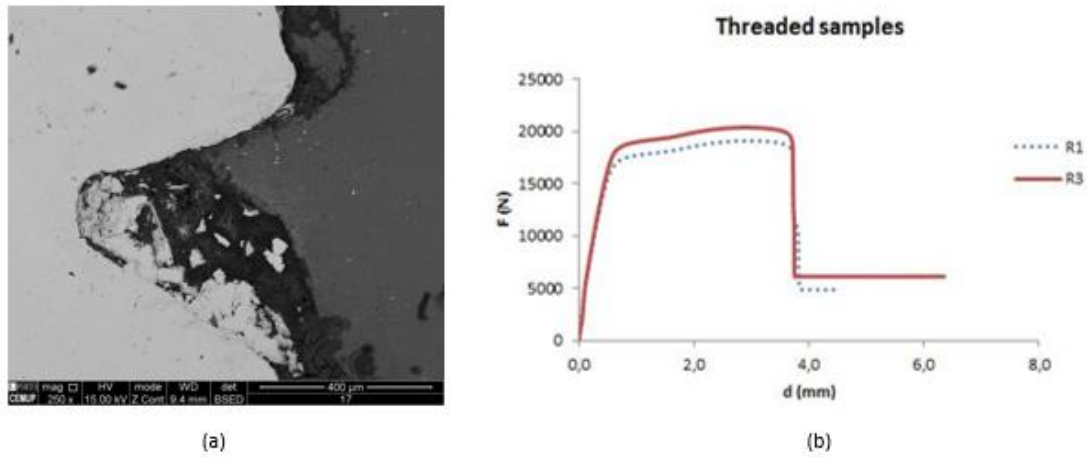


Figure 58: Threaded surface: a) weld interface SEM analysis for R1 (magn. 250x); b) Force-displacement curve for R2 and R3 threaded specimens.

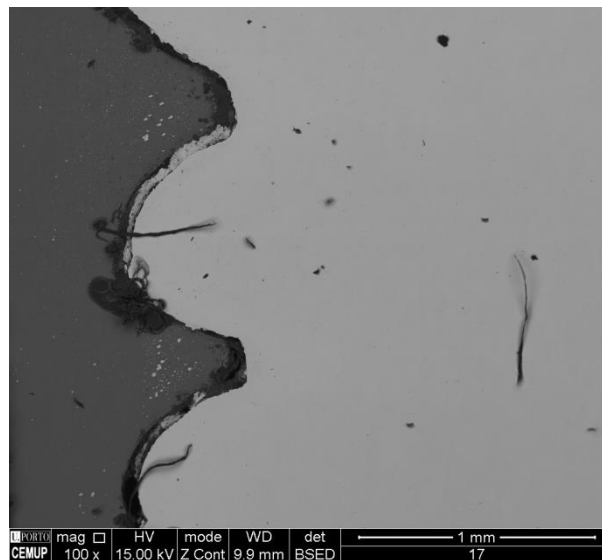


Figure 59: Weld interface for the R2 screwed specimen with almost non-intermetallic phase (magn. 100x).

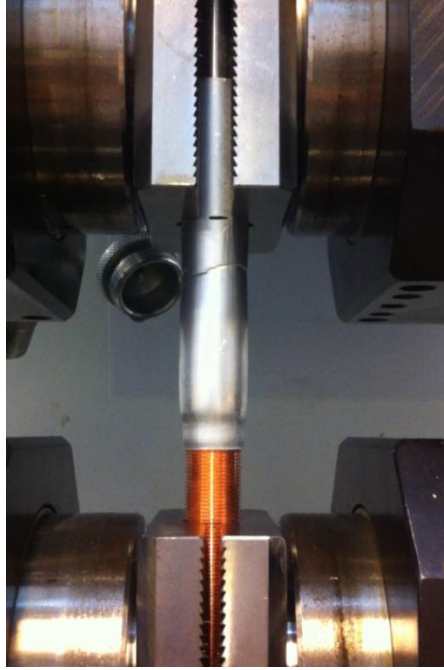


Figure 60: Failure occurred in the aluminum part at 19,70 kN load.

Specimen	Mechanical strength (kN)	Roughness ( $\mu\text{m}$ )	Wavy interface	Intermetallic phase
Machined (M)	12,1	1,5	yes	yes
Blasted (G)	12,1	4,8	yes	yes
Polished (P)	13,1	0,6	yes	yes
Chemically etched (Q)	14,3	2,1	yes	yes
Greasy surface (O)	9,6	1,5	no	no
Threaded (R)	19,7	-	no	no

Table 14: Surface roughness and average maximum bond strengths for different surface conditions

---

#### **4.4 Summary and Layout**

In this chapter, the weld between Al-Cu was investigated. The strength of the joints obtained was investigated through tensile tests. The microstructure examination allows us to distinct the samples welded from the not welded ones. The observation of the interface evidences the presence of melting and formation of intermetallic compounds. The values of mechanical strength for the different surface conditions are so similar (12,1 kN; 13,1 kN; 14,3 kN) that it is not possible to establish a relation between roughness and bonding strength. It is not possible to state that the increasing the surface's roughness would lead to an increasing strength, or vice-versa.



# 5 ANALYSIS OF THE RESULTS

---

## 5.1 Mechanical characterization of the joint

In the Fig.63 is clearly seen the occurrence of cracking. It can result from the formation of an intermetallic phase which consists in a source of residual tensions. Similar results between specimen M (Fig.62 a)) and [68] were expected as the process parameters are the same (1 mm gap, 8 mm overlap and 10.24 kJ). The only parameter that was modified between experiments was samples length. In [68] samples of 40 mm length were tested and in this thesis the samples have a length of 100 mm which may have an influence on the welding window. Probably it has an influence on the welding window and is necessary to re-optimize the process parameters for this length of sample.

The impact process welding provokes shock waves in the joining parts. Elastic and plastic deformation occurs in the target and flyer materials. Propagation and reflection of the waves may occur and its intersection can result in the fracture of the welded interface. This travel time of the waves depends on the materials and also on the geometrical properties of the sample. Changes in samples length can lead to the need of re-optimize the welding parameters.

Cracking can also have its origin on the residual stresses caused by the cooling rate of the solidification. The solidification generates a gradient of temperature in the sample [24] and this process may be similar with the one during casting where the intermetallic phase undergoes a rapid cooling soon the melting point is achieved. The solidification shrinkage and expansion is mainly due to the evolution of gases and the pressure drop over the intermetallic phase. It depends on the alloying system, melting, and solidification conditions [24]. The cooling curve derives from acquiring data of temperature against time and is processed in order to obtain information about critical temperatures and cooling rates.

Another possible source of pores formation is the phenomenon of cavitation. At the beginning of the solidification a drop of the temperature occurs and there is germination of bubbles. Then a coalescence with the increase of tension surface on the inner wall until the mechanical equilibrium is reached. Basically, the cavitation is about a hole formation when a liquid phase is subjected to rupture tensions [77, 97, 99].

The roughness of the different specimens was measured (Tab.11). Although the surface treatment may have an important influence on the weld quality, through the Tab.14 is not possible to establish a correlation between the values of roughness and mechanical strength, its influence on the wave pattern and wave expression. It is not possible to state that increasing the surface roughness leads to a stronger bond or vice-versa. The machined (Fig.62 a)) and blasted (Fig.62 b)) samples have very similar maximum forces: 12,14 kN and 12,11 kN, respectively. The increasing on the surface roughness (from 1,5  $\mu\text{m}$  to 4,8  $\mu\text{m}$ ) for blasted samples does not lead to an improvement regarding bond strength.

According to [102], besides the surface roughness, the scratch orientation also influences the wave formation. The direction of the surface features also affects the properties of the waves as the wavelength, amplitude, etc. This wavy interface of MPW joints consequently affects the mechanical behavior of the joint. However, the results obtained in this thesis do not support that idea in terms of tensile strength. For the machined and blasted surface (Fig.62), very similar bond strength was achieved for different scratch orientation.

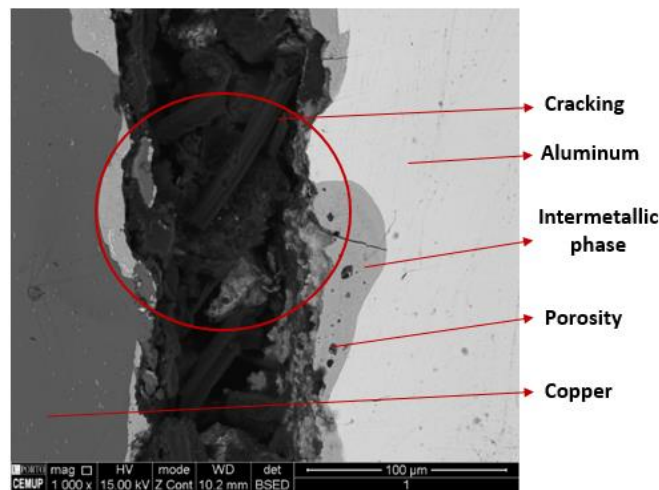


Figure 61: Cracking observation for machined sample (M).

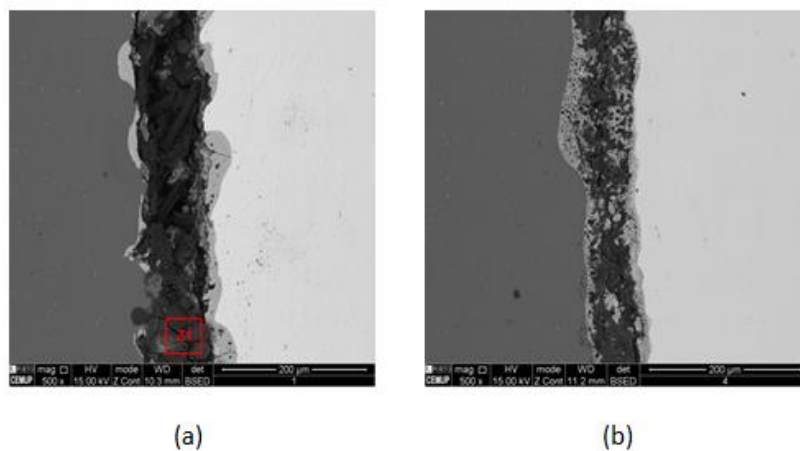


Figure 62: Weld interface (magnification 500x): a) Machined specimen (M1); b) Shot-blasted specimen (G1).

## 5.2 Intermetallic phase formation

In most of the samples, the appearance of an intermetallic phase is possible to recognize from the base materials. In this section, the microstructure will be analyzed in terms of the intermetallic phase formation. Welding dissimilar materials could lead to some changes on the mechanical properties of the joint. These changes can be due to the fine grained microstructure or as well by the stable or metastable intermetallic phase which can lead to a hardness increasing of the joint interface [58, 82, 105].

As described in the literature review, for aluminum and copper joints an intermetallic  $\gamma_1$  ( $\text{Cu}_2\text{Al}$ ) can be created and this phase increases the interfacial hardness. The melting and rapid solidification of the interface material is the possible cause of the formation of intermetallic compounds and voids. Through the equilibrium diagram (Fig.64) is possible to analyze the solidification process and the appearance of an intermetallic phase. This binary phase-equilibrium diagram is really important to show the physical and structural changes on metallic alloys, due to successive heating and cooling slow cycles. In the specific case of aluminum and copper diagram (Fig.64) the study of this diagram allows to understand how variations in the content of copper and aluminum can influence the achievement of different properties. The intermetallic phase has a certain quantity of Cu and Al and is exposed to a certain temperature during the welding process which will decrease from high temperatures to the room temperature along a time period. The combination of these two parameters, temperature exposed and percentage of copper leads to a certain position in the diagram. Then, following the lines in the diagram is possible to understand how the intermetallic phase undergoes the cooling process [15, 16].

Through the analysis of the Al-Cu phase diagram (Fig.64) and the EDS study on MPW welded Al-Cu interface-zones (Tab.15), it is possible to verify that, probably, intermetallic phases have been created. The melting and rapid solidification of interface material is the possible cause of the formation of intermetallic compounds and voids as well.

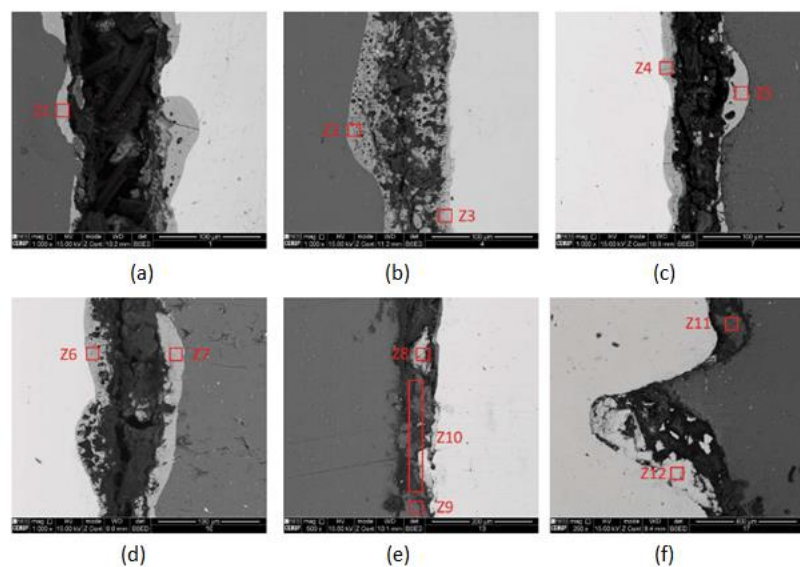


Figure 63: EDS study on MPW welded Al-Cu interface zones for different surface preparations: a) machined; b) blasted; c) polished; d) chemical etching; e) greasy; f) threaded

Zone	Al (At %)	Cu (At %)	Others (At %)
Z1	63	37	-
Z2	72	28	-
Z3	62	38	-
Z4	66	34	-
Z5	70	30	-
Z6	67	33	-
Z7	65	35	-
Z8	1.5	26	72.5
Z9	93	-	7
Z10	17	3	80
Z11	-	68	32
Z12	-	90	10

Table 15: EDS study on MPW welded Al-Cu interface-zones for different surface conditions.

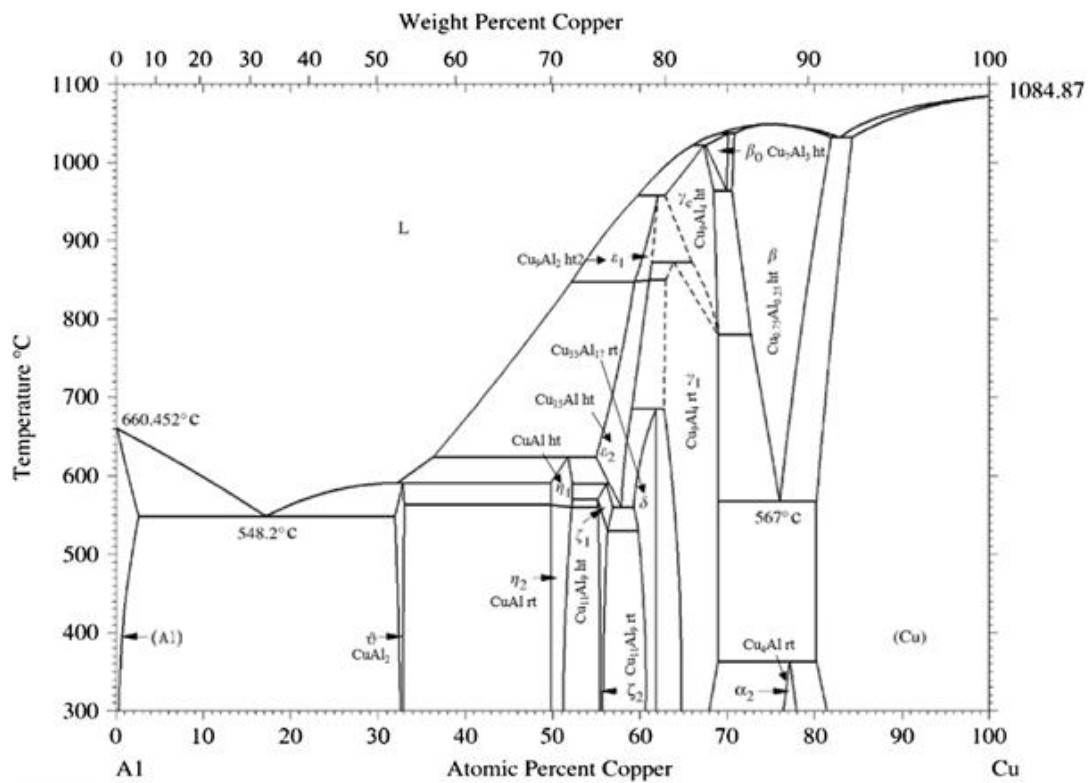


Figure 64: Analysis of the content for the different surface conditions.



### 5.3 Jetting formation

During the magnetic pulse welding, a jet was created along the interface for almost all the specimens. However, for the oil-contaminated and threaded surfaces the jet was not formed. For both of these specimens the wavy interface was not observed and a flat interface was obtained. This flat interface may be related to the absence of jet and can be represented in the Fig.65.

Through the literature review, it was found that welding could be possible without pre-cleaning the surface due to the jet, which can remove the contaminants from both surfaces. In order to study the influence of the surface on the welding quality and to test if the welding would occur in a greasy surface, the surface of the specimen O was covered with oil.

Through the analysis of the interface, the greasy samples are not welded. Thus, the jet seems not to be enough to clean the surface and it probably has an influence on the welding process. The specimens type O (Fig.65 a)) showed the lowest maximum load of all the experiments, nearby 9,57 kN. For the threaded specimens (R), the joint was reached through crimping and not welding, the jet was not registered maybe due to the threads which probably block the jet formation. The maximum mechanical strength was obtained for the threaded samples with an average tensile strength of nearby 19,70 kN (Tab.14). Thus, in this study, the process of crimping led to joints with higher values of mechanical strength than the welding did. Moreover, getting crimping joints is proved to be easier than obtaining welds as the requirements of this process are less demanding.

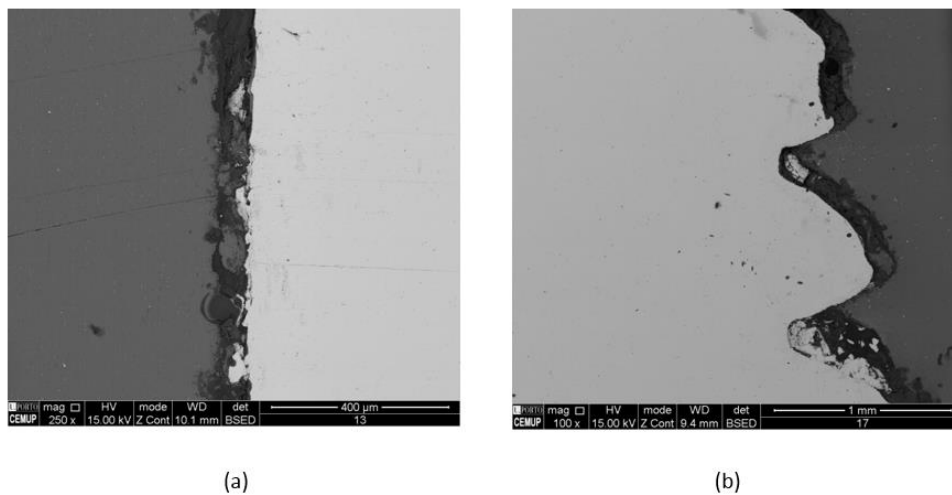


Figure 65: Flat interface observed a) Greasy surface b) Threaded surface.

## 5.4 Occurrence of melting

One purpose of this present thesis is to study if magnetic pulse welding can be effectively considered as a solid-state welding process. Although considered a “cold welding”, analyzing the aspect of the interfaces, is possible to verify the occurrence of melting.

The aspect of the interfaces obtained (Fig. 66) shows the presence of intermetallic compounds what can mean the existence of local melting. The temperature of the interface increases maybe due to the dissipation of kinetic energy at the interface, due to the jet, which is dependent on the impact angle, and the impact energy which determines the impact velocity. In order to avoid melting, the energy level can be decreased. Several papers support the theory of melting and the jet has been found to be the main source for the heating of the materials, apart from the heating due to the collision itself [73].

The big disadvantage of melting relies on the intermetallic phase which is a brittle layer and can have an important influence on the material strength creating residual stresses, susceptible of cracking.

In Fig. 66 is also possible to analyze the porosity which can probably influence the cracks propagation. It is possible to compare this phenomenon to the traditional fusion welding processes. Although called a “cold welding” process, during welding, the temperature can increase to values above the melting point.

During MPW, the interface experiences heating, melting and solidification. One of the reasons for the occurrence of failure can be probably the residual tensions arising during the solidification of the intermetallic compound.

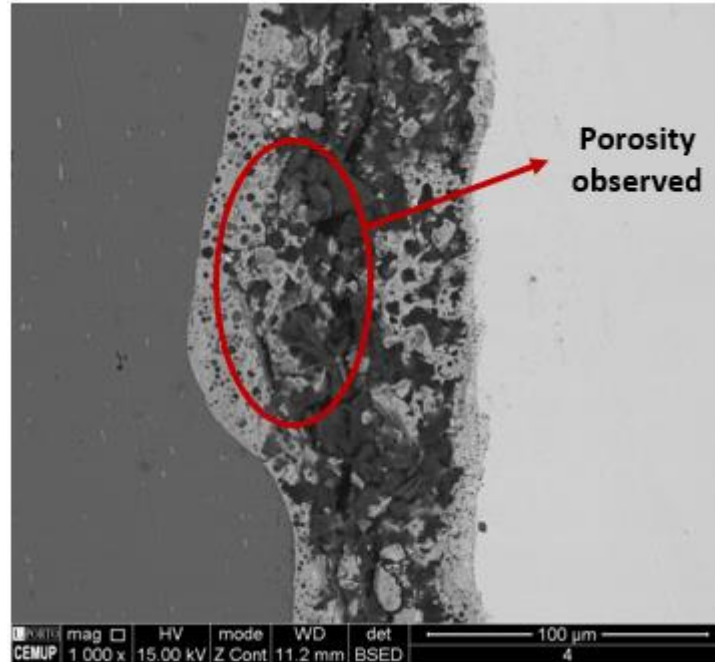


Figure 66: SEM observation for G1 workpiece.

---

## 5.5 Summary

In this chapter, a process of magnetic pulse welding between tubes of aluminum and copper rods was tested. Six different surfaces were tested in order to better understand how the surface influences the welding quality. The geometrical parameters were fixed and what differed from one experiment to another was just the surface preparation. Having the experimental background into consideration it is possible to outline the following points:

- The weld of Al/Cu dissimilar pair was investigated and it is possible to weld aluminum with copper through electromagnetic impact welding;
- The strength of the joints was investigated through tensile tests.
- During the welding it is often noticed the appearance of an intermetallic phase which can not be completely avoided when welding dissimilar materials as Al/Cu;
- Through the results obtained it is not possible to establish a relation between the values of roughness and mechanical strength;
- The welding was not established for the oil contaminated samples what means that probably the jet is not enough to clean the surface for bonding;
- Seems that surface condition has a certain influence on bond formation and interface morphology;
- The threaded samples were bonded through a process of crimping. The value for tensile strength obtained for these samples was the biggest one what means that strong connections can be achieved without metallurgical bonding. In MPW the bond created between the base materials is metallurgical and the results show that the tensile strength obtained is only a few kN.



---

# 6 CONCLUSIONS

---

## 6.1 Conclusions

The joining technology based on plastic deformation has been widely explored as an alternative to fusion conventional methods often used in the industry. Electromagnetic pulse technology consists in an alternative under study with an increasing number of applications due to the possibility of joining dissimilar materials. It is based on Faraday's law of electromagnetic induction where the driving force is the Lorentz force created by the electromagnetic field between the conductive materials. An electrical current is delivered from a capacitor bank into a coil. Then, an opposite current is induced in the metallic object. One of the two materials is fixed while the workpiece is repelled at a very high speed against the target object. The magnetic pulse welding process seems promising, but joining two workpieces wasn't found to be that easy as it is generally represented. This thesis investigates the influence of surface preparation on the weld quality of tubular parts. Different surfaces conditions were tested (machined, blasted, polished, greasy, chemical etched and threaded) with fixed gap, standoff distance and energy. To analyze the welding quality, for each surface condition, two welded samples were investigated through tensile tests and another one was used to examine the microstructure.

- The surface condition does have an influence on the welding quality. However, it was not possible to establish a correlation between the surface roughness and joint strength through the results obtained.
- Different interface morphologies were obtained, for each sample tested. Regarding the tensile tests, the strongest Al/Cu joint obtained was for the threaded samples but this bond was created through a process of crimping and not welding. For the threaded samples, the failure occurred in the aluminum part after exceeding the tensile strength. For some applications where a tight joint is not required, the process of crimping can be a better option than welding as a stronger joint can be achieved without metallurgical

bonding. For MPW higher values of temperature are involved leading to an increase in the problems associated with the setup used.

- Analyzing the aspect of the different interfaces is possible to conclude that the formation of an intermetallic layer, the presence of porosity and occurrence of cracking is affected by the surface topology. The porosity registered in some SEM images is very susceptible of cracking.
- The need of pre-cleaning the surface seems to be relevant. For the oil contaminated samples, the bond was not created. Probably, the jet formation was not enough to clean the contaminated surface.
- The parameters as the standoff distance, the voltage level and LWZ distance used in the experiments were fixed in order to study the influence of the surface conditions for the same working conditions. However, it was expected that the interface obtained for the machined samples was similar to the results presented in [68]. It was found that, probably, the samples' length may influence the joint formation. Thus, for different materials properties, the welding window and the process parameters should be re-optimized.
- Magnetic pulse welding has been considered as a solid state process. However, during the process, the occurrence of melting was verified. The growth of an intermetallic phase, composed by aluminum and copper, suggest the occurrence of fusion between both materials.

---

## 6.2 Future work

According to the experimental results and regarding the main propose of this thesis which was to analyze the surface influence on the weld quality, more variety of different surface conditions can be done in order to increase the reliability of the main conclusion of this thesis: the condition of the surface does have an influence on the welding quality.

Several considerations about future improvements of the present work are described in the following:

1. More material combinations: In this thesis experiments were all performed using the same combination of aluminum and copper, always using the aluminum as a flyer material and copper as a target one. In order to study different combinations of materials with different characteristics would be interesting to do the same experimental procedures using different materials.
2. Different experimental parameters: In this experimental work the same energy, standoff distance and LWZ were always used. Meaning that, varying this would result in a different impact angle and impact velocity which could lead to different weld results. Thus, would be interesting to optimize the process parameters for each specimen length and then tested different roughness values for each surface.
3. Development of different approaches for magnetic pulse technology besides welding should be also considered. For instance, the process of crimping because of the higher mechanical strength results obtained when comparing crimping with welding using the same technology. A stronger connection was obtained without metallurgical bonding.





## 7 REFERENCES

---

- [1] Mustafa Acarer, Behçet Guelenc, and Fehim Findik. Investigation of explosive welding parameters and their effects on microhardness and shear strength. *Materials & design*, 24(8):659-664, 2003.
- [2] Tomokatsu Aizawa, Mehrdad Kashani, and Keigo Okagawa. Application of magnetic pulse welding for aluminum alloys and spcc steel sheet joints. *Welding Journal*, 86(5):119-124, 2007.
- [3] S.A.A. Akbari-Mousavi, L.M. Barrett, and S.T.S. Al-Hassanib. Explosive welding of metal plates. *Journal of materials processing technology*, 2007.
- [4] Alexander Popo\_ Alexis. Explosive welding process, July 14 1964. US Patent 3,140,537.
- [5] Nicola Angelo. Kelvin-helmholtz instability in a fully ionized plasma in a magnetic field. *Physics of Fluids* (1958-1988), 8(9):1748{1750, 1965.
- [6] Masatada Araki. Explosive welding process, June 4 1974. US Patent 3,813,758.
- [7] T Baaten, Nicolas Debroux, Wim DeWaele, and K Faes. Joining of copper to brass using magnetic pulse welding. In *4th International Conference on High Speed Forming, March 9th-10th 2010 Columbus, Ohio, USA*. Institut fur Umformtechnik-Technische Universitaet Dortmund, 2010.
- [8] VS Balanethiram, Xiaoyu Hu, Marina Altynova, and Glenn S Daehn. Hyperplasticity: enhanced formability at high rates. *Journal of Materials Processing Technology*, 45(1-4):595-600, 1994.
- [9] John G Banker and Edward G Reineke. Explosion welding. *ASM International, ASM Handbook.*, 6:303{305, 1993.
- [10] A Ben-Artzy, A Stern, N Frage, V Shribman, and O Sadot. Wave formation mechanism in magnetic pulse welding. *International Journal of Impact Engineering*, 37(4):397-404, 2010.
- [11] A Berlin, TC Nguyen, MJ Worswick, and Y Zhou. Metallurgical analysis of magnetic pulse welds of az31 magnesium alloy. *Science and Technology of Welding and Joining*, 16(8):728-734, 2011.
- [12] Tadeusz Zdzislaw Blazynski. *Explosive welding, forming and compaction*. Springer Science & Business Media, 2012.
- [13] Jan Broeckhove, Len Willemsens, and Koen Faes. Magnetic pulse welding. *Sustainable Construction and Design*, 1(1):21, 2010.
- [14] Eric Carton. *Wave forming mechanisms in explosive welding*. In *Materials Science Forum*, volume 465, pages 219-224. Trans Tech Publ, 2004.
- [15] Vicente Chiaverini. *Aco e ferros fundidos*. São Paulo: ABM-Associação Brasileira de Metais, pages 321-358, 1982.
- [16] Alexandre Albarello Costa. *Tratamentos termicos*. PGETEMA/PUCRS.

- [17] GR Cowan, OR Bergmann, and AH Holtzman. Mechanism of bond zone wave formation in explosion-clad metals. *Metallurgical and Materials Transactions B*, 2(11):3145-3155, 1971.
- [18] Glenn S Daehn, M Altynova, VS Balanethiram, G Fenton, M Padmanabhan, A Tamhane, and E Winnard. *High-velocity metal forming an old technology addresses new problems*. *Jom*, 47(7):42-45, 1995.
- [19] Ines Vieira de Oliveira. Electromagnetic forming process: *Numerical modelling and analysis of process parameters*. Master's thesis, University of Porto, 2013.
- [20] TI DebRoy and SA David. *Physical processes in fusion welding*. *Reviews of modern physics*, 67(1):85, 1995.
- [21] Ahmet Durgutlu, Behcet Gulenc, and Fehim Findik. *Examination of copper/stainless steel joints formed by explosive welding*. *Materials & design*, 26(6):497{507, 2005.
- [22] Ahmet Durgutlu, Hasan Okuyucu, and Behcet Gulenc. *Investigation of effect of the stand-off distance on interface characteristics of explosively welded copper and stainless steel*. Elsevier, 2007.
- [23] A Elsen, P Groche, M Ludwig, and R Schaefer. *Fundamentals o empt-welding*. In 4th International Conference on High Speed Forming, March 9th-10th 2010 Columbus, Ohio, USA. Institut fur Umformtechnik-Technische Universitaet Dortmund, 2010.
- [24] DG Eskin, L Katgerman, JF Mooney, et al. *Contraction of aluminum alloys during and after solidification*. *Metallurgical and Materials Transactions A*, 35(4):1325{1335, 2004.
- [25] Fehim Findik. *Recent developments in explosive welding*. *Materials & Design*, 32(3):1081{1093, 2011.
- [26] Dhiraj Gayakwada, Mahesh Kumar Dargar, Pramod Kumar Sharma, Rajesh purohit, and R.S.Rana. *A review on electromagnetic forming process*. *Procedia Materials Science*, 2014.
- [27] Mohammad Tabatabaee Ghomi, Jafar Mahmoudi, Abolfazl Khalkhali, and Gholamhossein Liaghat. *Explosive welding of unequal surface using groove method*. Technology Development Institute (TDI) and ACECR Researcher, Tehran, Iran and Malardalen University (MDH), Sweden and School of Automotive Engineering, Iran University of Science and Technology, Tehran, Iran and Tarbiat Modares University, Tehran, Iran, 2012.
- [28] Gunther Goebel, Eckard Beyer, Joerg Kaspar, and Berndt Brenner. *Dissimilar metal joining: macro-and microscopic e\_ects of mpw*. In 5th International Conference on High Speed Forming, pages 179{188, 2012.
- [29] Gunther Goebel, Eckard Beyer, Joerg Kaspar, and Berndt Brenner. *Dissimilar metal joining: macro and microscopic effects of mpw*. 5th International Conference on High Speed Forming, 2012.
- [30] S Golovashchenko, N Bessonov, and R Davies. *Design and testing of coils for pulsed electromagnetic forming*. In Proceedings of the 2nd International Conference on High Speed Forming (ICHSF 2006), University of Dortmund, Germany, 2006.
- [31] F Grignon, D Benson, KS Vecchio, and MA Meyers. *Explosive welding of aluminum to aluminum: analysis, computations and experiments*. *International Journal of Impact Engineering*, 30(10):1333-1351, 2004.
- [32] Behcet Gulenc. *Investigation of interface properties and weldability of aluminum and copper plates by explosive welding method*. Elsevier, 2007.
- [33] Marlon Hahn, Christian Weddeling, Geo\_rey Taberb, Anupam Vivekb, Glenn S. Daehnb, and A. Erman Tekkaya. *Vaporizing foil actuator welding as a competing technology tomagnetic pulse welding*. *Journal of Materials Processing Technology*, 2015.
- [34] SR Hansen, A Vivek, and GS Daehn. *Control of velocity, driving pressure, and planarity during yer launch with vaporizing foil actuator*. In 6th International Conference on High Speed Forming, March 27th-29th 2014, Daejeon, Korea, 2014.
- [35] H Hokari, T Sato, K Kawauchi, and A Muto. *Magnetic impulse welding of aluminium tube and copper tube with various core materials*. *Welding international*, 12(8):619{626, 1998.
- [36] Ahmad K Jassim. *Magnetic pulse welding technology*. In Energy, Power and Control (EPC-IQ), 2010 1st International Conference on, pages 363-373. IEEE, 2010.

- 
- [37] AK Jassim. *Comparison of magnetic pulse welding with other welding methods*. Journal of Energy and Power Engineering, 5(12), 2011.
- [38] J.L. Robinson. *A fluid model of impact welding on metals: A mechanism wave formation and the effect of viscous energy dissipation*. 1974.
- [39] Nizamettin Kahraman and Behcet Gulen\_c. *Microstructural and mechanical properties of cu-ti plates bonded through explosive welding process*. Journal of Materials Processing Technology, 169(1):67{71, 2005.
- [40] Nizamettin Kahraman, Behcet Gulen\_c, and Fehim Findik. *Joining of titanium/stainless steel by explosive welding and effect on interface*. Journal of Materials Processing Technology, 169(2):127{133, 2005.
- [41] Kalpakjian and Schmid. *Solid-state welding processes*. In Manufacturing Engineering and Technology. Manufacturing Engineering and Technology, 2010.
- [42] Manish Kamal and Glenn S Daehn. *A uniform pressure electromagnetic actuator for forming at sheets*. Journal of Manufacturing Science and Engineering, 129(2):369{379, 2007.
- [43] Sung-Wook Kim, Chang-Keun Chun, and Sook-Hwan Kim. *Effects of the stand-off distance on the weld strength in magnetic pulse welding*. Journal of Welding and Joining, 26(6):48{53, 2008.
- [44] M Kimchi, H Shao, W Cheng, and P Krishnaswamy. *Magnetic pulse welding aluminium tubes to steel bars*. Welding in the World, 48(3-4):19-22, 2004.
- [45] Anna Kochan. *Magnetic pulse welding shows potential for automotive applications*. Assembly Automation, 20(2):129{132, 2000.
- [46] S DATE Kore, PP Date, and SV Kulkarni. *Effect of process parameters on electromagnetic impact welding of aluminum sheets*. International journal of impact engineering, 34(8):1327{1341, 2007.
- [47] Sachin D Kore, PN Vinod, Satendra Kumar, and MR Kulkarni. *Study of wavy interface in electromagnetic welds*. In Key Engineering Materials, volume 504, pages 729{734. Trans Tech Publ, 2012.
- [48] SD Kore, J Imbert, MJ Worswick, and Y Zhou. *Electromagnetic impact welding of mg to al sheets*. Science and Technology of Welding and Joining, 14(6):549-553, 2009.
- [49] H Kreye. *Melting phenomena in solid state welding processes*. Weld. J, 56(5):154{158, 1977.
- [50] Kwang-Jin Lee, Shinji Kumai, Takashi Arai, and Tomokatsu Aizawa. *Interfacial microstructure and strength of steel/aluminum alloy lap joint fabricated by magnetic pressure seam welding*. Materials Science and Engineering: A, 471(1):95{101, 2007.
- [51] Won-Bae Lee, Kuek-Saeng Bang, and Seung-Boo Jung. *Effects of intermetallic compound on the electrical and mechanical properties of friction welded cu/al bimetallic joints during annealing*. Journal of Alloys and Compounds, 390(1):212{219, 2005.
- [52] Yuri Livshiz and Oren Gafri. *Joining or welding of metal objects by a pulsed magnetic force*, October 20 1998. US Patent 5,824,998.
- [53] Yuri Livshiz and Oren Gafri. *Technology and equipment for industrial use of pulse magnetic fields*. In Pulsed Power Conference, 1999. Digest of Technical Papers. 12th IEEE International, volume 1, pages 475-478. IEEE, 1999.
- [54] Kevin Loncke. *An exploratory study into the feasibility of magnetic pulse welding*. Master's thesis, Ghent University, 2008-2009.
- [55] Pulsar Ltd. *New applications development*. Technical report, Presentation for internal use, 2008.
- [56] W Lucas, JD Williams, and B Crossland. *Some metallurgical observations on explosive welding*. In Second International Conference of The Center for High Energy Forming, 1969.
- [57] AG Mamalis, DE Manolakos, AG Kladas, and AK Koumoutsos. *Electromagnetic forming and powder processing: trends and developments*. Applied Mechanics Reviews, 57(4):299{324, 2004.
- [58] M Marya and S Marya. *Interfacial microstructures and temperatures in aluminium-copper electromagnetic pulse welds*. Science and technology of welding and joining, 9 (6):541{547, 2004.

- [59] Manuel Marya, Didier Priem, and Surendar Marya. *Microstructures at aluminum-copper magnetic pulse weld interfaces*. In Materials Science Forum, volume 426, pages 4001-4006. Trans Tech Publ, 2003.
- [60] James Clerk Maxwell. *A treatise on Electricity and Magnetism*. University of Oxford, 1873.
- [61] RM Miranda, B Tomás, TG Santos, and N Fernandes. *Magnetic pulse welding on the cutting edge of industrial applications*. Soldagem & Inspeção, 19 (1):69-81, 2014.
- [62] Lucio F Mondolfo. *Aluminum alloys: structure and properties*. Elsevier, 2013.
- [63] A.A. Akbari Mousavi and S.T.S. Al-Hassani. *Numerical and experimental studies of the mechanism of the wavy interface formations in explosive/impact welding*. Journal of the Mechanics and Physics of Solids, 2005.
- [64] SAA Akbari Mousavi and P Farhadi Sartangi. *Experimental investigation of explosive welding of cp-titanium/aisi 304 stainless steel*. Materials & Design, 30(3):459-468, 2009.
- [65] PRIMOZ Mrvar, M Terelj, Goran Kugler, Matevz Fazarinc, and Joze Medved. *Characterization of solidification and hot workability of mgal6mn foundry alloy*. Materials and Geoenvironment, 53 (2):175, 2006.
- [66] Keigo Okagawa and Tatsuhiko Aizawa. *Impact seam welding with magnetic pressure for aluminum sheets*. In Materials Science Forum, volume 465, pages 231-236. Trans Tech Publ, 2004.
- [67] Inês V. Oliveira, A. J. Cavaleiro, and A. Reis G. A. Taber. *Magnetic pulse welding of dissimilar materials: Aluminum-copper*. Advanced Structured Materials (SPRINGER), 2016.
- [68] Ines Oliveira, Pedro Teixeira, and Ana Reis. *Magnetic pulse welding of dissimilar metals: Influence of process parameters*. In 6th International Conference on High Speed Forming, 2012.
- [69] Mahadevan Padmanabhan. *Wrinkling and springback in electromagnetic sheet metal forming and electromagnetic ring compression*. PhD thesis, The Ohio State University, 1997.
- [70] Evandro Paese, Martin Geier, Roberto Petry Homrich, and Joyson Luiz Pacheco. *Simplified mathematical modeling for an electromagnetic forming system with a spiral coil as actuator*. Journal of the Brazilian Society of Mechanical Sciences and Engineering, 33 (3):324-331, 2011.
- [71] Chandrhas Patel and Sachin D Kore. *Dual electromagnetic forming using single uniform pressure coil*. In Key Engineering Materials, volume 611, pages 723-730. Trans Tech Publ, 2014.
- [72] Michael M Plum. *Electromagnetic forming*. ASM Handbook., 14:644-653, 1988.
- [73] V. Psyk, D. Risch, B.L. Kinsey, A.E. Tekkaya, and M. Kleiner. *Electromagnetic forming-a review*. Journal of Materials Processing Technology, 2010.
- [74] R Raelison, M Rachik, N Buiron, D Haye, M Morel, B Dos Santos, D Jouare, and G Frantz. *Assessment of gap and charging voltage influence on mechanical behaviour of joints obtained by magnetic pulse welding*. In Proceedings of the 5th International Conference on High Speed Forming, Dortmund, Germany, pages 207-216, 2012.
- [75] RN Raelison, N Buiron, M Rachik, D Haye, and G Franz. *Efficient welding conditions in magnetic pulse welding process*. Journal of Manufacturing Processes, 14 (3):372-377, 2012.
- [76] RN Raelison, N Buiron, M Rachik, D Haye, G Franz, and M Habak. *Study of the elaboration of a practical weldability window in magnetic pulse welding*. Journal of Materials Processing Technology, 213(8):1348-1354, 2013.
- [77] RN Raelison, D Racine, Z Zhang, N Buiron, D Marceau, and M Rachik. *Magnetic pulse welding: Interface of al/cu joint and investigation of intermetallic formation effect on the weld features*. Journal of Manufacturing Processes, 16(4):427-434, 2014.
- [78] RN Raelison, T Sapanathan, N Buiron, and M Rachik. *Magnetic pulse welding of al/al and al/cu metal pairs: Consequences of the dissimilar combination on the interfacial behavior during the welding process*. Journal of Manufacturing Processes, 20:112-127, 2015.
- [79] V. Robin, E. Feulvarch, and J.M. Bergheau. *Modelling of processes involving electromagnetic phenomena*. International Journal of Material Forming, 2008.
- [80] G. S. Sarkisov, K. W. Struve, and D. H. McDaniel. *Effect of current rate on energy deposition into exploding metal wires in vacuum*. AIP, 2004.

- 
- [81] R Schafer, P Pasquale, and S Kallee. *Industrial application of the electromagnetic pulse technology*. Alzenau, Germany, 2009.
- [82] Francis A Schunk. *Constitution of binary alloys*, second supplement McGraw-Hill, 1969.
- [83] V.S. Sedoi, G.A. Mesyats, V.I. Oreshkin, V.V. Valevich, and L.I. Chemezova. *The current density and the specific energy input in fast electrical explosion*. IEEETrans. Plasma Sci., 1999.
- [84] Ji-Yeon Shim, Ill-Soo Kim, Moon-Jin Kang, In-Ju Kim, Kwang-Jin Lee, and Bong-Yong Kang. *Joining of aluminum to steel pipe by magnetic pulse welding*. Materials Transactions, Vol. 52, No. 5, 2011.
- [85] V Shribman. *Magnetic pulse welding of automotive hvac parts*. Rapport technique, Pulsar Ltd, 8:41{42, 2007.
- [86] V Shribman. *Magnetic pulse welding for dissimilar and similar materials*. In 3rd International Conference on High Speed Forming, March 11-12, 2008, Dortmund, Germany. Institut fur Umformtechnik-Technische Universitat Dortmund, 2008.
- [87] V Shribman, A Stern, Y Livshitz, and O Gafri. *Magnetic pulse welding produces high-strength aluminum welds: welding aluminium*. Welding Journal, 81(4):33{37, 2002.
- [88] Muhammad Ali Siddiqui. *Numerical modelling and simulation of electromagnetic forming process*. PhD thesis, Ecola doctorale matematiques, 2009.
- [89] A Stern and M Aizenshtein. *Bonding zone formation in magnetic pulse welds*. Science and Technology of Welding & Joining, 2013.
- [90] A Stern, V Shribman, A Ben-Artzy, and M Aizenshtein. *Interface phenomena and bonding mechanism in magnetic pulse welding*. Journal of Materials Engineering and Performance, 23(10):3449-3458, 2014.
- [91] Milton Van Dyke and Milton Van Dyke. *An album of fluid motion*, volume 176. Parabolic Press Stanford, 1982.
- [92] A. Vivek, R.C. Brune, S.R. Hansen, and G.S. Daehn. *Vaporizing foil actuator used for impulse forming and embossing of titanium and aluminum alloys*. Journal of Materials Processing Technology, 2013.
- [93] A. Vivek, S.R. Hansen, B.C. Liu, and Glenn S. Daehn. *Vaporizing foil actuator: A tool for collision welding*. Journal of Materials Processing Technology, 2013.
- [94] A Vivek, BC Liu, and GS Daehn. *Collision welding of tungsten alloy 17d and copper using vaporizing foil actuator welding*. In 6th International Conference on High Speed Forming, March 27th-29th 2014, Daejeon, Korea, 2014.
- [95] Anupam Vivek and Glenn S Daehn. *Vaporizing foil actuator: a versatile tool for high energy-rate metal working*. Procedia Engineering, 81:2129-2134, 2014.
- [96] Mitsuhiro Watanabe and Shinji Kumai. *High-speed deformation and collision behavior of pure aluminum plates in magnetic pulse welding*. Materials transactions, 50 (8):2035{2042, 2009.
- [97] Mitsuhiro Watanabe and Shinji Kumai. *High-speed deformation and collision behavior of pure aluminum plates in magnetic pulse welding*. Materials transactions, 50 (8):2035{2042, 2009.
- [98] Mitsuhiro Watanabe and Shinji Kumai. *Interfacial morphology of magnetic pulse welded aluminum/aluminum and copper/copper lap joints*. Materials transactions, 50 (2):286-292, 2009.
- [99] Mitsuhiro Watanabe and Shinji Kumai. *Welding interface in magnetic pulse welded joints*. In Materials Science Forum, volume 654, pages 755-758. Trans Tech Publ, 2010.
- [100] Christian Weddeling. *Electromagnetic Form-Fit Joining*. 2015.
- [101] Jez Weston and Rob Wallach. *Mechanical properties of laser welds in aluminium alloys*. In Joints in Aluminium-Inalco, 1998: 7th International Conference, page 332. Woodhead Publishing, 1999.
- [102] Xin Wu and Jianhui Shang. *An investigation of magnetic pulse welding of al/cu and interface characterization*. Journal of Manufacturing Science and Engineering, 136 (5):051002, 2014.

- [103] Jun Rui Xu, Hai Ping Yu, and Chun Feng Li. *Effects of process parameters on electromagnetic forming of az31 magnesium alloy sheets at room temperature*. The International Journal of Advanced Manufacturing Technology, pages 1-12.
- [104] P Zhang, M Kimchi, H Shao, JE Gould, and GS Daehn. *Analysis of the electromagnetic impulse joining process with a field concentrator*. In AIP Conference Proceedings, volume 712, pages 1253-1258. IOP INSTITUTE OF PHYSICS PUBLISHING LTD, 2004.
- [105] Yuan Zhang. *Investigation of magnetic pulse welding on lap joint of similar and dissimilar materials*. PhD thesis, The Ohio State University, 2010.
- [106] Yuan Zhang, SS Babu, P Zhang, Edward A Kenik, and GS Daehn. *Microstructure characterisation of magnetic pulse welded aa6061-t6 by electron backscattered diffraction*. Science and Technology of Welding & Joining, 2013.
- [107] Yuan Zhang, Sudarsanam Suresh Babu, Curtis Prothe, Michael Blakely, John Kwasegroch, Mike LaHa, and Glenn S Daehn. *Application of high velocity impact welding at varied different length scales*. Journal of Materials Processing Technology, 211 (5):944-952, 2011.